Identification of unknown model parameters and sensitivity analysis for abrasive waterjet milling process

Vladimir Groza

▶ **To cite this version:**

Vladimir Groza. Identification of unknown model parameters and sensitivity analysis for abrasive waterjet milling process. General Mathematics [math.GM]. COMUE Université Côte d'Azur (2015 - 2019), 2016. English. NNT : 2016AZUR4094 . tel-01466734

HAL Id: tel-01466734
https://theses.hal.science/tel-01466734

Submitted on 13 Feb 2017

HAL is a multi-disciplinary open access archive for the deposit and dissemination of scientific research documents, whether they are published or not. The documents may come from teaching and research institutions in France or abroad, or from public or private research centers.

L'archive ouverte pluridisciplinaire **HAL**, est destinée au dépôt et à la diffusion de documents scientifiques de niveau recherche, publiés ou non, émanant des établissements d'enseignement et de recherche français ou étrangers, des laboratoires publics ou privés.

Université Nice Sophia Antipolis - UFR Sciences
École Doctorale de Sciences Fondamentales et Appliquées

Thèse

pour obtenir le titre de

Docteur en Sciences

de l'Université Nice Sophia Antipolis

Discipline : Mathématiques

présentée et soutenue par

Vladimir Groza

Identification de paramètres et analyses de sensibilité pour un modèle d'usinage par jet d'eau abrasif

---

Identification of unknown model parameters and sensitivity analysis for abrasive waterjet milling process

---

Thèse dirigée par

Didier Auroux

Soutenue le 9 Novembre 2016

Jury :

Directeur :	Didier Auroux	-	Université Nice Sophia Antipolis
Rapporteur :	John Billingham	-	University of Nottingham
Rapporteur :	Eric Blayo	-	Université Joseph Fourier, Grenoble
Examinateur :	Jacques Blum	-	Université Nice Sophia Antipolis
Examinateur :	Laurent Hascoët	-	INRIA Sophia-Antipolis
Examinateur :	Michel Kern	-	INRIA Rocquencourt

À ma famille.

"J'ai décidé d'être heureux parce que c'est bon pour la santé."

Voltaire

Remerciements

Tout d'abord, j'aimerais remercier chaleureusement mon directeur de thèse Didier Auroux de m'avoir permis d'effectuer une thèse sur un sujet très intéressant et important. Il m'a donné des conseils précieux et des orientations utiles. Je voudrais le remercier de m'avoir guidé, encouragé et soutenu avec son enthousiasme pendant ces trois années qui furent véritablement essentielles à l'avancée de mon travail d'une manière efficace. Je souhaiterais également lui exprimer toute ma reconnaissance de m'avoir accueilli avec une gentillesse et une attention qui ont fait minimiser toutes les difficultés culturelles et démarches administratives.

Mes remerciements vont également à John Billingham et Eric Blayo qui ont bien voulu faire le rapport de ma thèse. Vos remarques attentives ont contribué à l'amélioration du manuscrit.

I wish to thank John Billingham and Eric Blayo who kindly agreed to give a report on my thesis. I am thankful to them for their attentive remarks that contributed to the improvement of the manuscript.

Je suis très reconnaissant à Jacques Blum, Laurent Hascoët et Michel Kern d'avoir accepté de participer à mon jury.

I also would like to thank all the fellows and partners of Marie-Curie ITN project STEEP with whom I was working during these three years. It was a great pleasure to collaborate with young and experienced researchers in different areas on the edge between industry and science. I want to thank Dr. Pablo Lozano Torrubia for his contribution in preparing the experimental data required for my research. I also express my gratitude to all the project partners for given opportunities for the joint work and for great meetings during this project.

Je souhaite exprimer ma gratitude à tous les membres du laboratoire J.A. Dieudonné pour l'ambiance agréable au cours de ces trois années. Merci également à mes collègues de bureau Bastien, Nathalie et Kateryna.

Un remerciement amical à Jean-Marc Lacroix et à Roland Ruelle qui ont assuré les moyens informatiques nécessaires à mes travaux.

Je remercie mes parents qui ont su croire en moi et m'ont apporté toute leur aide quand j'en ai eu besoin. Je vous suis très reconnaissant d'avoir toujours été à mes côtés. Merci pour votre soutien et vos encouragements.

Je remercie ma femme Mayya qui a choisi de partager sa vie avec moi. Sans elle, je n'aurais pas pu surmonter les moments les plus difficiles du travail et il aurait été tout simplement impossible de trouver le vrai bonheur.

Enfin, je souhaite adresser un remerciements spéciaux à ma fille Varvara pour m'avoir inspiré et m'avoir laissé dormir les nuits.

Contents

Résumé. Ce travail fait partie du projet Marie-Curie ITN STEEP, dans le domaine des faisceaux énergétiques. Nous étudions ici l'identification de paramètres pour un modèle générique d'usinage par jet d'eau abrasif. Cela peut être vu comme un problème inverse mal posé.

L'étude de ce problème trouve son origine dans les applications industrielles d'usinage, où la nécessité de modéliser et prédire la surface finale avec une très grande précision est essentielle en l'absence de connaissance des paramètres du modèle.

Nous proposons ici une méthode d'identification des paramètres du modèle basée sur la minimisation d'une fonction coût, mesurant la différence entre la solution numérique et les observations expérimentales. L'approche variationnelle, basée sur le Lagrangien, permet de considérer l'adjoint, et l'utilisation d'un logiciel de différentiation automatique (TAPENADE) conduit à une identification rapide et précise des paramètres, quelles que soient la complexité et la taille du problème étudié.

La qualité de l'identification peut être fortement instable et dépendre largement des données expérimentales en cas de bruit. Nous introduisons alors des termes de régularisation permettant de gérer la présence d'erreurs de mesure et d'améliorer l'estimation des paramètres.

Plusieurs cas d'usinage par jet abrasif sont considérés: problème stationnaire, jet qui se déplace à vitesse constante, ou en accélérant, utilisation de données synthétiques ou réelles. L'étude de sensibilité faite dans ces différents cas montre la robustesse de l'approche, qui permet d'obtenir de très bons résultats, à la fois acceptables d'un point de vue industriel, et permettant de prédire la surface avec une grande précision.

Mots-clés: Equations aux dérivées partielles, Problèmes inverses, Approche variationnelle, Optimisation, Identification de paramètres, Usinage par jet d'eau abrasif, Différentiation automatique, TAPENADE, Prévision de surfaces.

Abstract. This work is part of STEEP Marie-Curie ITN project, covering the research in field of energy beam processing. We focus on the identification of unknown parameters of the proposed generic Abrasive WaterJet Milling (AWJM) model. This problem appears as an ill-posed inverse problem.

The necessity of studying this problem comes from the industrial milling applications where the possibility to predict and model the final surface with high accuracy is one of the primary tasks in the absence of any knowledge of the model parameters that should be used.

We propose the method of the model parameters identification by minimizing a cost function, measuring the difference between experimental observation and numerical solution. The variational approach based on corresponding Lagrangian allows to obtain the adjoint state and the involvement of the automatic differentiation software tool (TAPENADE) leads to fast and efficient parameters identification regardless the complexity and size of particular studied problem.

In fact the parameter identification problem is highly unstable and strictly depends on quality of input data. Regularization terms could be effectively used to deal with the presence of measurement errors and to improve the identification correctness.

Various cases of the AWJM process such as a stationary problem and moving with constant feed speed or acceleration are studied based on both artificial and real experimental data. The sensitivity study related to these particular problems demonstrates the strong capability of the proposed approach to obtain acceptable results for manufacturing and to predict the required surface geometry with high accuracy.

Keywords: Partial differential equations, Inverse problems, Variational approach, Optimization, Parameters identification, Abrasive waterjet milling, Automatic differentiation, TAPENADE, Surface prediction.

Résumé étendu

Ce travail s'inscrit dans le cadre du projet ITN Marie Curie STEEP, qui porte sur l'étude de faisceaux énergétiques, et plus particulièrement sur l'usinage par jet d'eau abrasif (abrasive waterjet, AWJ).

L'usinage par jet d'eau abrasif (abrasive waterjet, AWJ) est un problème industriel pour lequel la théorie des problèmes inverses n'a pas encore été très étudiée et peut apporter beaucoup. Cette problématique fait partie de la classe des procédés industriels pour l'usinage mécanique de matériaux, où la pièce à usiner est soumise à des forces mécaniques spécifiques causées par l'impact de particules abrasives présentes dans le jet d'eau. Ce proecessus d'usinage est réalisé à l'aide d'un jet d'eau à très haute pression, envoyé par une pompe dans un petit orifice de la tête d'usinage afin de réaliser un jet à très haute vitesse. Dans la chambre de mélange, un système de dépression permet l'aspiration de particules abrasives. Cela résulte en un mélange d'eau et de particules abrasives accéléré à très haute vitesse, générant un panache agressif qui attaque la surface du matériau et crée une empreinte.

Le principal objectif de ce travail est de mettre au point une méthode mathématique permettant d'identifier les paramètres inconnus du modèle générique d'usinage par jet d'eau abrasif. Ce modèle a été décrit et étudié dans [6, 31, 14, 36] et a été développé pour tenir compte des contraintes industrielles pour la prévision des empreintes formées par le jet d'eau. En supposant que les paramètres du modèle et les termes sources sont connus, on peut trouver la forme du profil de la tranche usinée. Il s'agit ici du problème direct, qui repose sur une EDP non-linéaire. L'identification des paramètres du modèle est alors un problème inverse.

Cette étude est motivée par les applications industrielles d'usinage, pour lesquelles il est important de pouvoir modéliser et prédire avec une grande précision la forme finale de la pièce usinée. Il est donc nécessaire de pouvoir fournir une information sur les paramètres du modèle à utiliser.

Le premier objectif de cette thèse est de développer une méthode mathématique pour l'identification de paramètres du modèle d'usinage par jet d'eau abrasif considéré.

Ce modèle a été précédemment développé dans le contexte industriel de l'usinage de matériaux cassants par jet d'eau.

L'identification des paramètres inconnus du modèle est un problème inverse. Notre but est d'identifier ces paramètres, qui sont a priori inaccessibles à partir des données expérimentales, afin de pouvoir prédire l'usinage d'une surface avant d'effectuer des simulations de fabrication. Nous utilisons pour cela une approche variationnelle, dans laquelle la minimisation d'une fonction coût permet d'identifier les paramètres optimaux (dans un sens à définir).

Il se trouve que dans ce cadre, l'identification de paramètres est fortement instable, et dépend beaucoup de la qualité des données disponibles. Lorsque le problème inverse (d'identification des paramètres) est mal posé, la solution n'est pas unique - la fonction coût peut présenter plusieurs minima - ou peut présenter une grande instabilité par rapport aux données. Dans ce cas, une approche classique consiste à régulariser le problème, en apportant par exemple des informations supplémentaires. L'ajout de termes de régularisation dans la fonction coût à minimiser permet a priori de mieux gérer le bruit dans les données et d'améliorer l'identification des paramètres.

L'approche considérée consiste à minimiser une fonction coût mesurant la différence entre les données expérimentales et la solution numérique correspondante du modèle. En introduisant le Lagrangien associè à la minimisation sous contrainte de modèle dans cette approche variationnelle, nous pouvons en déduire le modèle adjoint, nécessaire pour effectuer la minimisation en un temps raisonnable. L'utilisation d'un algorithme de différentiation automatique permet d'obtenir efficacement le modèle adjoint, et ainsi de mener à bien la minimisation et l'identification des paramètres, même lorsque la taille du problème est grande.

La minimisation numérique de la fonction coût peut être faite par différents algorithmes. Une approche classique repose sur des algorithmes itératifs de descente de gradient. Nous utilisons ici l'une de ces méthodes, l'algorithme L-BFGS (Broyden-Fletcher-Goldfarb-Shanno à mémoire limitée), mis en œuvre numériquement dans la routine N2QN1 de la librairie de minimisation MODULOPT développée à INRIA.

Le gradient de la fonction coût, nécessaire pour la minimisation, peut être vu comme le multiplicateur de Lagrange associé à la contrainte de modèle, solution du modèle adjoint. L'adjoint est obtenu numériquement à l'aide d'un logiciel de différentiation automatique, TAPENADE, développé par l'équipe Tropics d'INRIA Sophia Antipolis. Il s'agit d'une des méthodes les plus efficaces et les moins coûteuses pour obtenir l'adjoint. En effet, ce logiciel génère automatiquement les codes tangent et/ou adjoint à partir du code direct correspondant au modèle.

Notre étude a porté sur différents cas d'usinage par jet d'eau abrasif: problème stationnaire avec un jet immobile, déplacement du jet à vitesse constante ou non (accélération / décélération du jet). L'identification de paramètres a été testée en utilisant soit des données synthétiques, soit des données réelles expérimentales, pour chacun de ces cas. Les données synthétiques ont été générées en utilisant le modèle numérique, et ont permis de mettre au point et démontrer le potentiel de l'approche proposée. Afin de faire le lien entre la technique développée et le processus industriel d'usinage, plusieurs jeux de données réelles et de paramètres de machines d'usinage ont été étudiés.

Les techniques que nous avons utilisées pour identifier les paramètres inconnus du modèle et pour prédire l'évolution géométrique de la surface ont d'abord été introduites et testées dans le cas d'usinage stationnaire.

Le modèle proposé d'usinage par jet d'eau abrasif est le suivant:

$$\frac{\partial \boldsymbol{Z}}{\partial t} = -\frac{\boldsymbol{E}(x,y)\mathrm{e}^{a\boldsymbol{Z}}}{\left(1+|\nabla \boldsymbol{Z}|^2\right)^{k/2}}. \tag{1}$$

Dans un premier temps, nous étudions le cas stationnaire avec des données synthétiques (générées par le modèle), puis expérimentales. Nous présentons les résultats, à la fois en ce qui concerne l'identification des paramètres du modèle, mais aussi pour l'évolution de la surface usinée. Nous étudions ensuite particulièrement l'identification de la fonction de vitesse de gravure (etching rate function) dans le cadre d'une analyse de sensibilité par rapport au bruit dans les données.

Le bruit est considéré comme un paramètre du modèle, qui une fois identifié, permet d'améliorer l'identification des autres paramètres. Nous présentons plusieurs résultats

numériques dans ce cadre. Nous étudions également la possibilité de modifier la fonction coût pour tenir compte de la disponibilité de plusieurs jeux de données bruitées correspondant à la même expérience. Cela apporte une flexibilité supplémentaire à l'approche proposée, pour tenir compte des données disponibles, et surtout une efficacité accrue pour l'identification de paramètres et la prédiction de l'usinage.

L'identification de paramètres a également été testée dans le cas de jets instationnaires. Nous avons considéré deux sous-cas, avec une vitesse constante ou non du jet d'eau abrasif. Les simulations numériques ont là aussi été faites avec des données synthétiques générées par le modèle, puis avec des données expérimentales réelles. Dans le cas d'une vitesse constante, nous avons notamment étudié l'identification simultanée de tous les paramètres du modèle.

Enfin, l'étude se termine par une étude de sensibilité par rapport au bruit de mesure dans le cas d'un jet qui se déplace de façon uniforme. Étant donné le coût très élevé des simulations expérimentales sur des machines industrielles, nous n'avons pu traiter ici que le cas de données synthétiques, générées par le modèle. Les résultats numériques confirment l'efficacité de la méthode, et démontrent que l'approche développée permet de traiter des données issues de beaucoup de cas tests différents (jet stationnaire ou non, vitesse du jet constante ou non, présence ou non de bruit de mesure, ...).

Afin de pouvoir prévoir la surface usinée dans des conditions bruitées, nous avons aussi mis en œuvre une méthode d'identification dans laquelle le bruit est identifié seul, indépendamment des autres paramètres du modèle. L'idée consiste alors à utiliser le bruit identifié pour le retirer des données, puis à identifier les autres paramètres du modèle avec ces nouvelles données. Cela augmente la qualité de l'identification des paramètres. Et les résultats numériques correspondants pour la surface usinée confirment l'intérêt de cette approche. Nous avons enfin présenté une approche d'identification globale de tous les paramètres simultanément, afin de montrer l'étendue des capacités de la méthode proposée.

Les études numériques proposées dans les cas stationnaire et instationnaire montrent que la méthode que nous avons développée permet d'obtenir des résultats sat-

isfaisants pour la fabrication industrielle, permettant d'identifier les paramètres du modèle et ainsi de prévoir la construction d'une surface souhaitée avec une grande précision.

Chapter 1

Introduction (français)

Le domaine des problèmes inverses a connu un intérêt grandissant et une expansion à de nombreux nouveaux domaines ces dernières années, suite à de nouveaux besoins apparus aussi bien dans le monde industriel que scientifique. Une attention particulière a été portée aux problèmes non-linéaires, notamment en raison de leurs applications dans un contexte industriel.

Afin de mieux comprendre ce qu'est un problème inverse, nous parlons tout d'abord de problème direct, qui se réfère généralement à la phase de modélisation, par exemple d'un phénomène physique. La résolution d'un problème direct consiste alors à identifier une fonction qui décrit le processus physique en tout point et à chaque instant d'un domaine prédéfini. Cela nécessite de connaître à l'avance tous les paramètres physiques nécessaires, comme par exemple des cœfficients, ou des termes sources. La résolution du problème direct permet alors de prédire l'évolution du système à partir de la connaissance de son état initial et des lois physiques qui le gouvernent. Dans le problème inverse, le but est de remonter aux paramètres (inconnus) du modèle à partir de données correspondant à l'état du système. Très souvent, ces paramètres ne sont pas directement reliés aux données, et doivent donc être identifiés à partir des données et du modèle.

Les problèmes inverses sont devenus très populaires et développés ces dernières années, grâce notamment au développement de méthodes numériques sophistiquées et à l'augmentation de la puissance de calcul. La théorie et la mise en œuvre numérique des problèmes inverses sont également fortement répandues dans la résolution de problèmes industriels de grande complexité. Les domaines d'application recouvrent par exemple la physique (mécanique quantique, acoustique), la géophysique (océanogra-

phie, sismologie, volcanologie, étude du champ magnétique), la médecine (rayons X, tomographie RMN, croissance tumorale), l'écologie (qualité de l'air et de l'eau, agriculture), l'économie et la finance, ...

Les problèmes inverses se décomposent en une multitude de cas différents, suivant les domaines d'application et la nature du problème posé. L'un de ces cas, crucial dans un grand nombre d'applications, consiste à identifier les paramètres et termes sources inconnus du modèle. Cela peut se faire en comparant les données expérimentales (provenant des systèmes réels) et les simulations numériques (calculées à partir des modèles mathématiques).

Cependant, l'identification de paramètres est généralement un problème inverse mal posé [32, 43] lorsque par exemple il y a du bruit dans les données ou dans le modèle, et cela même si le problème direct est bien posé. On parle de problème mal posé (par opposition à un problème bien posé) lorsque la solution n'existe pas, ou n'est pas unique, ou n'est pas stable (au sens où une petite perturbation sur les données d'entrée peuvent conduire à des écarts considérables dans la solution identifiée). Ce dernier point représente d'ailleurs souvent l'une des plus grandes difficultés lors de la résolution d'un problème inverse mal posé.

Cet aspect peut néanmoins être traité en utilisation des techniques de régularisation [3, 45, 46], largement étudiées [44, 17, 29, 19], et l'identification de paramètres peut alors être réécrite sous la forme stable d'un problème de minimisation de la somme de l'écart aux données et d'un terme de régularisation.

L'usinage par jet d'eau abrasif (abrasive waterjet, AWJ) est un problème industriel pour lequel la théorie des problèmes inverses n'a pas encore été très étudiée et peut apporter beaucoup. Cette problématique fait partie de la classe des procédés industriels pour l'usinage mécanique de matériaux, où la pièce à usiner est soumise à des forces mécaniques spécifiques causées par l'impact de particules abrasives présentes dans le jet d'eau. Ce proecessus d'usinage est réalisé à l'aide d'un jet d'eau à très haute pression, envoyé par une pompe dans un petit orifice de la tête d'usinage afin de réaliser un jet à très haute vitesse. Dans la chambre de mélange, un système de dépression permet

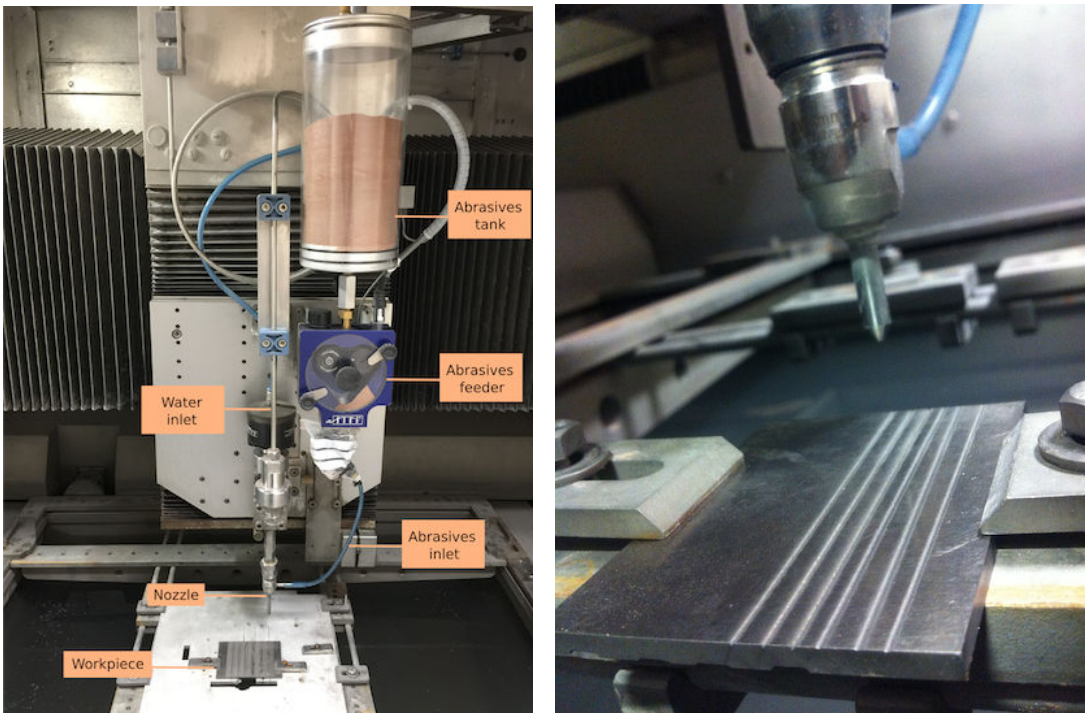

(a) microwaterjet machine (b) Example of milled trenches

Figure 1.1: Système d'usinage par jet d'eau abrasif (gauche) et exemples de tranches usinées (droite).

l'aspiration de particules abrasives. Cela résulte en un mélange d'eau et de particules abrasives accéléré à très haute vitesse, générant un panache agressif qui attaque la surface du matériau et crée une empreinte. L'illustration et les notations pour une machine d'usinage par jet d'eau abrasif sont présentées en Figure 1.1 avec quelques exemples de tranches usinées.

L'usinage par jet d'eau abrasif est une méthode industrielle non conventionnelle et polyvalente d'usinage à moindre coût, permettant de traiter presque n'importe quel type de matériaux, sans se soucier de ses propriétés physiques ou chimiques. Le jet d'eau abrasif est par exemple très largement utilisé pour l'usinage de matériaux en acier, titane, aluminium, verre, diamant polycristallin, céramique, carbure de silicium, ainsi que pour différents composites [41, 7, 47], et dans de nombreux domaines d'application comme les technologies médicales, l'électronique, l'industrie automobile, la bijouterie,

l'industrie du verre, et même en aéronautique et espace. En effet, l'un des avatanges de l'usinage par jet d'eau abrasif est la possibilité de traiter des matériaux non homogoènes, fragiles, extrêmement durs. D'autres avantages résident dans (i) l'utilisation de forces physiques de découpage relativement faibles, permettant de réduire les risques d'endommager la zone de travail; (ii) le fonctionnement de la machine à faible température et l'absence de dommages causés par la chaleur; (iii) la possibilité de découper des formes complexes en 3D grâce à la légèreté de l'équipement.

De plus, le jet d'eau abrasif peut servir à différentes applications comme le découpage, l'usinage, le forage, le polissage, ... d'une pièce. L'un des grands défis est justement l'usinage avec une grande précision et une profondeur controllée. Comme la technique met en jeu un grand nombre de processus physiques, avec plusieurs paramètres comme la pression de la pompe, la vitesse d'alimentation du jet, le flux de matière abrasive, la distance entre le jet et la pièce, le diamètre de l'orifice, ..., il est assez délicat de prédire la forme de la surface créée. Ainsi, la prévision du profil géométrique de la surface à l'aide d'un modèle mathématique devient nécessaire pour contourner ces difficultés.

Ce travail s'inscrit dans le cadre du projet Européen Marie Curie ITN (Initial Training Network) STEEP, qui porte sur l'étude de faisceaux énergétiques. Ce projet intègre des partenaires à la fois académiques et industriels, avec le but de mener à bien des recherches pluri-disciplinaires, un programme de formation scientifique et des interactions entre les universités et partenaires industriels et privés suivants:

- University of Nottingham
- Université Nice Sophia Antipolis
- University of Birmingham
- Friedrich-Alexander University of Erlangen-Nürnberg
- Katholieke Universiteit Leuven
- Swiss Federal Laboratories for Materials Science and Technology

- Fundaciòn TEKNIKER
- WATERjet AG
- TESCAN a.s.
- ZEEKO Ltd

Le principal objectif de ce travail est de mettre au point une méthode mathématique permettant d'identifier les paramètres inconnus du modèle générique d'usinage par jet d'eau abrasif. Ce modèle a été décrit et étudié dans [6, 31, 14, 36] et a été développé pour tenir compte des contraintes industrielles pour la prévision des empreintes formées par le jet d'eau. En supposant que les paramètres du modèle et les termes sources sont connus, on peut trouver la forme du profil de la tranche usinée. Il s'agit ici du problème direct, qui repose sur une EDP non-linéaire. L'identification des paramètres du modèle est alors un problème inverse, et certaines études de ce problème inverse portant uniquement sur un modèle linéaire ont été présentées dans [13].

Notre but consiste à déterminer les paramètres du modèle, qui sont a priori inaccessibles à partir des données expérimentales, afin de prédire la construction de la surface usinée, avant de réaliser la simulation industrielle. Nous considérons alors une approche variationnelle, dans le but de déterminer les paramètres qui vont minimiser une fonction objectif. Il est alors possible de reformuler le problème sous la forme d'une minimisation d'une fonction coût mesurant la différence entre les données expérimentales et la solution correspondante du modèle.

Lorsque le problème inverse est mal posé, sa solution n'est pas unique, ou comme indiqué précédemment, elle n'est pas stable par rapport aux données. Dans ce cas, la fonction coût présente plusieurs minima locaux. De façon assez classique, une solution consiste à utiliser des techniques de régularisation. Il est nécessaire d'ajouter des informations supplémentaires (par exmeple de régularité) sur les paramètres à identifier, afin de rendre le problème bien posé.

La minimisation numérique de la fonction objectif peut être réalisée avec un grand nombre de méthodes. Nous avons considéré une approche classique, basée sur des

algorithmes itératifs de descente de gradient qui convergent vers le minimum. Plus particulièrement, nous avons utilisé l'algorithme à mémoire limitée Broyden-Fletcher-Goldfarb-Shanno (L-BFGS) [21, 35, 48], qui est au cœur de la routine N2QN1 de la librairie de minimisation MODULOPT développée à INRIA [22].

Le gradient de la fonction coût est obtenu numériquement grâce au logiciel de différentiation automatique TAPENADE, développé par l'équipe Tropics à INRIA Sophia Antipolis [27]. Le gradient peut être vu comme un multiplicateur de Lagrange dans le cadre de la minimisation sous contrainte de modèle, permettant d'introduire le modèle adjoint [38, 34]. Nous avons sélectionné cette méthode qui se trouve être particulièrement efficace et peu coûteuse en temps de calcul. Dans le but de calculer le gradient, TAPENADE génère automatiquement les codes tangent et/ou adjoint à partir du code direct. Le code adjoint généré comprend deux étapes générales: un mode direct résolvant le code source original permettant de calculer la fonction coût et de sauver certaines informations au cours de la résolution, et un mode rétrograde, qui utilise ces informations pour calculer les dérivées de la fonction coût.

Cette thèse est organisée sous la forme suivante:

- **Chapitre 3**

  Ce chapitre présente le modèle mathématique proposé pour le procédé d'usinage par jet d'eau abrasif et ses propriétés physiques. Puis nous introduisons les principes généraux sur les problèmes inverses et leurs applications à notre cas. Nous présentons ensuite l'approche variationnelle basée sur le Lagrangien, permettant d'obtenir le gradient de la fonction coût. Nous donnons ensuite une courte description des méthodes de descente de gradient qui sont utilisées pour minimiser la fonction coût. Le cas particulier d'un jet stationnaire est étudié à part dans une section suivante afin de montrer l'efficacité de l'approche proposée. Ce chapitre se termine avec la liste des étapes de notre algorithme d'identification.

- **Chapitre 4**

  Dans ce chapitre, nous étudions tout d'abord l'identification de paramètres pour

le problème de jet stationnaire. Des résultats numériques sont donnés dans le cas de données synthétiques (générées par le modèle) ainsi que pour des données expérimentales. Nous montrons ainsi la capacité de notre approche à identifier les différents paramètres inconnus du modèle, ainsi que l'influence du bruit de mesure et du terme de régularisation sur la prévision de formation de la surface.

- **Chapitre 5**

  Ce chapitre présente des résultats numériques pour la prévision de formation de la surface dans le cas stationnaire, avec une étude de sensibilité par rapport aux différents bruits de mesure. Nous comparons ensuite différentes modifications de la fonction coût lorsque plusieurs jeux de données sont disponibles. Nous pouvons alors considérer le bruit comme un paramètre du modèle et nous présentons des résultats numériques de l'identification. Le chapitre se termine par un cas d'utilisation de mauvaises estimations initiales des paramètres.

- **Chapitre 6**

  Dans ce chapitre, nous étudions l'identification de paramètres du modèle et présentons les résultats numériques correspondants dans le cas d'un jet d'eau instationnaire, qui se déplace avec une vitesse fixe ou variable. Nous donnons des résultats portant sur la prévision de reconstruction de la surface géométrique dans les cas de données artificielles et expérimentales. Dans le cas d'un jet qui se déplace de façon uniforme, nous présentons des résultats numériques pour l'identification simultanée de tous les paramètres du modèle.

- **Chapitre 7**

  Ce chapitre présente une étude de sensitivité par rapport au bruit de mesure pour le modèle d'usinage par jet d'eau abrasif dans le cas d'un jet se déplaçant de façon uniforme. Nous étudions l'influence du bruit, et différentes approches sont proposées pour améliorer l'efficacité de la méthode et la précision de la surface prédite. L'avantage de pouvoir identifier le bruit comme un paramètre

supplémentaire du modèle nous permet d'améliorer la prévision de l'évolution de la surface usinée.

- **Conclusions**

  Enfin, ce travail se termine par des conlusions et perspectives en rapport avec l'identification de paramètres pour un modèle d'usinage par jet d'eau abrasif.

Chapter 2

Introduction (english)

Caused by the growth of application needs and interest both in science and industry, the area of inverse problems has undergone increasing interest and expansion in the last years. A significant effort has been observed more strongly than before on nonlinear problems due to high motivation of their application in manufacturing.

In order to better understand what an inverse problem is, we first note that a direct problem is usually a problem of modeling of some physical process or phenomena. The aim of solving a direct problem is to discover a function which describes this physical process at any point and any time in the predefined domain. It is required to know in advance all the involved physically relevant parameters such as coefficients or sources characteristics to solve the direct problem and predict the evolution of the described system from knowledge of its given state and governing physical laws. In the inverse problem, the goal is to find the unknown functions or parameters used in the formulation of a direct problem from the observations or input data. And very often these parameters are totally unknown or inaccessible and have to be identified only from experimental measurements.

The inverse problems became very popular and widely spread in the last years with the development of sophisticated numerical techniques and powerful computing capabilities. The theory and application of inverse problems is also widely used in solving applied and completely industrial problems on a level of high complexity. Different types of inverse problems can be met in almost all fields of science such as physics (quantum mechanics, acoustics), geophysics (oceanography, seismic exploration, volcanology, electrical and magnetic phenomena), medicine (X-ray and NMR tomography, tumor growth), ecology (air and water quality control, agriculture), economics and financial

mathematics.

Inverse problems of mathematical physics can be divided into a wide range of different groups depending either on fields of application or on the nature of their occurrence. One of the crucial problems in this variety of inverse problems of natural, industrial and economical phenomenas is the identification of unknown sources and model parameters by suitable comparison between the experimental observations referred to the real systems and the simulations by the mathematical models.

However, parameter identification is generally an ill-posed inverse problem [32, 43] under some considerations due to the measurement or modelling errors, even if the direct problems are well-posed. The ill-posed problem is a problem which either does not have or has many solutions, or the solution is not stable (small perturbations in the input data may lead to serious discrepancies in the solutions). Exactly the last point of instability brings the biggest difficulties in solving ill-posed inverse problems.

This kind of problems can be partially overcome by using regularization methods [3, 45, 46], studied by many authors [44, 17, 29, 19], and parameters identification could be reformulated in a stable case as a minimization problem with a data mismatch and a regularization term.

One of the industrial problems which is not widely studied by the inverse problems theory and application, and where it can be efficiently used is the Abrasive waterjet (AWJ) machining. It relates to the class of mechanical material removal machining processes, where the workpiece is subject to some specific mechanical force caused by impact of abrasive particles. The AWJ machining process is performed by a high pressured water powered by a pump through the small orifice in the cutting head, where it is generated to a high speed water jet. In the mixing chamber the abrasive particles are entrained by creared vacuum inside the system. As a results, the highly accelerated mixture of abrasives and water generates the aggressive jet plume, which hits the target surface and generates a footprint. The illustration and notations of the abrasive waterjet machine with the example of milled trenches are presented on Figure 2.1.

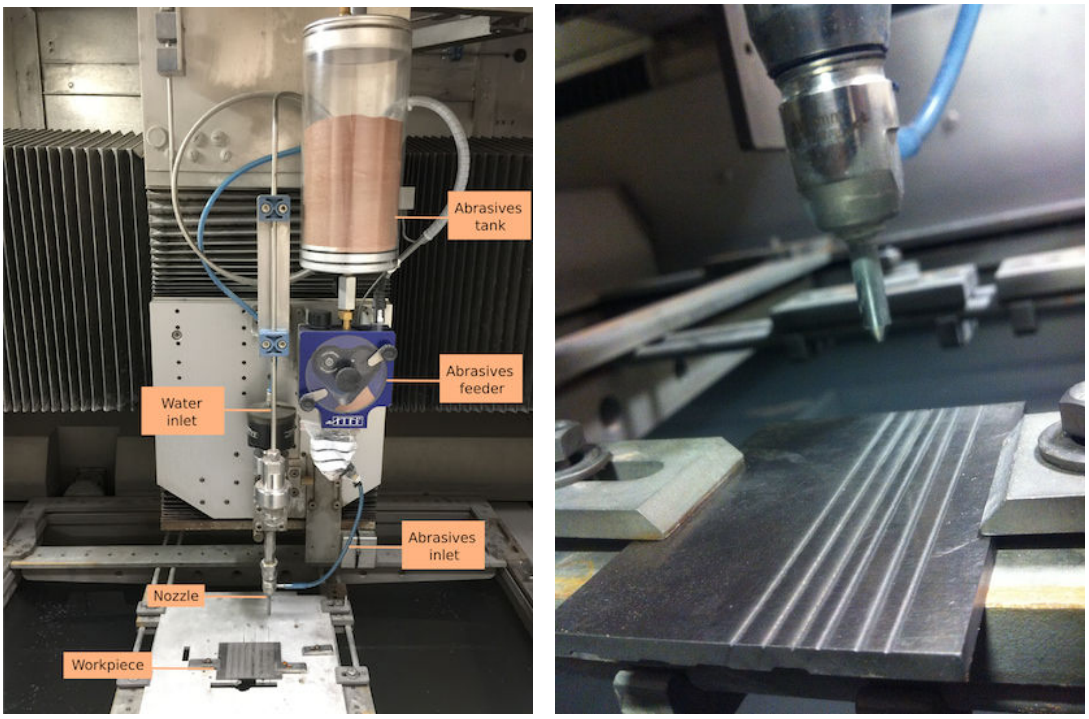

(a) microwaterjet machine

(b) Example of milled trenches

Figure 2.1: Abrasive microwaterjet machine system (left) and examples of the milled trenches (right).

AWJ machining is a fast-growing non-conventional and versatile material removal technology that is capable to process almost any material regardless its properties and keeping manufacturing costs low. AWJ is widely used in the machining of materials such as steel, titanium, aluminium, glass, polycrystalline diamond, ceramics, silicon carbide and different composites [41, 7, 47] for various fields of application as medical technologies, electronics and automotive industry, jewelry and glass industry or even aircraft and aerospace manufacturing needs. Thus, one of the main advantages of the AWJ machining is the ability to proceed with the brittle/ultra-hard/non-homogenous materials. Other important advantages are (i) the involvement of very low cutting forces, hence reducing the risk to damage the workpiece; (ii) no heat affected zones and low machining temperatures; (iii) complex 3D shapes can be obtained due to the facilities of the AWJ machine according to required surface geometry.

Moreover, AWJ machining can be used in a variety of applications such as cutting, milling, drilling, polishing etc. One of the main challenges is the accurate shape and depth-controlled milling, which plays an important role in the Abrasive waterjet milling (AWJM) technology. Since there are a lot of independent process parameters as pump pressure, jet feed speed, abrasive mass flow, stand-off distance, nozzle diameter, it turns out difficult to predict the surface shape formation. Thus, a forecast of the surface profile geometry by a mathematical model is essential to bypass most of issues.

This work is a part of European Marie Curie Initial Training Network project STEEP covering the research in field of energy beam processing. This involves both academia and industry in the multi-disciplinary scientific training, research and interaction between the full partners from universities and industrial and private companies:

- University of Nottingham
- Université Nice Sophia Antipolis
- University of Birmingham
- Friedrich-Alexander University of Erlangen-Nürnberg

- Katholieke Universiteit Leuven
- Swiss Federal Laboratories for Materials Science and Technology
- Fundaciòn TEKNIKER
- WATERjet AG
- TESCAN a.s.
- ZEEKO Ltd

The main objective of this work is to present the mathematical method to identify unknown parameters of the proposed generic Abrasive Waterjet milling (AWJM) model which was previously described and studied in [6, 31, 14, 36] and was developed according to the industrial needs for waterjet footprints prediction. Assuming that model parameters and source terms are known, one can find the shape of the milled trench profile. In this context this is the direct problem that in our case involves a nonlinear PDE. The identification of the model parameters is the inverse problem and some studies of other linear AWJM inverse problems were previously presented in [13].

Our goal is to determine the model parameters inaccessible from the experiments to predict the surface construction before performing the manufacturing simulations. Following this requirement we base our work on the variational approach to find a function or parameters the use of which will minimize the objective functional. The problem may be reformulated as a minimization problem, that in its turn can be presented as search of the minimum of a cost function measuring the difference between the process observations and the corresponding model solution.

If the inverse problem is ill-posed, the solution of the inverse problem is not unique or as it was mentioned above not stable. In this case, the cost function may have several local minima. Commonly, these problems can partially be overcome by the use of regularization techniques. It is necessary to consider some additional information which can help to stabilize the problem.

The numerical minimization of the objective functional can be realized by using various methods, but the most common minimization techniques are gradient descent algorithms which are iterative processes converging to the minimum. We use the one, based on the limited memory Broyden-Fletcher-Goldfarb-Shanno (L-BFGS) algorithm [21, 35, 48] underlying the N2QN1 minimization package from the INRIA MODULOPT library [22].

The gradient vector is obtained numerically using the automatic differentiation (AD) software TAPENADE developed by the Tropics team at INRIA Sophia-Antipolis [27], which can be interpreted as the Lagrange multiplier of the model equations in terms of adjoint problem [38, 34]. It was chosen as the most effective technique with low computational costs. In order to compute the gradients, it automatically generates the tangent and/or adjoint code from the direct source code. AD adjoint code consists of two general steps: a forward mode running the original source code and remembering certain information, and a backward mode, which uses this information to compute the derivatives.

This thesis is organized as follows:

- **Chapter 3**

  This chapter consists of representation of the proposed mathematical model describing the AWJM process and its physical properties. Further, the general principles of the inverse problems and their application to given problem is explained, leading to a variational approach based on corresponding Lagrangian, which is used to obtain the gradient of the cost function. Then the short description of gradient descent algorithms, which are used for the minimization problem, and related adjoint approach are presented. The special case of stationary waterjet problem is studied separately in the next section to demonstrate the proposed method. This chapter ends up with the listing of the identification algorithm.

- **Chapter 4**

  In this chapter the parameters identification starts with the case of stationary

waterjet problem. Numerical results are given for both self-generated data and averaged experimental measurements used as problem input. We demonstrate the ability to identify different unknown model parameters and influence of considered measurement errors and regularization technique on the surface formation prediction.

- **Chapter 5**

  This chapter presents the numerical results in surface geometry prediction for stationary jet problem, corresponding to the sensitivity study of the model in case of various measurement errors. Further, comparison of the use of different modifications of the cost function according to available input data and their amount is given. Next, we show the appropriate numerical results by considering the existing measurement noise as AWJM model parameter, and in the end of this chapter the case of wrong initial estimation of the model parameters is studied.

- **Chapter 6**

  In this chapter we present the model parameters identification and actual numerical results for a moving waterjet with fixed and varied feed speed. Numerical results of the surface geometry forecast are based on artificial and experimental observations. In case of evenly moving waterjet setup we give the results of the joint identification of all unknown model parameters.

- **Chapter 7**

  This chapter presents the sensitivity study of the given AWJM model in case of uniform waterjet movement, where the influence of the various measurement noise is studied and several approaches to improve the accuracy in the surface prediction are demonstrated. The opportunity to identify the measurement errors from the input data leads to sufficient improvement in the prediction of the evolution of the surface geometry.

- **Conclusions**

Finally, this work ends up in this chapter with some conclusions and outcomes about the possibilities in the parameters identification and surface prediction for Abrasive waterjet milling model.

Chapter 3

Problem formulation and methods

Contents

3.1 Introduction

We will introduce and explain the mathematical formulation of the physical problem and will present the model, which describes the abrasive waterjet milling process and surface geometry evolution. The goal is to propose, implement and study the mechanism for the optimal model parameters identification in different cases and situations close to the real experimental conditions. We will describe several techniques used to formulate the adjoint problem and solve it numerically. Also, we will demonstrate the possibility to avoid different difficulties related to the ill-posedness of the inverse problem by the use of regularization methods.

3.2 Physical model

Fundamentally, the Abrasive Waterjet milling process (AWJM) is based on a surface evolution under the jet plume impact, whose characteristics (specific erosion rate) depend on process parameters as water pressure, mass flow and abrasive particles. During the milling process, a mixture of water and abrasive particles is pressured to ultrahigh pressure through a small orifice, forming an intense cutting stream which hits a target surface and generates the footprint (Figure 2.1).

The final form of the trench, which is described as a function $\boldsymbol{Z}(x, y, t)$, depends on the different physical parameters such as pump pressure, abrasives mass flow, velocity and waterjet nozzle diameter. These machine settings could be described and represented all together as set of model parameters u, defining the intensity of the jet impact. Separately, the forces caused by the jet may be described as erosion rate function $\boldsymbol{E}$, which includes the pressure, mass flow and particles velocity; and the scalar parameter a describes the jets nozzle radius. The etching rate function reaches its maximum in the center of the jet and decreases near its sides. The scalar parameter k describes the dependence of the erosion rate and arrises from a cosine law for the jet impact angle for brittle materials [42].

The intensity of the jets impact during the process strictly depends on the slopes of the trench. When the trench become more deep, the efficiency of the impact decreases due to the verticality of the slopes. This may be described by the cosine of the angle between the jet stream and the normal $\vec{n}$ to the target surface and given by $\frac{1}{\sqrt{1+|\nabla \boldsymbol{Z}|^2}}$.

The impact angle of the waterjet is defined as an angle between the jet vertical axis and a tangent to the surface. For brittle materials, maximum of erosion occurs when the jet is perpendicular to the workpiece. Thus, we consider only a case when the impact occurs on the initially flat surface $\boldsymbol{Z}(x, y) = 0$ at 90° impact angle. The vertical position of the jet is fixed during the process relative to the zero-level of the workspace, and the intensity of the jet impact continuously depends on the trench depth. Other model components such as the exponent and the gradient of the surface parametrization were included to consider these influences and model the process more

precisely and believable.

The milling process perpetrated by Abrasive Waterjet machine is represented as a nonlinear partial differential equation with initial and boundary conditions. To define the problem we consider the time interval of the continuous milling process $[0, T]$ and denote by Ω a bounded domain of $\mathbb{R}^2$ where the process takes place.

The proposed Abrasive Waterjet Milling model introduced in [6, 31, 14] then is given by:

$$\frac{\partial \boldsymbol{Z}}{\partial t} = -\frac{\boldsymbol{E}(x,y)\mathrm{e}^{a\boldsymbol{Z}}}{\left(1+|\nabla \boldsymbol{Z}|^2\right)^{k/2}} \qquad \text{in } \Omega \times [0,T], \tag{3.1}$$

with initial and boundary conditions:

$$\begin{cases} \boldsymbol{Z}(x,y,t) = 0 & \text{on} \quad \partial\Omega, \\ \boldsymbol{Z}(x,y,t) = \boldsymbol{Z}_0 & \text{at} \quad t = 0, \end{cases}$$

where

- $(x, y) \in \Omega$
- $\boldsymbol{Z}(x, y, t) \in \mathbb{H}_0^1(\Omega, \mathbb{R}^+)$ is the parametrization of the surface,
- $a, k \in \mathbb{R}^+$ are the model parameters,
- $\boldsymbol{E}(x, y) \in \mathbb{L}^2(\Omega)$ is the Etching rate function which is also model parameter.

This model is well suitable for the abrasive waterjet milling process. It characterizes the process of the trench surface formation by the jet impact on the workpiece and is suitable for various jet feed speeds regardless of the target material properties. The etching rate function $\boldsymbol{E}$, which describes most of the machine settings, has strong influence on the surface formation. The simple example of the surface geometries obtained with the use of various Etching rate functions can be observed on Figure 3.1. For this demonstration scalar parameters $a = 0.7$ and $k = 3$ were chosen without connection to real experimental settings.

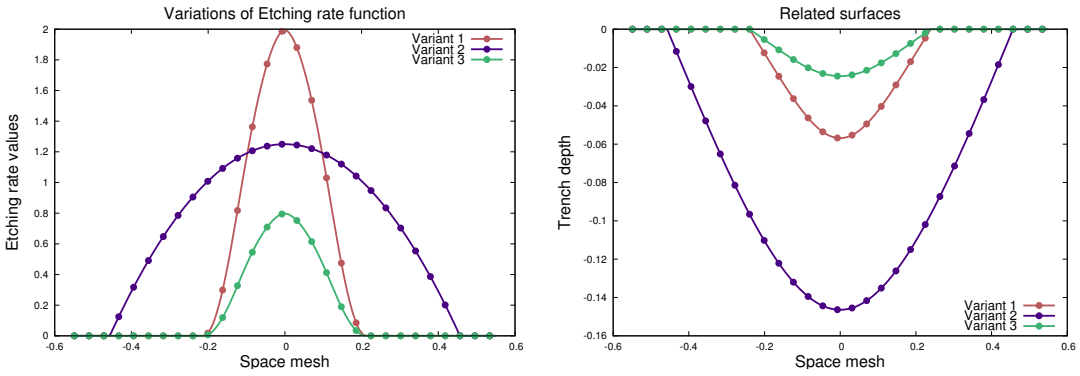

(a) Used Etching rate functions

(b) Related surfaces

Figure 3.1: Example of the model outcome by the use of different Etching rate functions.

Further the AWJM model could be rewritten in general as:

$$\frac{\partial \boldsymbol{Z}}{\partial t} = \boldsymbol{F}(\boldsymbol{Z}, \nabla \boldsymbol{Z}, x, y, t, \boldsymbol{u}), \tag{3.2}$$

where $\boldsymbol{u} = \{a, k, \boldsymbol{E}\}$ is a set of model parameters.

During the reporting time period jet moves in the y-direction with permanent or varied feed speed what determines the final structure of the surface. The use of the experimental data allows us to calibrate the Etching rate function $\boldsymbol{E}$ using the experimental data, because of its dependency on physical properties of the workpiece material and waterjet machine parameters, described above.

Schematically AWJM process and jet footprint at some time moment $t \in [0, T]$ could be presented as on the Figures 3.2(a) and 3.2(b).

3.3 Inverse Problem

The modeling of the surface geometry knowing the values of model parameters is the general direct problem. The prediction of the surface formation from some estimations of the paramteres is also the direct problem, when we are interested in results of the model by assuming some properties in advance. Lack of knowledge about the model parameters initiates another problems called inverse problems.

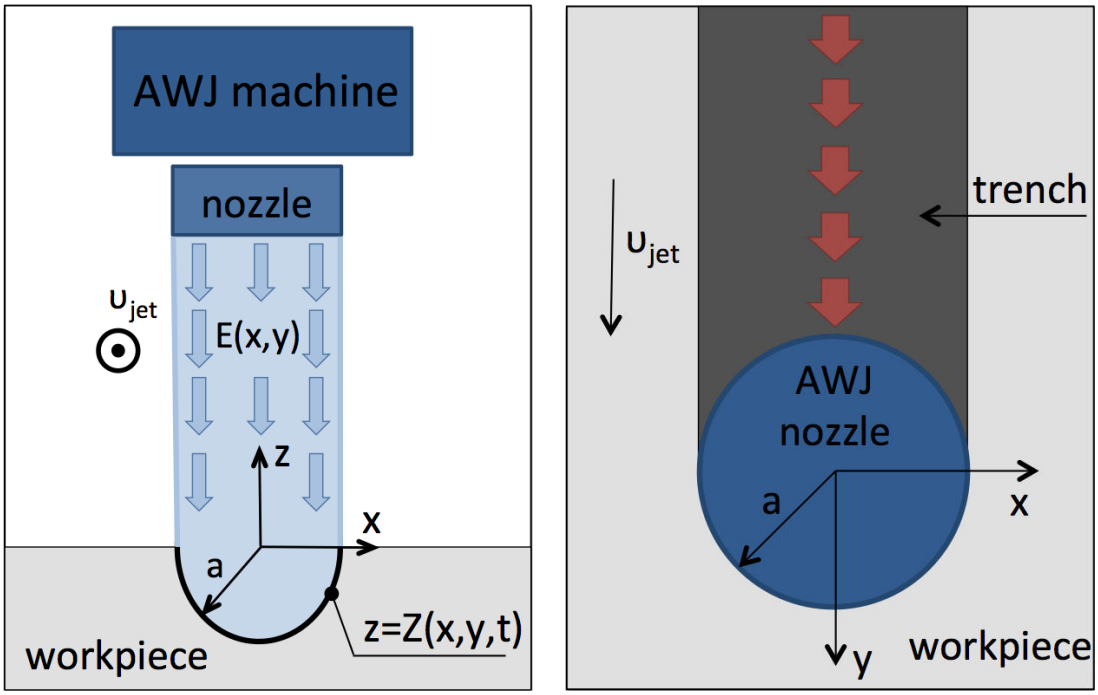

(a) Cross section (b) Top view

Figure 3.2: Schematic of the AWJM process and jet footprint.

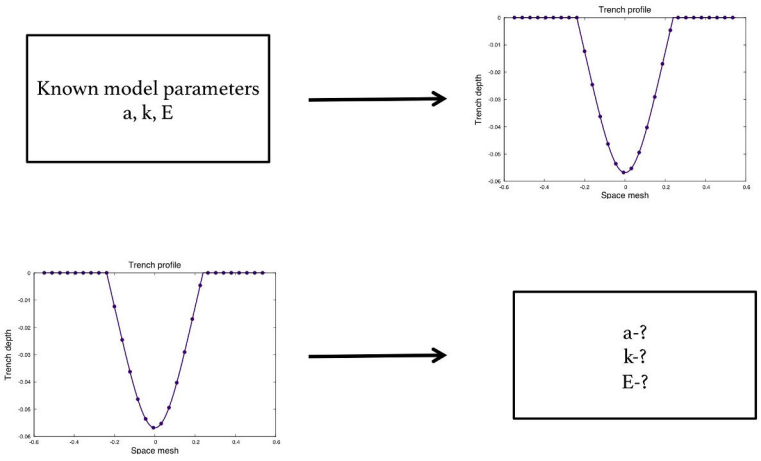

Figure 3.3: Demonstration of direct (top) and inverse problems (bottom).

Schematically, it can be demonstrated as on Figure 3.3.

Suppose, that it is necessary to describe the behavior of some physical process. The primary sources of information, based on which it is possible to study the process, are observations and experiments. If in the observations only behavioral traits can be fixed, the experiments allow to actively influence on the process and register the respond of the system by changing the input properties. Mainly, in the inverse problems it is necessary to determine the reasons of system behavior or effects.

Inverse problems are very active research fields in the applied science, with a fast growing interest among the industry. Wide range of their application includes signal and image processing [12, 51, 10], invsere scattering [16, 39], tomography [37], inverse heat conduction problems [20, 11], parameters identification [8, 28] and many more classes [19, 18, 23, 30, 9, 49]. One reason for this is that conditions and properties of the physical processes underlying the actual results are usually not known.

Following David Colton, Heinz Engl et al. [15], inverse problems are concerned with determining causes for a desired or an observed effect or calibrating the parameters of a mathematical model to reproduce observations.

Generally, parameters identification problems face with the reconstruction and estimation of unknown functions or physical effects appearing in systems of differential equations as coefficients, terms, boundary or initial conditions. This type of problems requires some information about the process behavior or experimental observations needed to estimate the unknowns which should be used in order to correctly forecast the process outcome.

The abrasive waterjet techniques are used to produce extremely small elements in the macro or micro areas for medical technologies, electronics and automotive industry, jewelry and glass industry or even aircraft and aerospace manufacturing needs. In all these directions, the main interest comes from the desire to predict the evolution of the surface and to improve the quality of manufacturing. This milling process is difficult to control due to the aggressive nature and high pressure of the jet. The use of the correct simulation predictions of the surface formation can provide good opportunity

to adjust the machining parameters in advance instead of performing the numerous of expensive experiments to calibrate them.

In fact, we are interested in the identification of unknown model parameters, the use of which in direct milling model will lead to the desired accuracy in the surface reconstruction or further forecast. A common feature of most parameter identification problems is their ill-posedness.

In the sense of Hadamard's postulates [24, 25], a mathematical problem is well-posed if it satisfies the required conditions:

- A solution exists.
- The solution is unique.
- The solution's behavior changes continuously with the problem parameters.

When one of these three conditions is not fulfilled, the problem called ill-posed. It means that these problems might not have a strict solution either it can be not unique or not depend continuously on the input data. Nevertheless such problems are very common in engineering, physics and other areas and have to be studied and solved numerically. In general, the most often case for applied problem is the failure to comply the third condition.

Particularly in our problem, the dependencies on input model parameters and sensitivity of the AWJM model on measurement or model errors effort the instability in the surface prediction. Numerical simulation of the direct problem clearly demonstrates that the use of different Etching rate functions leads to simillar trench profiles (Figure 3.4).

These simple implementations of the direct problem with difference only in one model parameter $\boldsymbol{E}$ and fixed others demonstrates the absence of continuous dependence on the input data in a stable way. Moreover, if the stability condition is ignored, the numerical solution of the inverse problem is problematic even if the input data is perfect.

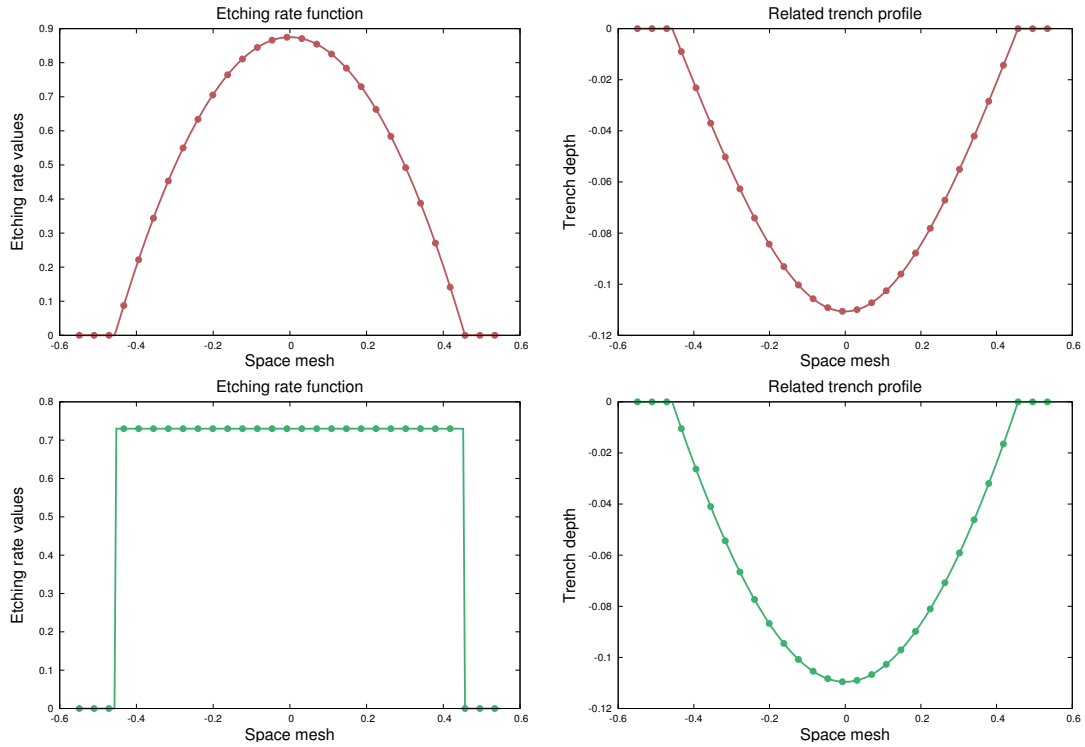

Figure 3.4: Example of ill-posedness of the problem. Different types of Etching rate function lead to simillar trench surfaces.

Detailed study and observation of these effects provides us the opportunity to see which are there possibilities to reconstruct the required shape of the trench regardless of the input data.

3.4 Variational approach

The main objective of the variational approach is to find the function or parameters, the use of which will make the functional attain its the minimum or maximum under the given constraints. Typically, the constrained variational problem focuses on the minimization of the cost function that measures the distance between the given observation and the predicted state.

Thus, the constrained variational problem is to find $\boldsymbol{u}^*$ which minimizes the following cost function:

$$\boldsymbol{J}(\boldsymbol{u}) = \frac{1}{2}\int\limits_{\Omega} \|\boldsymbol{Z}(x,y,T) - \boldsymbol{Z}_{\text{exp}}(x,y)\|^2 \mathrm{d}x\mathrm{d}y, \tag{3.3}$$

where the $\boldsymbol{Z}_{\text{exp}}$ are the experimental measurements and $\boldsymbol{Z}$ is the predicted state of the direct problem.

It means that in order to identify the optimal AWJM model parameters $\boldsymbol{u} = \{a, k, \boldsymbol{E}\}$ we formulate the minimization problem:

$$\boldsymbol{J}(\boldsymbol{u}^*) = \inf_{\boldsymbol{u}} \boldsymbol{J}(\boldsymbol{u}). \tag{3.4}$$

The goal is to identify the set of parameters acceptable for manufacturing process, the use of which in direct model will fit the input data, in other words will lead to correct surface reconstruction.

If the direct or even inverse problem are ill-posed, the solution of the inverse problem may not be unique. In this case, the cost function $\boldsymbol{J}$ may have several local minimums, and the minimization process may stop not only at the seddle point. It is possible to partially overcome this problem by introducing the regularization techniques. It is

necessary to consider additional information which can help to regularize the problem. The additional Tikhonov's regularization term can be added to the cost function.

The corresponding cost function $\boldsymbol{J}(\boldsymbol{u})$ takes next form, where the regularization term generally can be chosen as difference with available background information about the model parameters:

$$\boldsymbol{J}(\boldsymbol{u}) = \frac{1}{2}\int\limits_{\Omega} \|\boldsymbol{Z}(x,y,T) - \boldsymbol{Z}_{\text{exp}}(x,y)\|^2 \mathrm{d}x\mathrm{d}y + \frac{\alpha}{2}\|\boldsymbol{u} - \boldsymbol{u}_{\text{b}}\|^2, \tag{3.5}$$

subject to the model constraint that $\boldsymbol{Z}$ is the solution of the direct problem, obtained with input set of parameters $\boldsymbol{u} \in \mathbb{R}^+ \times \mathbb{R}^+ \times \mathbb{L}^2(\Omega, \mathbb{R}^+)$. We also assume that required observations are available at every moment of each studied problem.

In the expression above (3.5) $\boldsymbol{Z}_{\text{exp}}$ are the process observations, by $\boldsymbol{u}_{\text{b}}$ we denote an a priori estimation of the set of AWJM model parameters $\boldsymbol{u}$, and $\alpha > 0$ is the Tikhonov regularization coefficient [45]. Due to the available information or special conditions, regularization term can be changed in order to better satisfy the problem requirements. As this is the additional information, it can be varied to any applicable form. In case of inaccessible background information about the Etching rate function, we propose following variant with a gradient of unknown function $\boldsymbol{E}$:

$$\boldsymbol{J}(\boldsymbol{u}) = \frac{1}{2}\int\limits_{\Omega} \|\boldsymbol{Z}(x,y,T) - \boldsymbol{Z}_{\text{exp}}(x,y)\|^2 \mathrm{d}x\mathrm{d}y + \frac{\alpha}{2}\int\limits_{\Omega} \|\nabla \boldsymbol{E}\|^2 \mathrm{d}x\mathrm{d}y. \tag{3.6}$$

In terms of ill-posedness, regularization part plays an important role to overcome the instability and reduce the inaccuracy in the identification of acceptable unknown parameters. The type of the regularization term can be changed accordingly to exact problem and requirements (e.g. when the sought unknown function has to be smooth, one can use the gradient of it as a regularization part).

3.5 Minimization process

One of the steps in the identification process is the minimization of the cost function, which measures the difference between experimental measurements and estimated state of the system. The numerical minimization of the cost function can be performed by using various methods such as conjugate gradient methods or Newton/quasi-Newton algorithms.

From the first order Taylor expansion of the cost function $\boldsymbol{J}(\boldsymbol{u})$ for any two iterations $\boldsymbol{u}_j$ and $\boldsymbol{u}_{j+1}$ we have:

$$\begin{aligned}\boldsymbol{J}(\boldsymbol{u}_{j+1}) = \boldsymbol{J}(\boldsymbol{u}_j) + \nabla\boldsymbol{J}(\boldsymbol{u}_j)(\boldsymbol{u}_{j+1} - \boldsymbol{u}_j) + \\ +\frac{1}{2}(\boldsymbol{u}_{j+1} - \boldsymbol{u}_j)^T\nabla^2\boldsymbol{J}(\boldsymbol{u}_j)(\boldsymbol{u}_{j+1} - \boldsymbol{u}_j).\end{aligned} \tag{3.7}$$

The objective function $\boldsymbol{J}(\boldsymbol{u})$ is minimized by solving $\nabla\boldsymbol{J}(\boldsymbol{u}) = 0$. Thus, it is necessary to solve:

$$\nabla\boldsymbol{J}(\boldsymbol{u}_j) + \nabla^2\boldsymbol{J}(\boldsymbol{u}_j)(\boldsymbol{u}_{j+1} - \boldsymbol{u}_j) = 0,$$

which yields

$$\boldsymbol{u}_{j+1} = \boldsymbol{u}_j - \boldsymbol{H}(\boldsymbol{u}_j)^{-1}\nabla\boldsymbol{J}(\boldsymbol{u}_j),$$

where $\boldsymbol{H}(\boldsymbol{u}_j) = \nabla^2\boldsymbol{J}(\boldsymbol{u}_j)$ is the Hessian of the cost function $\boldsymbol{J}$ at iteration j.

The classical Newton's type of minimization algorithms uses $\boldsymbol{d}_j = -\boldsymbol{H}(\boldsymbol{u}_j)^{-1}\nabla\boldsymbol{J}(\boldsymbol{u}_j)$ as the direction of descent.

The descent step-size $\boldsymbol{\rho}_j$ is calculated so that:

$$\boldsymbol{J}(\boldsymbol{u}_j + \boldsymbol{\rho}_j\boldsymbol{d}_j) \leq \boldsymbol{J}(\boldsymbol{u}_j),$$

ensuring that $\boldsymbol{d}_j$ is a descent direction:

$$\boldsymbol{d}_j^T\nabla\boldsymbol{J}(\boldsymbol{u}_j) < 0.$$

The computation of $\boldsymbol{\rho}_j$ is called line search, and this is usually an inner iterative loop. It might be exact or inexact to adapt the stepsize by involving additional criterias [2, 50].

Starting from the initial given position $\boldsymbol{u}_0$ (which is defined from some background estimation $\boldsymbol{u}_0 = \boldsymbol{u}_\mathrm{b}$), one has to compute the cost function $\boldsymbol{J}(\boldsymbol{u}_j)$ on each iteration and its gradient $\nabla \boldsymbol{J}(\boldsymbol{u}_j)$ to shift to the next discretized step and update the solution:

$$\boldsymbol{u}_{j+1} = \boldsymbol{u}_j + \boldsymbol{\rho}_j \boldsymbol{d}_j.$$

However, the method requires computing the Hessian matrix at each iteration and this is not always feasible due to the size of the problem. The sufficiently difficult minimization of the functional is realized in fact with the use of quasi-Newton type methods, which differ from the Newton type methods by the involvement of the approximations of the inverse of the Hessian functional at the current point and does not demand the direct computation of it.

The most common minimization techniques are gradient descent algorithms which are iterative processes converging to the minimum. The minimization of the cost function could be realized in such a way, where the descent step is computed by quasi-Newton's type algorithms. In quasi-Newton's type algorithms the Hessian does not need to be computed and inverted, but it can be replaced by a symmetric positive approximation ($\boldsymbol{Q}_j$) to $\boldsymbol{H}^{-1}$. It is much less expensive than implementation of the real Hessian. Due to the limitation in memory facilities we use the limited-memory algorithm which keeps only fixed amount information about the previous steps needed to update the approximation of the Hessian.

Particularly, the inverse limited-memory minimization algorithm L-BFGS (Broyden-Fletcher-Goldfarb-Shanno) [35] implemented in N2QN1 minimization algorithm from "MODULOPT" library [22] was chosen as the most efficient and suitable. It is a BFGS algorithm in the quasi-Newton's family methods which uses an approximation of the inverse Hessian, but with limited amount of memory: it stores only m last values of $\boldsymbol{u}_j$ and $\nabla \boldsymbol{J}(\boldsymbol{u}_j)$. During the minimization of the functional, it construct the approximation of the inverse Hessian. The update formulas for L-BFGS algorithm are presented

in [21]. In practice, the minimization stops before the convergence in order to reduce the calculation costs.

3.6 Adjoint model

Very often the size and complexity of the studied problem is such that it can not likely be solved directly without reducing the amount of unknowns or simplifying the initial model. An important point is to clearly express the dependence between the variations of input data and the related variations of the cost function. In the other words, it requires the computation of the gradient of cost function with respect to the unknown parameters. A possible way to implement it is to perturb each component of the set of unknowns separately and to integrate the model equations for each perturbation. However, the numerical cost of this method is so high that it is almost impossible to apply it for any practical problems.

From the other side, there is another approach, which allow to avoid several difficulties in implementation, called the adjoint approach. In general, the optimal control theory [34] provides the possibility to observe how the behavior of the process can be controlled by changing the input process parameters. The adjoint technique gives the efficient way to numerically compute the local gradient of a cost function included a set of arguments. This gradient is further used to perform the descent minimization algorithm to minimize the differnce to observations.

Depending on each particular case and size of the problem in our work, the time consumption can be reduced in dozens or hundreds of times, needless to say about the computational costs required for numerical implementation. In the simple case of stationary jet, based on self-generated input data (see Chapter 4), the use of adjoint technique allows to decrease the clear computational time (not including the preparation of each case and collecting the results) from 4 hours to approximately 1 minute. Furthermore, in case of more complex problem of moving waterjet (notably with varied jet's feed speed), the gain in time is proportionally substantial.

The minimization problem (3.4) could be regarded as an optimal control problem, and the approach based on Lagrangian multipliers could be used to get the solution of it [38, 34]. The solution of the optimal control problem can therefore be regarded as the search of critical "points" of the Lagrangian functional $\boldsymbol{L}(\boldsymbol{u}, \boldsymbol{Z}, \boldsymbol{P})$ associated to the constrained minimization, that we introduce as following:

$$\boldsymbol{L}(\boldsymbol{u}, \boldsymbol{Z}, \boldsymbol{P}) = \boldsymbol{J}(\boldsymbol{u}) + \int_0^T \int_\Omega \boldsymbol{P}(t, x, y) \left(\frac{\partial \boldsymbol{Z}}{\partial t} - \boldsymbol{F}(\boldsymbol{Z}, t, \boldsymbol{u}) \right) \mathrm{d}x\mathrm{d}y\mathrm{d}t, \tag{3.8}$$

where $\boldsymbol{P}$ is called Lagrangian multiplier or adjoint variable associated to the constraint that $\boldsymbol{Z}$ is a solution of (3.1) from the same space $\mathbb{H}_0^1(\Omega)$.

The minimum of cost function $\boldsymbol{J}(\boldsymbol{u})$ is given by the saddle point of functional $\boldsymbol{L}$ when all partial derivatives of the Lagrangian are equal to zero.

We get the optimal system:

$$\frac{\partial \boldsymbol{L}}{\partial \boldsymbol{P}} = 0, \tag{3.9}$$

$$\frac{\partial \boldsymbol{L}}{\partial \boldsymbol{Z}} = 0, \tag{3.10}$$

$$\frac{\partial \boldsymbol{L}}{\partial \boldsymbol{u}} = 0. \tag{3.11}$$

Considering the general foundations of Lagrange parameters theory [43] we have that $\frac{\partial \boldsymbol{Z}}{\partial t} = \boldsymbol{F}(\boldsymbol{Z}, t, \boldsymbol{u})$, where $\boldsymbol{Z}$ is solution of the direct model from the (3.9):

$$\frac{\partial \boldsymbol{L}}{\partial \boldsymbol{P}} = \frac{\partial \boldsymbol{Z}}{\partial t} - \boldsymbol{F}(\boldsymbol{Z}, t, \boldsymbol{u}) = 0 \tag{3.12}$$

Adjoint equation can be found from the expression (3.10), where $\boldsymbol{P}$ has to be a solution. To calculate the derivative of the Lagrangian with respect to $\boldsymbol{Z}$, we can more efficiently use the integration by parts, which will give us the derivative of $\boldsymbol{P}$ with respect to t instead of the derivative of $\boldsymbol{Z}$ with respect to t.

Consequently, nulling of the derivative of $\boldsymbol{L}$ with respect to $\boldsymbol{Z}$ leads to the following adjoint problem:

$$\frac{\partial \boldsymbol{P}}{\partial t} = -\left(\frac{\partial \boldsymbol{F}}{\partial \boldsymbol{Z}} \right)^{\mathrm{T}} \boldsymbol{P} + (\boldsymbol{Z} - \boldsymbol{Z}_{\mathrm{exp}})\, \boldsymbol{\delta}(t - T), \tag{3.13}$$

$$\begin{cases} \boldsymbol{P}(x, y, T) = 0, \\ \boldsymbol{P}(x, y, t) \mid_{\partial\Omega} = 0. \end{cases}$$

And finally the derivative of $\boldsymbol{L}$ with respect to $\boldsymbol{u}$ (3.11) gives us the gradient of the cost function from the initial adjoint state $\boldsymbol{P}(0)$, in conditions that $\boldsymbol{Z}$ is a solution of the direct problem (3.2), related to the set of AWJM model parameters $\boldsymbol{u}$. This gives us the following expression for the variational derivative of the cost function:

$$\nabla \boldsymbol{J}(\boldsymbol{u}) = \frac{\partial \boldsymbol{L}}{\partial \boldsymbol{u}} = -\int_0^T \boldsymbol{P}(t, x, y) \frac{\partial \boldsymbol{F}}{\partial \boldsymbol{u}} (\boldsymbol{Z}, t, \boldsymbol{u}) \, \mathrm{d}t + \alpha(\boldsymbol{u} - \boldsymbol{u}_b), \tag{3.14}$$

To solve the minimization problem and find an optimal solution $\boldsymbol{u}^*$ the gradient of the cost function $\nabla \boldsymbol{J}(\boldsymbol{u})$ is needed for the iterative gradient descent minimization algorithms from the quasi-Newton family.

Thus, to calculate the gradient of the cost function, one has to integrate the adjoint model backward in time with final conditions $\boldsymbol{P}(x, y, T) = 0$ to obtain initial $\boldsymbol{P}(0)$. The interest to use the adjoint method to calculate the gradient of $\boldsymbol{J}$ is the comparatively low numerical cost needed when the number of unknowns is large. The usage of the adjoint method requires only one adjoint model integration, while the standard implementation of the evolution of the gradient will ask a number of model integrations equal to the size of the control space.

3.7 Case of stationary jet

Considering the special case of stationary waterjet problem, when there is no movement in the y-direction and $\frac{\partial Z}{\partial t} = 0$, the general AWJM model (3.1) could be reduced to:

$$\frac{\partial \boldsymbol{Z}}{\partial t} = -\frac{\boldsymbol{E}(x) \mathrm{e}^{a\boldsymbol{Z}}}{\left(1 + \left(\frac{\partial \boldsymbol{Z}}{\partial x}\right)^2\right)^{k/2}} \qquad \text{in } \Omega \times [0, T], \tag{3.15}$$

with initial and boundary conditions:

$$\begin{cases} \boldsymbol{Z}(x) = 0 & \text{on} \quad \partial\Omega_1, \\ \boldsymbol{Z}(x) = 0 & \text{at} \quad t = 0. \end{cases}$$

In this case we define a symmetric domain $\Omega_1 = \{x : x \in [-x_1; x_1]\}$, where x_1 always depends on the actual experimental parameters or measurements, due to the changes of the jets radius. Thereby, the cost function takes next form with the unknown Etching rate function $\boldsymbol{E}$:

$$\boldsymbol{J}(\boldsymbol{E}) = \frac{1}{2}\int\limits_{\Omega_1} \|\boldsymbol{Z}(x,T) - \boldsymbol{Z}_{\exp}(x)\|^2 \mathrm{d}x + \frac{\alpha}{2}\int\limits_{\Omega_1} \|\nabla \boldsymbol{E}\|^2 \mathrm{d}x. \tag{3.16}$$

Actually, the right side of announced model (3.15) can written as $\boldsymbol{F}(\boldsymbol{Z}, \boldsymbol{Z}_x, t, \boldsymbol{E})$ and Lagrangian functional $\boldsymbol{L}(\boldsymbol{E}, \boldsymbol{Z}, \boldsymbol{P})$ associated to the constrained minimization takes following form:

$$\boldsymbol{L}(\boldsymbol{E}, \boldsymbol{Z}, \boldsymbol{P}) = \boldsymbol{J}(\boldsymbol{E}) + \int\limits_0^T \int\limits_\Omega \boldsymbol{P}(t,x) \left(\frac{\partial \boldsymbol{Z}}{\partial t} - \boldsymbol{F}(\boldsymbol{Z}, \boldsymbol{Z}_x, t, \boldsymbol{E}) \right) \mathrm{d}x\mathrm{d}t. \tag{3.17}$$

By nulling of the derivative of $\boldsymbol{L}$ with respect to $\boldsymbol{Z}$ we obtain the following adjoint problem for the linearized 2D case:

$$\begin{aligned} \frac{\partial \boldsymbol{P}(x,t)}{\partial t} = &- \left(\frac{\partial \boldsymbol{F}}{\partial \boldsymbol{Z}} \right)^{\mathrm{T}} \boldsymbol{P}(x,t) + \left(\frac{\partial \boldsymbol{F}}{\partial \boldsymbol{Z}_x} \right)^{\mathrm{T}} \frac{\partial \boldsymbol{P}}{\partial x} + \\ &+ \left(\frac{\partial}{\partial x} \frac{\partial \boldsymbol{F}}{\partial \boldsymbol{Z}_x} \right)^{\mathrm{T}} \boldsymbol{P}(x,t) + (\boldsymbol{Z} - \boldsymbol{Z}_{\exp})\, \boldsymbol{\delta}(t - T), \end{aligned} \tag{3.18}$$

$$\begin{cases} \boldsymbol{P}(x,T) = 0, \\ \boldsymbol{P}(x,t) \mid_{\partial\Omega_1} = 0. \end{cases}$$

It is necessary to consider not the continuous but the discrete system to figure out numerically with the optimal problem and to find its solution. Indeed we need to minimize the discrete cost function what requires the gradient of the discrete cost

function. Commonly the discretized adjoint statement comes from the discretized forms of the Lagrangian and its discrete derivatives.

In the particular linearized case for the stationary waterjet it is possible to discretize the direct problem (3.19), for example with a central difference scheme, and get the adjoint problem of it (3.22), to obtain the gradient of the cost function and to perform the minimization problem after. But again, the very important key point that the gradient of the cost function has to be derived from the adjoint of the discrete direct problem, not by the discretization of the continious problem (3.18).

3.7.1 Discretization of stationary problem

In the assumption that domain Ω_1 is discretized into N points of regular grid with a step Δx, and the time interval $[0, T]$ into M points with a step Δt, the numerical scheme for the direct model is given as:

$$Z_i^{m+1} = Z_i^m - \Delta t \frac{e^{aZ_i^m} E_i}{\left(1 + \left(\frac{Z_{i+1}^m - Z_{i-1}^m}{2\Delta x}\right)^2\right)^{k/2}}, \tag{3.19}$$

with initial and boundary conditions:

$$\begin{cases} Z_1^m = Z_N^m = 0 \qquad \forall m \in [1, M]\,, \\ Z_i^1 = 0 \qquad \forall i \in [1, N]\,. \end{cases}$$

The discrete cost function is:

$$J(E) = \frac{1}{2} \sum_{i=2}^{N-1} \left(Z_i^M - Z_{exp_i}\right)^2 + \frac{\alpha}{2} \sum_{i=2}^{N-1} \left(\frac{E_{i+1} - E_{i-1}}{2\Delta x}\right)^2, \tag{3.20}$$

where $E = (E_1, ..., E_N)$ and $\left(Z_i^M\right)$ is the solution of the direct problem (3.19) at final time M.

Associated disctrete analog of the Lagrangian is obtained by the switching to the summation from the integration and by discretizing it in the defined domain Ω_1:

$$L(E,Z,P) = \frac{1}{2}\sum_{i=2}^{N-1}\left(Z_i^M - Z_{exp_i}\right)^2 + \frac{\alpha}{2}\sum_{i=2}^{N-1}\left(\frac{E_{i+1}-E_{i-1}}{2\Delta x}\right)^2 + \\ + \sum_{i=2}^{N-1}\sum_{m=1}^{M-1} P_i^m \left(\frac{Z_i^{m+1}-Z_i^m}{\Delta t} - \frac{e^{aZ_i^m}E_i}{\left(1+\left(\frac{Z_{i+1}^m - Z_{i-1}^m}{2\Delta x}\right)^2\right)^{k/2}}\right). \tag{3.21}$$

The numerical scheme for the adjoint problem, which comes from the derivative of the Lagrangian with respect to the Z, is solved backwards and for $i = 2, \ldots, N-1$ could be written as:

$$P_i^{m-1} = P_i^m - \Delta t P_i^m \frac{a e^{aZ_i^m}E_i}{\left(1+\left(\frac{Z_{i+1}^m - Z_{i-1}^m}{2\Delta x}\right)^2\right)^{k/2}} + \\ + \left(1-\delta_i^2\right)\Delta t P_{i-1}^m \frac{k e^{aZ_{i-1}^m}E_{i-1}}{\left(1+\left(\frac{Z_i^m - Z_{i-2}^m}{2\Delta x}\right)^2\right)^{k/2+1}} \frac{Z_i^m - Z_{i-2}^m}{4\Delta x^2} - \\ - \left(1-\delta_i^{N-1}\right)\Delta t P_{i+1}^m \frac{k e^{aZ_{i+1}^m}E_{i+1}}{\left(1+\left(\frac{Z_{i+2}^m - Z_i^m}{2\Delta x}\right)^2\right)^{k/2+1}} \frac{Z_{i+2}^m - Z_i^m}{4\Delta x^2} + \\ + \delta_m^M \sum_{i=2}^{N-1}\left(Z_i^M - Z_{exp_i}\right), \tag{3.22}$$

where δ_m^M is the Kronecker's delta and with initial and boundary conditions:

$$\begin{cases} P_1^m = P_N^m = 0 \qquad \forall m \in [1, M], \\ P_i^M = 0 \qquad \forall i \in [1, N]. \end{cases}$$

Further, the gradient of the discrete cost function with respect to the unknown model parameter Etching rate function E_i at some point $i = 3, \ldots, N-2$ could be found using the following expression:

$$\frac{\partial J}{\partial E_i} = \Delta x \sum_{m=1}^{M-1} \Delta t P_i^m \frac{e^{aZ_i^m}}{\left(1+\left(\frac{Z_{i+1}^m - Z_{i-1}^m}{2\Delta x}\right)^2\right)^{k/2}} + \alpha \frac{(2E_i - E_{i+2} - E_{i-2})}{4\Delta x^2}. \tag{3.23}$$

For $i = 1, 2$ this expression transforms to:

$$\frac{\partial J}{\partial E_i} = \delta_i^2 \Delta x \sum_{m=1}^{M-1} \Delta t P_i^m \frac{e^{aZ_i^m}}{\left(1 + \left(\frac{Z_{i+1}^m - Z_{i-1}^m}{2\Delta x}\right)^2\right)^{k/2}} + \alpha \frac{(E_i - E_{i+2})}{4\Delta x^2}, \tag{3.24}$$

and for $i = N - 1, N$:

$$\frac{\partial J}{\partial E_i} = \delta_i^{N-1} \Delta x \sum_{m=1}^{M-1} \Delta t P_i^m \frac{e^{aZ_i^m}}{\left(1 + \left(\frac{Z_{i+1}^m - Z_{i-1}^m}{2\Delta x}\right)^2\right)^{k/2}} + \alpha \frac{(E_i - E_{i-2})}{4\Delta x^2}. \tag{3.25}$$

In general case (3.1) it leads to enormous complication and moreover possible inability to execute it manually. To implement it more efficiently and gain the time and resource facilities we involve the automatic differentiation software (i.e. TAPENADE) which is based on the techniques described above and provides the gradient of the discretized cost function from the discrete realization of the direct problem. Once the gradient is computed we can solve the minimization problem (3.4) using it. After that suitable and optimal values of the model parameters can be found from only the trench experimental measurements.

3.8 Identification algorithm

In manufacturing, the numerical prediction of the surface formation is based on a good estimation of the model parameters which will be used to simulate the evolution of the system. This estimation could be done with the use of the available observation of the physical experiments done with appropriate machining tools.

The identification process consists of the search of unknown values of required model parameters to be used for correct surface geometry prediction from only the experimental observation used as input. The implementation of this process involves several steps and techniques. Thus the identification algorithm is then the following:

- Numerical implementation of the direct problem accordingly to the predefined domain $\Omega \times [0, T]$.

- Specification of the unknwon AWJM model parameters $\boldsymbol{u}$, which need to be identified.
- Formulation of the cost function and minimization problem related to the parameters $\boldsymbol{u}$.
- Calculation of the discrete gradient of the cost function with respect to $\boldsymbol{u}$ via the discrete analog of the adjoint state by use of TAPENADE software package.
- Selection of the available experimental observations to be used in the cost function and as only input in the identification process.
- Calculation of the model parameters via minimizing the functional $\boldsymbol{J}(\boldsymbol{u})$ with N2QN1 minimizer from the "MODULOPT" library based on gradient descent L-BFGS method.
- Analysis and comparison of obtained results and adjustment of the regularization term to improve accuracy in surface prediction and to achieve required properties of unknowns and applicability in the manufacturing.

Finally, the evolution of the surface geometry can be predicted by the use of the obtained correct model parameters.

Chapter 4

Model parameters identification for stationary problem

Contents

4.1 Introduction

This chapter introduces and presents the general principles of the parameter identification used in this thesis. The main objective here is to use the linearized model corresponding to the case of steady AWJM model to demonstrate the possibility of identification of unknown model parameters to predict the required surface formation.

Simple reminder how the AWJM model works and how the surface formation depends on the input model parameters is given on Figure 4.1, where different examples of surfaces is obtained with the use of different types of Etching rate function and fixed scalar parameters $a = 0.7$ and $k = 3$.

The presented results may be devided into two parts: identification based on an artificial input data, generated manually by ourselves, and involvement of the averaged experimental observations as input.

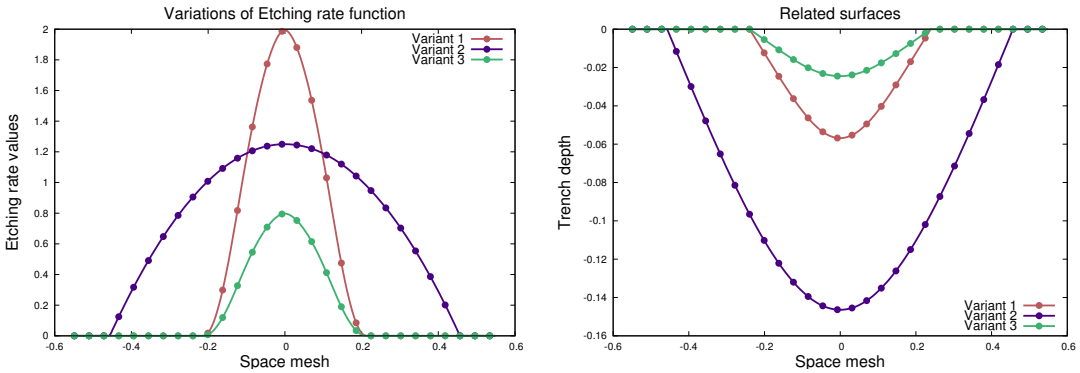

(a) Variations of Etching rate functions

(b) Corresponding surfaces

Figure 4.1: Dependence of surface formation on input model parameters.

First, the results of the identification of scalar model parameters a and k from the noisy data conditions and with the use of regularization term are presented. The correctness and capability of the proposed approach are demonstrated and proved in terms of this case. Inaccessibility of a priori information about the unknown Etching rate function makes us to change the regularization term in order to meet predefined requirements. Identification of function $\boldsymbol{E}$ is performed by the use of quasi-Newton's minimization method. Then, the use of the automatic minimization algorithm, realized in the N2QN1 package from "MODULOPT" library, demonstrates the opportunity to improve the speed and quality of the identification process in more complex cases. The limited-memory BFGS (Broyden-Fletcher-Goldfarb-Shanno) algorithm is used to perform the minimization. During the minimization of the functional it builds the approximation of the inverse Hessian. In both cases the appropriate results are demonstrated. The work described in this chapter has been partially submitted for a publication and is currently under review [4].

4.2 Identification based on self-generated surface profiles

Evolution of abrasive waterjet footprint is described by the nonlinear PDE [6, 31, 14] with the set of model parameters which can not be obtained directly from an experiment

or machine settings.

In this section we consider the particular non-moving abrasive waterjet formulation. The jet strikes the initially flat surface at vertical impact angle. In this case we define a symmetric domain $\Omega_1 = \{x : x \in [-x_1; x_1]\}$, where x_1 always depends on the actual experimental parameters or measurements, due to the changes of the jets radius.

From equation (3.1) we get the AWJM model corresponding to steady problems, with initial and boundary conditions:

$$\frac{\partial \boldsymbol{Z}}{\partial t} = -\frac{\boldsymbol{E}(x)\mathrm{e}^{a\boldsymbol{Z}}}{\left(1+\boldsymbol{Z}_x{}^2\right)^{k/2}}\ , \tag{4.1}$$

$$\begin{cases} \boldsymbol{Z}\mid_{t=0} = 0, \\ \boldsymbol{Z}\mid_{\partial\Omega_1} = 0. \end{cases}$$

Let us remind that scalar parameter a describes the radius of an abrasive waterjet and scalar parameter k describes the dependence of the erosion rate. The Etching rate function $\boldsymbol{E}(x)$ represents the energy characteristics of the blast of abrasive-laden water stream.

Parameter identification problems usually bring many difficulties due to model and measurement errors. First we assume that these kind of errors $\boldsymbol{\varepsilon}_{\mathrm{exp}}$ are random variables with a Gaussian probability density function and a zero mean, normalized to the maximum depth of the trench.

We introduce the following model:

$$\frac{\partial \boldsymbol{Z}}{\partial t} = -\frac{\boldsymbol{E}(x)\mathrm{e}^{a\boldsymbol{Z}}}{\left(1+\boldsymbol{Z}_x{}^2\right)^{k/2}} + \lambda\,\boldsymbol{\varepsilon}_{\mathrm{exp}}\ , \tag{4.2}$$

where λ is the factor corresponding to the percentage of the errors. This model is also used to generate the noisy input data.

4.2.1 Identification of the parameters a and k

Identification of the scalar model parameters a and k requires the modification of the cost function:

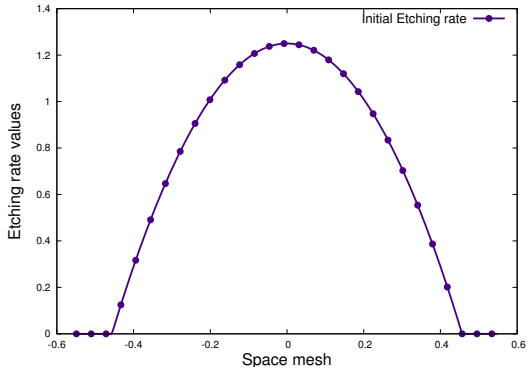

Figure 4.2: Initially used Etching rate function $\boldsymbol{E}_0$.

$$\boldsymbol{J}(\widetilde{\boldsymbol{u}}) = \frac{1}{2}\int\limits_{\Omega_1} \|\boldsymbol{Z}(x,T) - \boldsymbol{Z}_{\exp}(x)\|^2 \mathrm{d}x + \frac{\alpha}{2}\|\widetilde{\boldsymbol{u}} - \widetilde{\boldsymbol{u}}_b\|^2, \tag{4.3}$$

where the $\widetilde{\boldsymbol{u}} = (a, k)$ is a pair of unknown AWJM model parameters.

For the first numerical experiments, "pseudo-experimental" surface profiles are generated with arbitrary values of model parameters $\widetilde{\boldsymbol{u}}_b = (2, 3)$ and Etching rate function $\boldsymbol{E}_0(x)$ (Figure 4.2) defined on $\Omega_1 = \{x : x \in [-0.55; 0.55]\}$. To discretize the domain Ω_1, a regular grid of 228 points with a step $\Delta x = 0.0048$mm is used and the time period is taken as unit $t \in [0, 1]$ with $\Delta t = \frac{\Delta x^2}{4}$. In this particular case the standart Newton method is used to find the minimum of the cost function.

In order to verify the correctness of the minimization process, we demonstrate the behavior of the gradients of the cost function with respect to the parameters a and k and the evolution of the parameters approximation on the Figures 4.3(a) and 4.3(b) respectively. The continuous decreasing of the values shows us the proper work of the minimization.

First we assume the clear case when there is no measurement errors in the input data. Thus we are able to identify the required model parameters. The Figures 4.4(a) and 4.4(b) present the influence of the selection of Tikhonov regularization coefficient α on speed and precision of the identification. The reasonable choice of suitable values allows to reduce the amount of minimization iterations in 4-5 times without sufficient

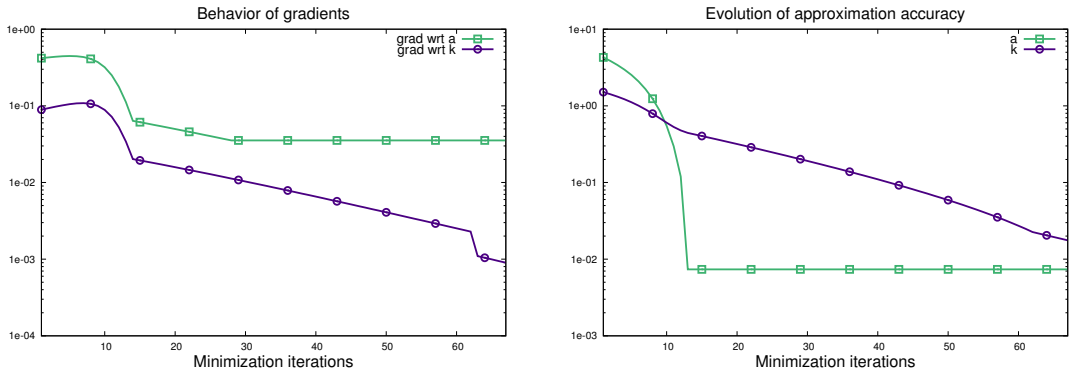

(a) Gradients

(b) Parameters approximation

Figure 4.3: Behavior of the gradients of cost function and approximation of the parameters a and k during the minimization process.

lost in accuracy even with wrong first guess.

Next, we compare the capabilities to identify the required model parameters from the noisy data. Numerical results of the identification of scalar parameters a and k are listed on Figures 4.5(a) and 4.5(b), where the cases with assumed measurement errors of levels 1%, 10% and 40% are compared with the identification based on original data. It is possible to notice that the presence of the errors in data does not influence a lot on the identification of parameter a. It is opposite with the case of parameter k, where the identification process highly depends on the quality of input data. Moreover, the identification process proceeds much slower in this case.

Further, we generated the noisy input data from the initial input surface by considering the measurement errors of different levels (10 and 30%), which is used for identification of both model parameters a and k. A Tikhonov regularization term is used with two different values of the factor α in order to demonstrate the improvement either in noisy conditions. This allows us to neutralize problems in identification process regarding the ill-posedness of the inverse problem and to accelerate the minimization process.

Results and comparisons are shown on Figure 4.6. One can find that the background estimation of the unknown model parameters accelerates the minimization process (in

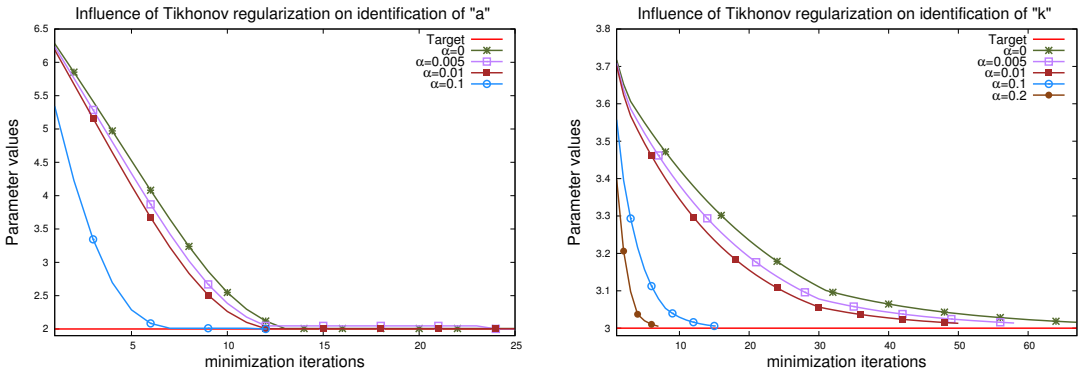

(a) parameter "a" (b) parameter "k"

Figure 4.4: Influence of the regularization term on the identification of scalar model parameters.

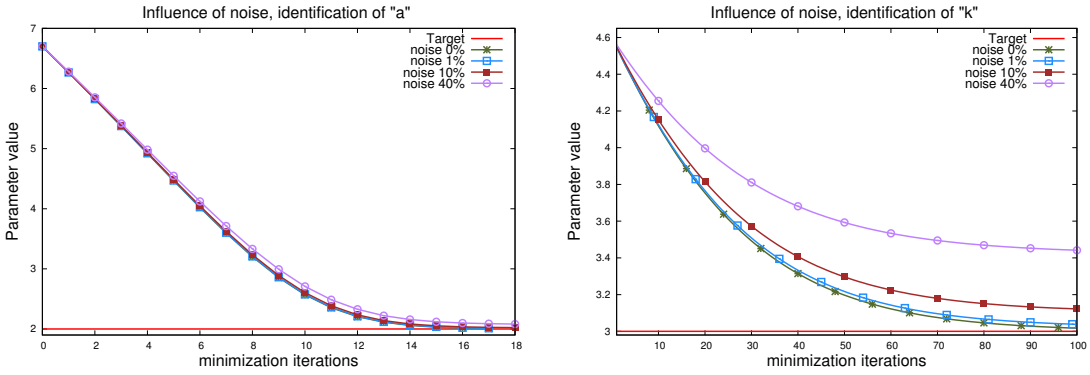

(a) parameter "a" (b) parameter "k"

Figure 4.5: Comparison of the identification capabilities of parameters a and k from the noisy data.

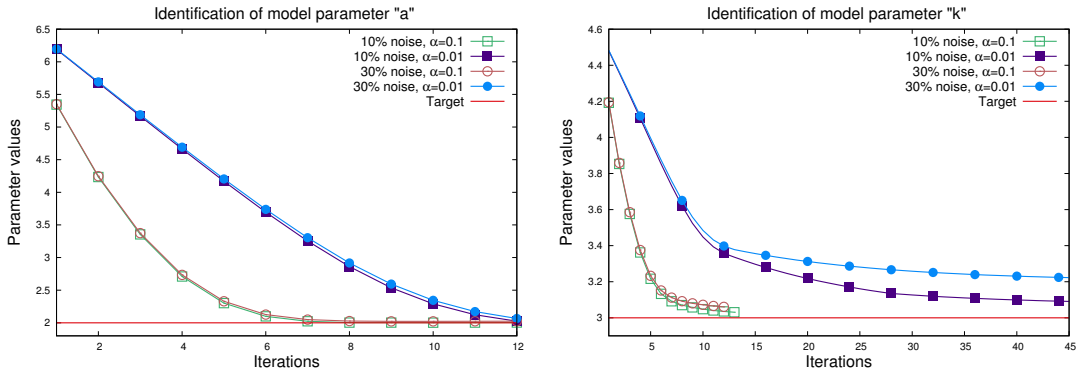

Figure 4.6: Results of the identification of model parameters a and k under the conditions of noisy data with errors equal to 10% and 30%, using different values of Tikhonov regularization coefficient.

compare with given results on Figure 4.5), but the higher the level of errors in the input data the less accurate the identification results. Even with a high level of errors, identification works properly and allows us to determine the unknowns being far enough from the first estimations. The choice of the regularization coefficient plays a very important role in the identification problem, especially dealing with noisy data.

In this particular case $\alpha = 0.1$ gives the opportunity to identify initial model parameters within 8 and 15 iterations respectively, but with the value $\alpha = 0.01$ it takes more time to approach the required precision. The use of too large or small values may prevent to identify the parameters at all.

Identified values of parameter a are always very close to the initial one and do not lead to serious mismatch in the surface prediction. From the other side, the results of the identification of parameter k from the data with 30% of the measurement errors sufficiently differ according to different values of regularization factor α. Comparison of the reconstructed and original surfaces is presented on Figure 4.7. Regardless the high level of the measurement errors, the mismatch between predicted forms of the trench and original very small, what can be explained by little influence of parameter k on surface formation.

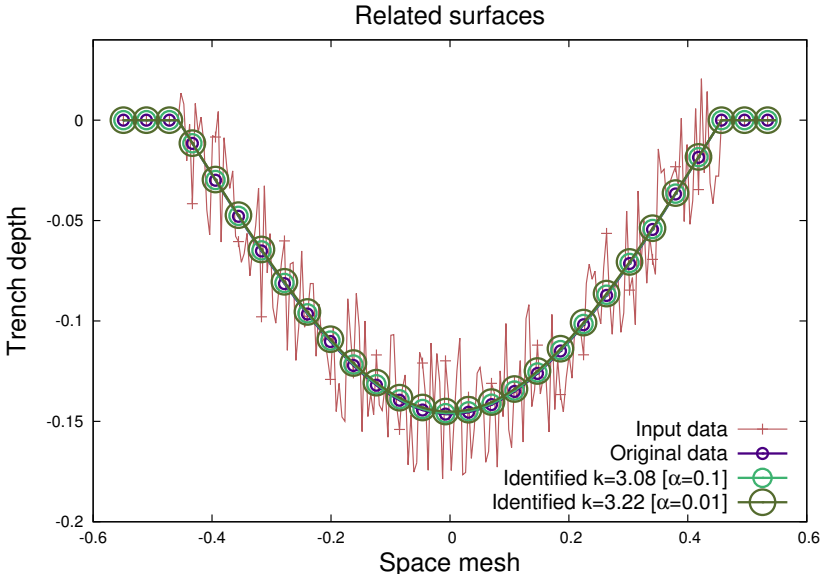

Figure 4.7: Numerical results of the trench surface reconstruction with identified values of parameter k.

4.2.2 Identification of the Etching rate function

The milling process depends on the numerous of the factors and model parameters, but the most significant effect of the impact in the material removal mechanism is caused by the Etching rate function, which can not be clearly estimated from the technical properties of the AWJ machine. This function should be determined from the experimental observations to be used for the surface prediction.

Previous chapter describes the experiments, which only includes the identification process corresponding to the cost function (3.5). The Etching rate function can be considered as the set of parameters $E = E_1, ..., E_m$ in accordance with the discretized domain $\Omega_1 = \{x : x \in [-1; 1]\}$. A regular grid of 200 points with a step $\Delta x = 0.01$mm is used. Unlike the previous case, these parameters are not independent and relate to the single function.

In principle, there is no a priori information about the behavior of unknown function $\boldsymbol{E}$, which can be obtained from real experiments and be used as background estimation.

Moreover, in order to obtain a smooth solution ($\boldsymbol{E}(x) \in \mathbb{H}^1(\Omega_1)$ instead of $\mathbb{L}^2(\Omega_1)$), we now change the cost function and regularization term in it to the one with the gradient of the Etching rate function:

$$\boldsymbol{J}(\boldsymbol{E}) = \frac{1}{2}\int\limits_{\Omega_1} \|\boldsymbol{Z}(x,T) - \boldsymbol{Z}_{\exp}(x)\|^2 \mathrm{d}x + \frac{\alpha}{2}\|\nabla \boldsymbol{E}\|^2. \tag{4.4}$$

The improvement of the results, obtained by the use of another type of regularization term can be clearly observed on Figure 4.8(a), where one of the identified Etching rate functions (named "No regularization") belongs to the not regularized case of the identification process. The form of the identified function $\boldsymbol{E}$ in this case does not satisfy the required smoothness conditions, though, leads to the good surface prediction.

Because of the absence of the general solution for the problem, we use another acceptable approach to estimate the values of regularization multiplier. For this particular problem, the closest to the optimal value of Tikhonov regularization term is chosen as $\alpha = 10^{-6}$. It is obtained by L-curve method which was first applied by Lawson and Hanson [33] and more recently by Hensen and O'Leary [26].

The main objective of this subsection is to correctly identify the Etching rate function $\boldsymbol{E}$ regardless the type of the unknown function, shape of the surface and difference between first assumption and target. Firstly, it was used to generate the surface profile in the perfect conditions without any noises or errors accounted in the model. Obtained trench surface is recorded and used as input in the identification process (Figure 4.8(b)). The other values of the model parameters $a = 2, k = 3$ are fixed. Results of the identification are presented on Figure 4.8(a). The point of identifying the Etching rate function is to focus on the most influential term of AWJM model and to demonstrate the possibility to identify various parameters. In addition, this case increases the number of unknowns in many times and lead to the complification of the problem.

The numerical results shown on Figure 4.8(a) confirm the possibility to identify unknown Etching rate function in the ideal situation even with a wrong and completely free-form first estimation. Here the total number of unknowns is 200 which is the

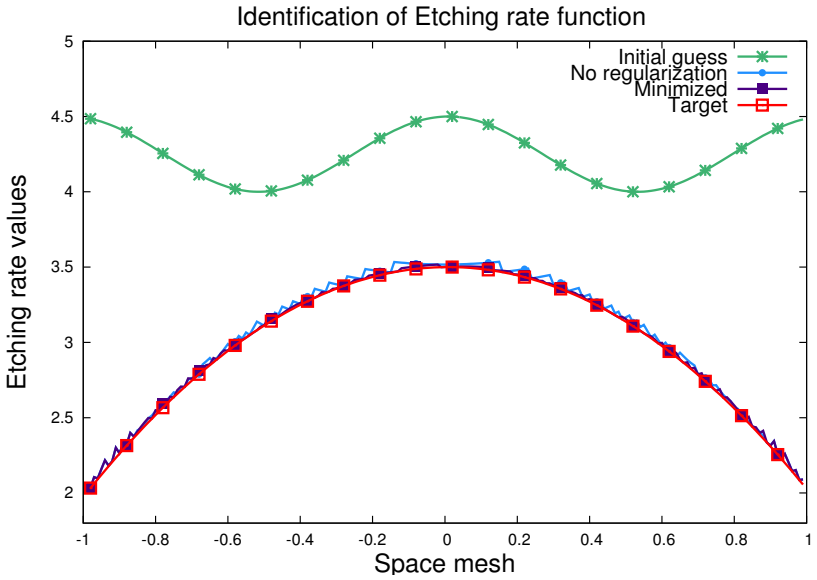

(a) Identification of Etching rate function

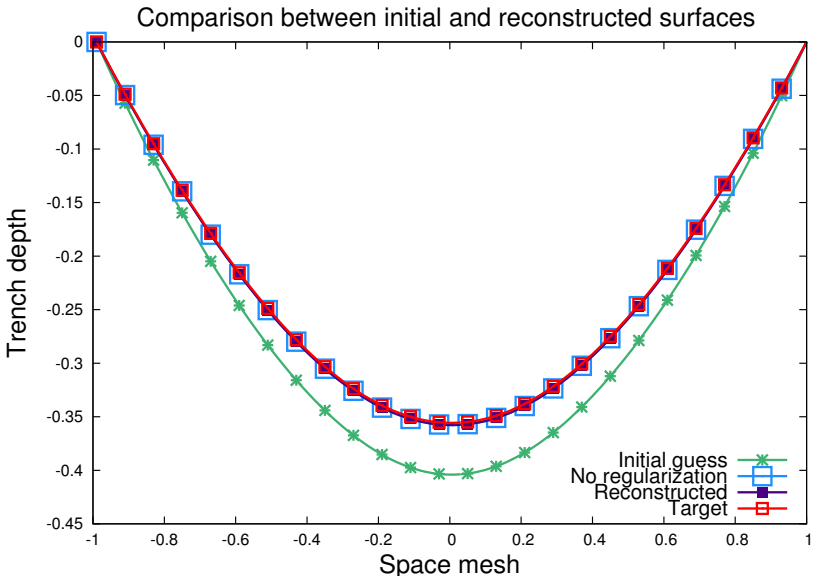

(b) Comparison of related surfaces

Figure 4.8: Results of the identification of Etching rate function E starting from different initial conditions.

number of mesh points. In case of a really wrong first assumption the minimization process stops after 19 iterations by reaching the defined precission of the gradient equal to 10^{-4}, what takes approximately 10 minutes, simply running on PC with 2.8GHz Intel Core i7 and 16GB RAM on board without parallel usage of the cores.

More interesting is the case when the Etching rate function is not so smooth and uniform, or evenmore is unknown, and the trench profile has some specialties caused ratherish by measurement errors and physical effects, undescribed by the considered AWJM model.

4.3 Real experiment measurements

The most interest of the model parameters identification and surface prediction concerns the case of real experimental observations. Usually, the available data is not perfectly smooth, noisy and has specialties. The milling process is very aggressive towards the workpiece and provokes the deformations of the surface such as so-called redeposition and damage of the material near the border of the trench. These actions are not included in the AWJM model 3.2 and we have to not consider them.

Operating with the experimental measurements, we use the averaging of the numerous of the cross-sections of the surface to obtain smooth and uniform trench profile. Furthermore, assuming that the waterjet plume is symmetrical, the trench profile is also symmetrical relative to the center. It allows us to state that identified unknowns will satisfy the requirements in some average approximation in accordance with input data.

For the simulation in this section, we use the measurements which were recorded from experiments done in collaboration with STEEP project partners. This data corresponds to the abrasive waterjet milling process with a feed speed of 2000 mm/min, and nozzle diameter of AWJ machine of 0.5 mm. This value is used as a background estimation of model parameter a. The number of mesh points in this case equals 228 with the step $\Delta x = 0.0048$ mm and Ω_1 is defined according the data by setting

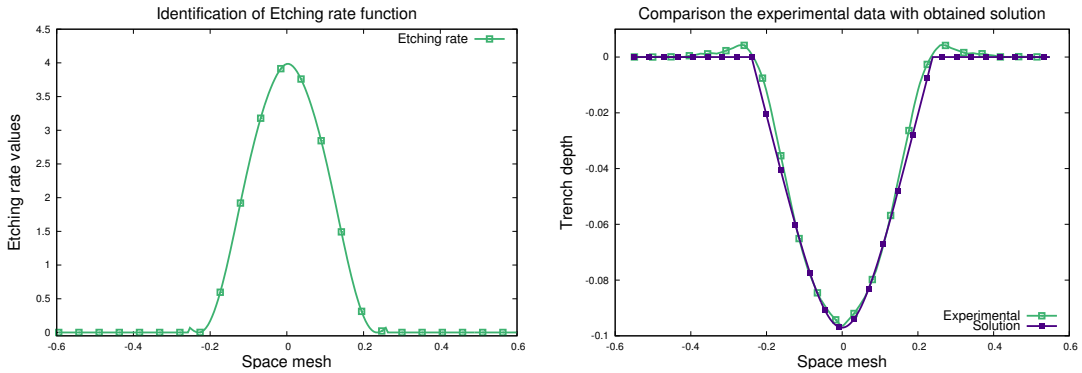

Figure 4.9: Results of the identification of Etching rate function and corresponding trench profile in comparison with experimental measurements.

$x_1 = 0.55$mm.

To identify the Etching rate function we involve the N2QN1 minimizer from the "MODULOPT" library, which bases on the L-BFGS algorithm, in order to speed up the process and improve the precision. The minimization process is realized using the regularization factor $\alpha = 10^{-5}$ that was obtained numerically by L-curve method. As it was noticed before, the physical parameters of the set up, can not provide any information about the behavior of the Etching rate function, and in lack of such knowledge we start the identification from the zero assumption $\boldsymbol{E}_0 = \mathbf{0}$.

Further, we present the results of identification of the Etching rate function which should be used in the direct AWJM model to be able to reproduce the required trench profile, and comparison of the predicted surface with the observations.

The identified Etching rate function gives us the opportunity to simulate numerically the trench profile with an accuracy in terms of L^2 norm smaller than 3% (Figure 4.9), which was estimated as ε in (4.5).

$$\varepsilon = \frac{\sqrt{\int_{\Omega_1} \left(\boldsymbol{Z}(x) - \boldsymbol{Z}_{exp}(x)\right)^2 \mathrm{d}x}}{\sqrt{\int_{\Omega_1} \left(\boldsymbol{Z}_{exp}(x)\right)^2 \mathrm{d}x}} \tag{4.5}$$

Figures 4.10(a) and 4.10(b) show respectively the behavior of the cost function and of the norm of its gradient during the minimization process. It shows that the

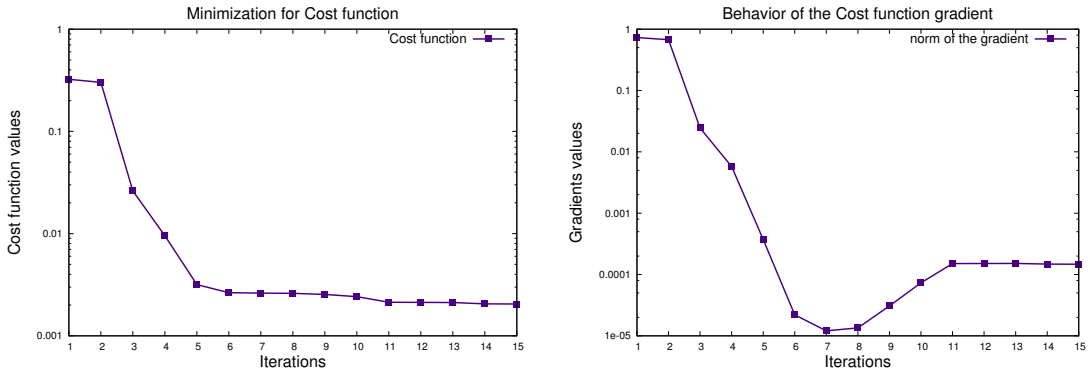

(a) Cost function

(b) Gradient of cost function

Figure 4.10: Behavior of the cost function and its gradient in the minimization process, corresponding to the real measurement data.

minimizer N2QN1 works properly. Using 15 minimization iterations, the Etching rate function is identified with the accuracy of 4×10^{-3}.

The used mathematical model (3.1) has some limitations itself and can not cover some effects on the edges of the trench which in practice is explained by redeposition of the surface material. These secondary effects appearing as the result of high power of the waterjet impact should be studied separately and are not considered in this work.

Chapter 5

Sensitivity analysis for the stationary problem

Contents

5.1 Introduction

The basic definition of sensitivity analysis can be formulated as following: The study of how uncertainty in the output of a model can be apportioned to different sources of uncertainty in the model input [40]. Sensitivity analysis in parameters identification problem of abrasive waterjet milling model is a key faeture, which can help to reduce the model calibration uncertainty, and enhance the parameters estimation efficiency.

Unlikely the well-posed problem when several different approaches for studying the sensitivity of the model could be used, we partially focuse on the variance-based method and propose an outlook on the behavior of the accuracy of the surface prediction depending on the level of errors in the data and wrong initial estimation of the independent model parameters.

In this chapter we propose the results of the identification of Etching rate function, which is one of the most valuable parameters of Abrasive Waterjet Milling model. The focus is on the capability to identify required information and accuracy of the surface formation prediction in case of noisy input data. The linearized AWJM model concerning to the steady problem is used to generate the input trench measurements.

The method using analysis of variance is used to understand how errors that arise in the measurements and modeling phase impact the final surface geometry formation. Sensitivity analysis demonstrate how the dependent variable of the process model and observation errors reflects the accuracy of parameters identification and prediction of the surface.

One of the significant roles in our problem play the measurement errors which present in the experimental data. Study the influence of it on the identification process could give us the opportunity to provide correct AWJM model parameters to reproduce required shape of the trench.

Consideration of the measurement errors as model parameter demonstrates the availability of the proposed approach to identify it a part from the other parameteres and high improvement in the trench profile prediction. This chapter jointly with the research presented in chapter 4 has led to a publication [4].

5.2 Variety of input measurements

The object of this section is to study the capacity of the approach, and to observe the possibilities to identify model parameters even with high level of measurement errors which are always present in the provided input data.

We assume the presence of the measurement errors in the input data. To generate the required amount of diverse noisy trench profiles we use given AWJM model (4.2) through which we simulate the initial smooth profiles with predefined values of $\boldsymbol{E} = \boldsymbol{E}_0, a = a_0, k = k_0$. Respectively to required conditions and according to depth of the trench, we add random uncorrelated noise corresponding to different predefined

levels up to 40% directly to the input data, to obtain new noisy inputs for the series of identification. We also assume the normal distribution of the random values in numerical implementation.

Further, we use these noisy profiles as the only input of the method and we try to identify the Etching rate function that can be acceptable by the machining settings and lead to the precise surface forecast. As this part of the study is based again on self-generated input data, we use the same numerical parameters and initial assumptions as in section 4.3. We also assume that initial Etching rate function $\boldsymbol{E}_0$ has symmetrical gaps corresponding to the edges of the trench. Abrasive waterjet has very powerfull impact over the entire impact area, what causes the form of the Etching rate function and jump of the values on the boundaries of the trench.

Initially our inverse problem is ill-posed and in order to identify the unknown parameters we use the regularization techniques. After shifting to the sensitivity analysis we worsen the situation by adding the perturbation to the input data. Thus, we have to adapt the regularization term for each particular case to make the Etching rate function smooth.

Tikhonov regularization and its variations have a very strong influence on the results of the identification process. It allows us to handle the identification results between accuracy and smoothness. We can then choose the optimal values that can be acceptable and suitable in the real experiments and lead to reconstruction of the surface profile with high precision at the same time.

The identification of the model parameter $\boldsymbol{E}$ is based only on the experimental data which include the measurement errors. We simulate such data (Figure 5.1) by adding to the initial surface profile a random Gaussian white noise with adjusting it to the trench depth and predefined error level. The initial surface profiles are generated by use of the Etching rate function named "Original" on Figures 5.2 - 5.4 and 5.6.

The goal of this part is to identify the unknown $\boldsymbol{E}$ the use of which in the AWJM model (4.1) will form the closest trench to the initial one, named "Target" on Figures 5.2 - 5.4, 5.6, 5.8.

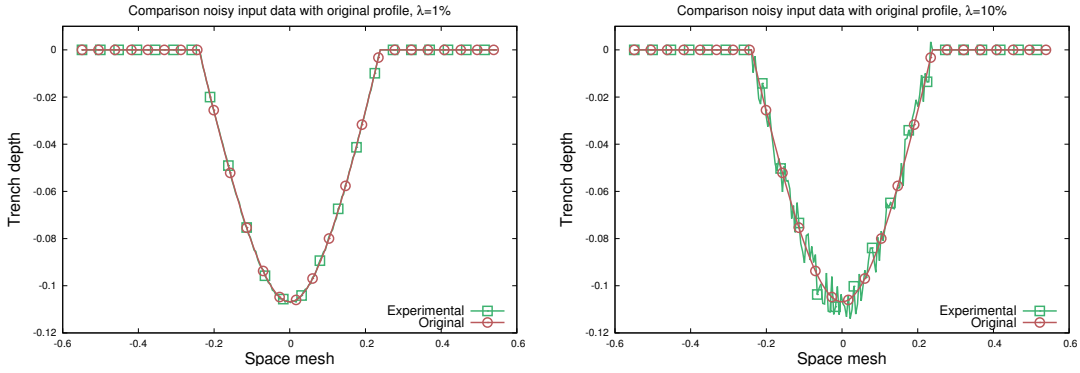

(a) Input noisy profiles, 1% and 10% of noise

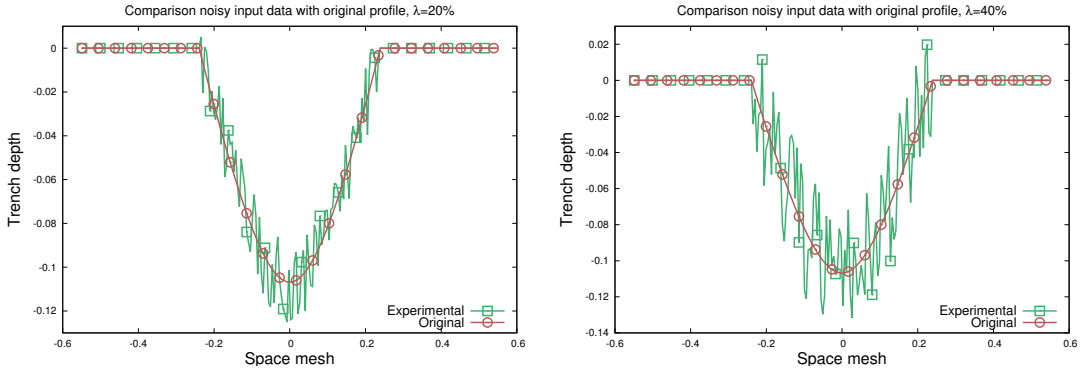

(b) Input noisy profiles, 20% and 40% of noise

Figure 5.1: Demonstration of self-simulated noisy data in compare to original profile according to different levels of considered noise.

Noise level	1%	2%	5%	10%	15%	20%	30%	40%
Precision	2.37×10^{-3}	2.24×10^{-3}	1.87×10^{-2}	2.38×10^{-2}	6.08×10^{-2}	6.14×10^{-2}	8.78×10^{-2}	0.272735

Table 5.1: Corresponding accuracy of "single input" surface prediction in dependence of the noise level.

In order to obtain a smooth solution, we again use the cost function (4.4) with the regularization term on the gradient. This will ensure the absence of high oscillations. For each special case the regularization coefficient needs to be newly estimated through a L-curve method due to the random distribution of the applied noise and its level.

The selection of the regularization parameters is very costly process and one has to guarantee the correctness for all the cases, thus we demonstrate the numerical results of the identification of Etching rate function and corresponding surface prediction for a band of considered errors with levels from 1% to 40% (Figures 5.2(a) - 5.4(b)).

Figures 5.2(a) - 5.4(b) demonstrate the results of identification of the Etching rate function $\boldsymbol{E}$ in case of noise with levels of 1% - 40%, and comparison of reproduced trenches with original profiles.

One could also notice that even with considering a very high level of errors in the measurements, it is still possible to identify the model parameter $\boldsymbol{E}$. Taking these founded values, we can then model and forecast the shape of the surface, even if the form and view of the founded function $\boldsymbol{E}$ is not perfectly matching. Summary of detailed values of accuracy in the surface prediction are listed in Table 5.1.

Analyzing the obtained numerical results, we can conclude that the surface prediction is very accurate for the case up to 10% of the measurement errors in the data. The reconstructed surfaces are almost identical to the initial one. But, one can see that the identified Etching rate functions for each case are different and not perfectly match the original. It happens due to the ill-posedness of the inverse problem and not-uniqness of the solution. Such issues are very often in the parameters identification problems and nearly inevitable. Moreover, we notice the dependence that less the applied noise to the initial input data less smooth the identified Etching rate function. It can be

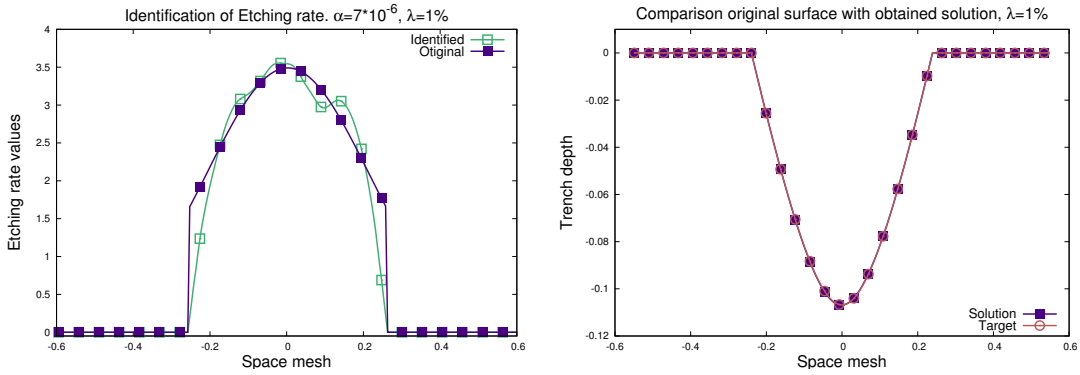

(a) Single profile, 1% of noise

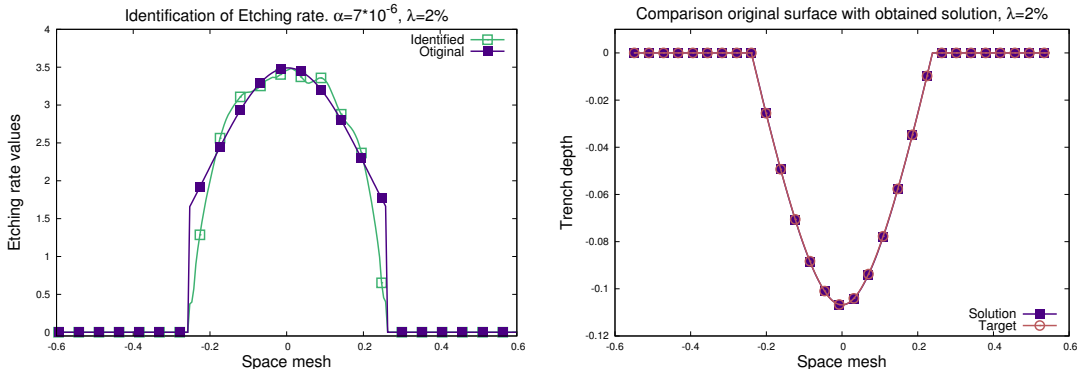

(b) Single profile, 2% of noise

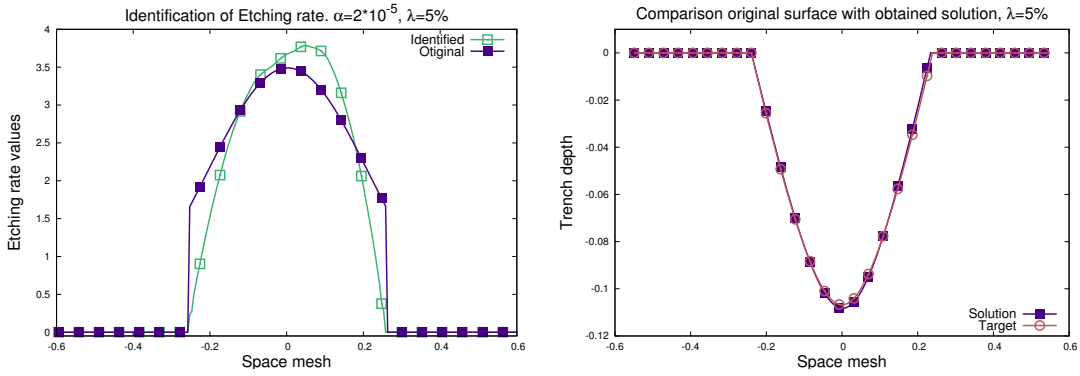

(c) Single profile, 5% of noise

Figure 5.2: Results of numerical experiments in the identification the Etching rate functions for AWJM model and reconstruction of the surface shapes based on single trench profiles for the range of measurement errors of 1% - 5%.

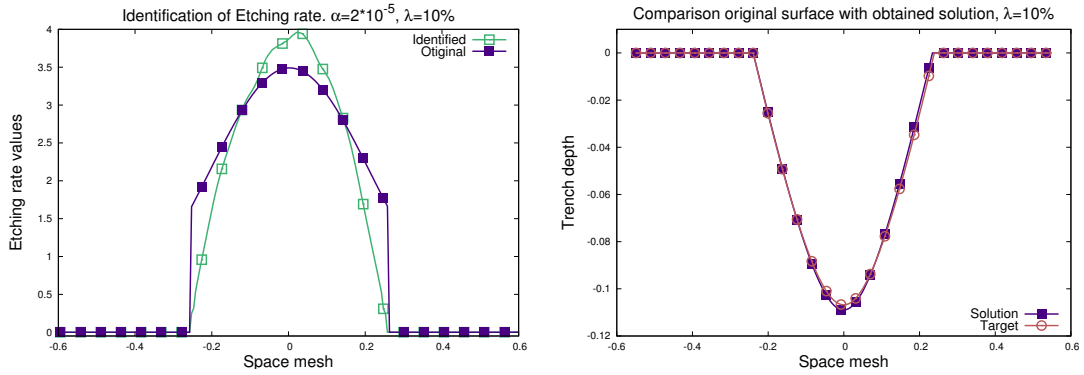

(a) Single profile, 10% of noise

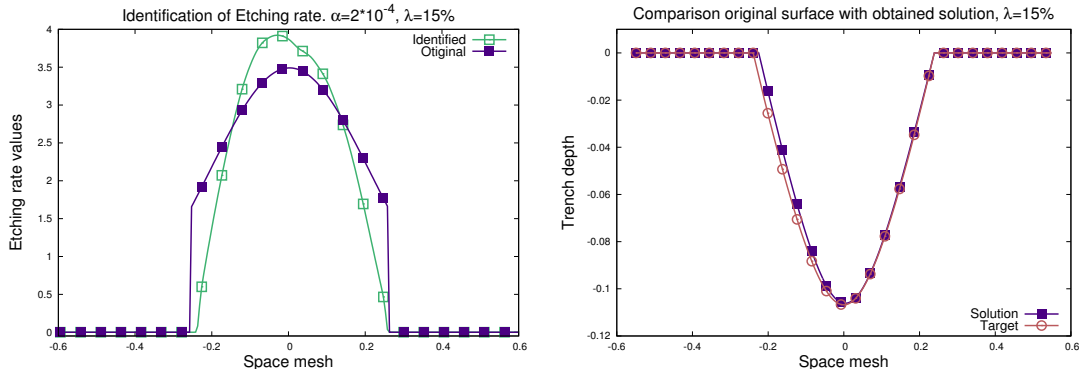

(b) Single profile, 15% of noise

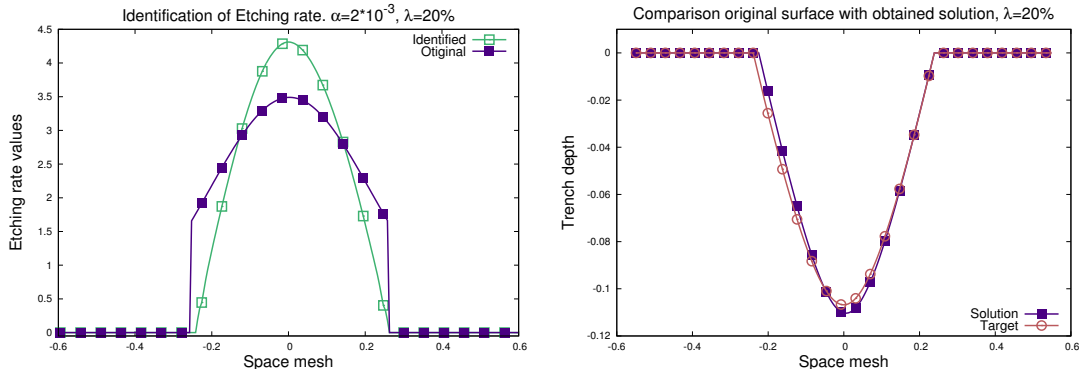

(c) Single profile, 20% of noise

Figure 5.3: Results of numerical experiments in the identification the Etching rate functions for AWJM model and reconstruction of the surface shapes based on single trench profiles for the range of measurement errors of 10% - 20%.

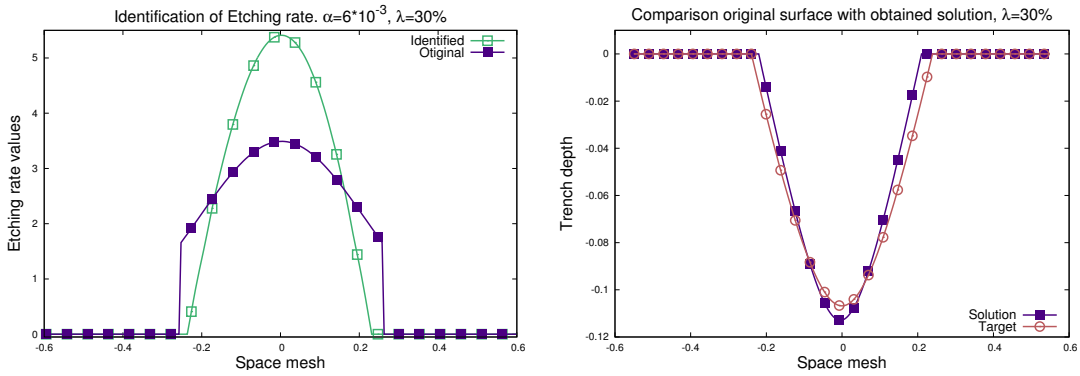

(a) Single profile, 30% of noise

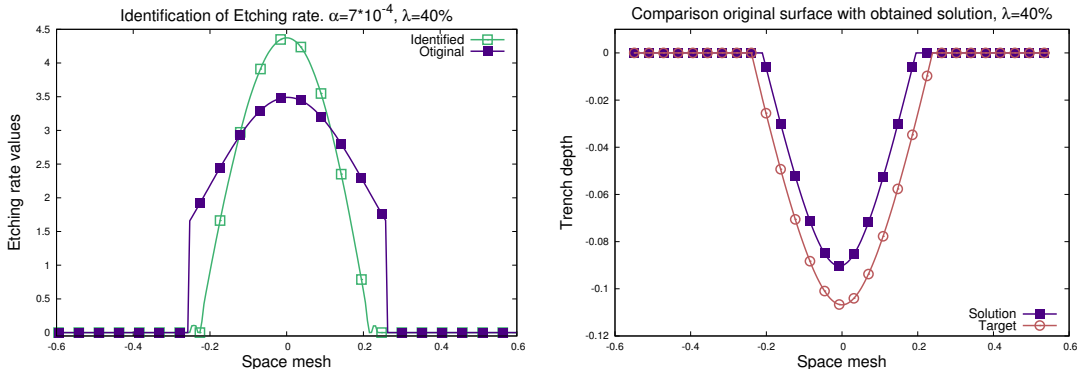

(b) Single profile, 40% of noise

Figure 5.4: Results of numerical experiments in the identification the Etching rate functions for AWJM model and reconstruction of the surface shapes based on single trench profiles for the range of measurement errors of 30% and 40%.

explained by the impact of the regularization term and not the optimal choice of the values of regularization factor α used for these simulations, but despite this inaccuracy we can achieve required results in the surface prediction even with not optimal model parameters.

The tricky point that for the small level of errors the regularization terms is always quite big and from time to time can even interfere with the minimization process.

Another predictable relation can be observed - with increase of the errors in the measurements, the mismatch between original Etching rate function and identified icreases and we lose in surface forecast accuracy. Finally, for the noise more than 20% and especially for 40% we completely far with simulated profile from the initial form and cannot figure out with high oscillations.

The question of the search of the optimal regularization parameters is open and very difficult, because very often the minimization process cannot deal with the problem and stuck in the local minimums.

These problems encouraged us to improve the identification mechanism by involvemet of the several independant trench measurements and change the cost function respectively.

5.3 Modifications of the cost function

Theoretically, the involvement of several measurements in cases of noisy input data could give the opportunity to obtain more smooth and usable surface profile by averaging of them. From the other side, the use of these measurements independently can indicate where it is necessary to level the noise. Moreover, it can help to understand which points are completely wrong and what can be reduced to improve the shape of the trench. It works very nice and properly in the ideal situation with the thousands or more of available measurements, what is nearly impossible in practise.

Assume now that we have more than one different measurements of exactly the same experiment. As it is explained above, the difference between them is only in

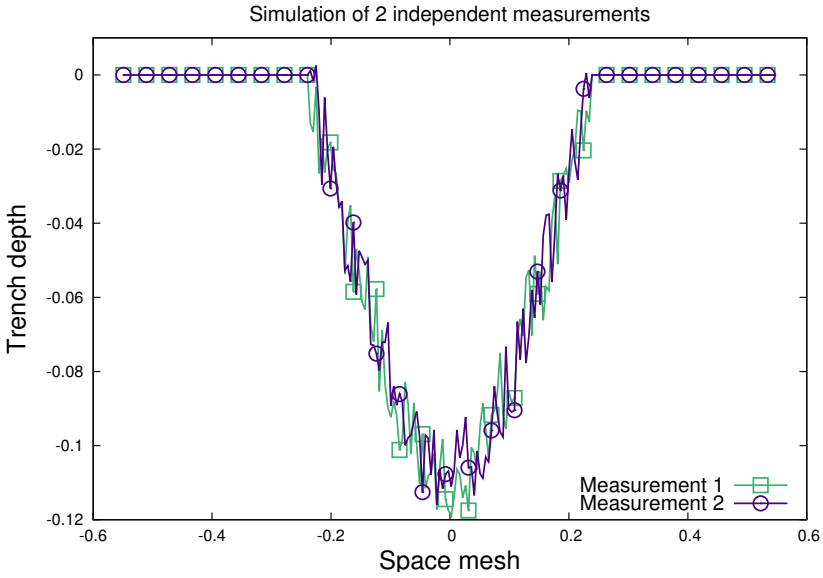

Figure 5.5: Simulation of the 2 independent trench measurements with the level of noise = 15%.

random noises that are present in measurements and influence the available input. We generate such inputs for our identification problem and comparison of two independent simulated inputs with applied noise of 15% is given on Figure 5.5 to show how they differ from each other.

Consider for this part of the work only two available observations, and in this case the cost function transforms to

$$\boldsymbol{J}(\boldsymbol{E}) = \frac{1}{4}\int\limits_{\Omega} \|\boldsymbol{Z}(x,T) - \boldsymbol{Z}_{\exp_1}(x)\|^2 \,\mathrm{d}x + \\ + \frac{1}{4}\int\limits_{\Omega} \|\boldsymbol{Z}(x,T) - \boldsymbol{Z}_{\exp_2}(x)\|^2 \,\mathrm{d}x + \frac{\alpha}{2}\|\nabla \boldsymbol{E}\|^2. \tag{5.1}$$

This form of the cost function presents the sum of separate calculations of the difference between each numerical simulation and experimental input. To keep the order of values the same, we devide each sum by half and use simillar regularization factors.

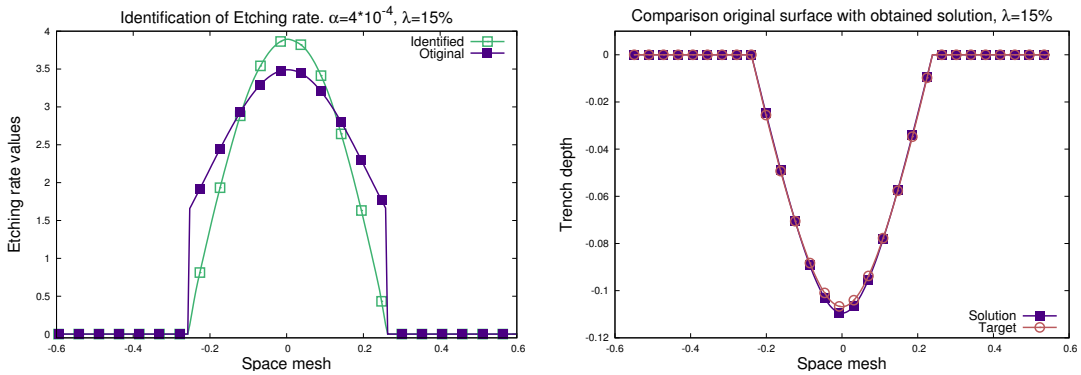

Figure 5.6: Results of numerical experiments in the identification the Etching rate functions for AWJM model and reconstruction of the surface shapes based on two different measurements of one trench profile in case the level of the measurement errors is 15%.

In case of 15% of the noise in measured profiles (Figure 5.5), it leads to the following results for the identification process (Figure 5.6).

In the previous section of the identification simulations there was a very problematic case when the noise was applied with the level of 40%. By considering actual changes in the cost function, the most significant improvement is achieved exactly for this case. The accuracy of the trench profile prediction rises up in four times. It is possible to notice that identified Etching rate function still is not perfect and differs from the original - more narrow at the bottom and top values are much higher, but it leads to good trench profile reconstruction (Figure 5.7).

Also we mark that in general the obtained results are much more precise than in the case with only one trench profile. Another improvement is the symmetry of the identified function $\boldsymbol{E}$ obtained from very unclear measurements and increased accuracy of the trench reconstruction.

More detailed information and summary is given in the Table 5.2. Mostly all the cases confirm the reasonability of proposed approach, except the case of 20% of measurement noise. It means that probably we were very lucky to obtain such accurate results basing only on one input measurement.

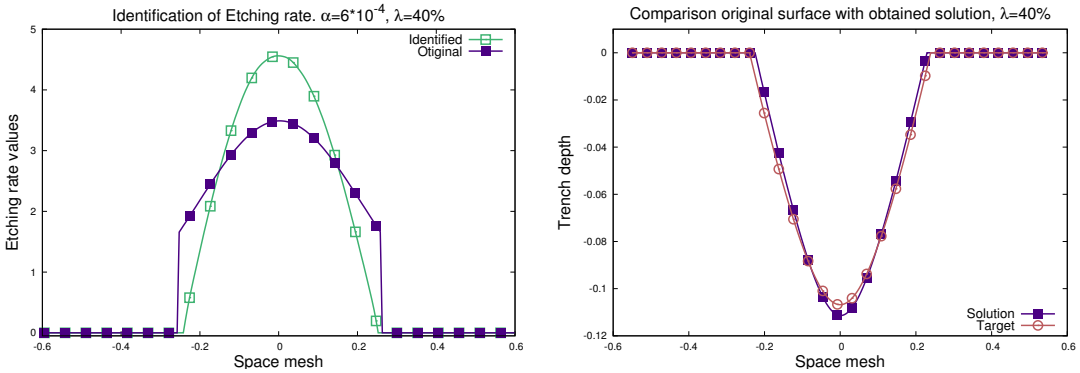

Figure 5.7: Results of numerical experiments in the identification the Etching rate functions for AWJM model and reconstruction of the surface shapes based on two different measurements of one trench profile in case the level of the measurement errors is 40%.

The joint use of more than one measurement of the only experimental data in theory will provide some kind of averaging of the trench profiles that should lead to smoothing of the input data. It might give higher opportunity to reconstruct the surface more precisely. Based on that assumption we introduce the superposition of exactly the same two different measurements for each case, which were used previously. It transforms the cost function as follows:

$$\boldsymbol{J}(\boldsymbol{E}) = \frac{1}{2}\int\limits_{\Omega} \left\| \boldsymbol{Z}(x,T) - \left(\frac{\boldsymbol{Z}_{\exp_1}(x) + \boldsymbol{Z}_{\exp_2}(x)}{2} \right) \right\|^2 \mathrm{d}x + \frac{\alpha}{2}\|\nabla \boldsymbol{E}\|^2. \qquad (5.2)$$

Here we take the average of two inputs and minimize the difference between it and numerical solution. All the minimization procedure remains the same as in the previous case.

As an example of these numerical implementations we demonstrate the view of the input, obtained by superposition of two independent trench profiles with 15% of the noise and final match between initial and reconstructed surfaces (Figure 5.8(a)).

Numerical results of this particular case show that the accuracy of the reconstruction of the trench profile is also higher in comparison with the case where two trenches are used independently (Figure 5.6). The whole description of the results is specified in

the Table 5.2. Mostly the accuracy of the surface prediction is a bit higher or on the same level as in case of independent measurements.

Considering some improvement above, we now include one more additional separate experimental measurement. We introduce it independently from other measurements, so that the corresponding cost function is:

$$\boldsymbol{J}(\boldsymbol{E}) = \frac{1}{6}\sum_{i=1}^{3}\int_{\Omega} \left\|\boldsymbol{Z}(x,T) - \boldsymbol{Z}_{\exp_i}(x)\right\|^2 \mathrm{d}x + \frac{\alpha}{2}\|\nabla \boldsymbol{E}\|^2, \tag{5.3}$$

As before, we have the difference between the model solution and each of the observations, which we devide by the number of observations. We supplement the cost function with the regularization term, multiplied by factor α which again has to be determined by L-curve method.

Numerical results of this approach for the chosen case of 15% of noise are displayed on the Figure 5.8(b), where one could see that mismatch between solution and "Target" is still very low. Note that identified Etching rate function already keeps the smooth and symmetric form. For all the range of applied noise, the identified form of the function $\boldsymbol{E}$ does not visually differ from the previous cases.

Finally, all the three measurements used before can also be combined together into the formation of the input for minimization process. They are involved into the superposition of trenches to form the input for minimization process. This leads to the following cost function:

$$\boldsymbol{J}(\boldsymbol{E}) = \frac{1}{2}\int_{\Omega} \left\|\boldsymbol{Z}(x,T) - \left(\frac{\boldsymbol{Z}_{\exp_1}(x) + \boldsymbol{Z}_{\exp_2}(x) + \boldsymbol{Z}_{\exp_3}(x)}{3}\right)\right\|^2 \mathrm{d}x + \\ + \frac{\alpha}{2}\|\nabla \boldsymbol{E}\|^2. \tag{5.4}$$

The results, presented on Figure 5.8(c), rely on the superposition of the three different measurements of the same trench which takes corresponding averaged form. The surface forecast is again very close to the previous cases and keeps the level of error around 2% in terms of L^2 norm.

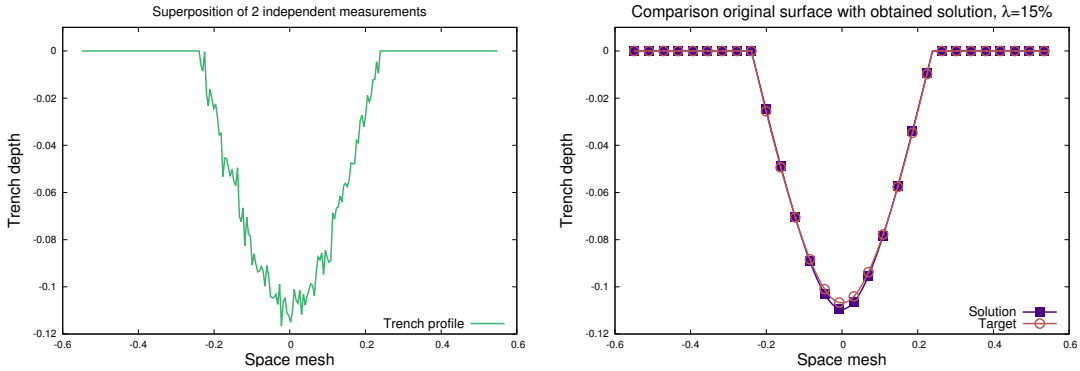

(a) Superposition of two trenches

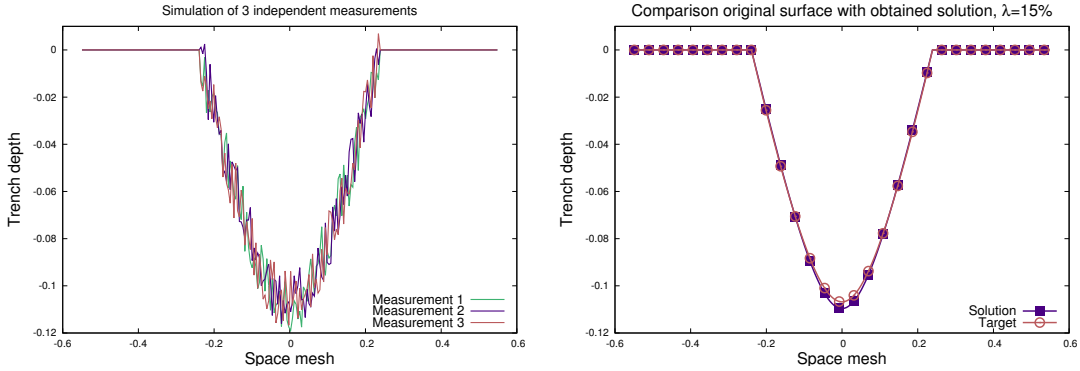

(b) Three independent trenches

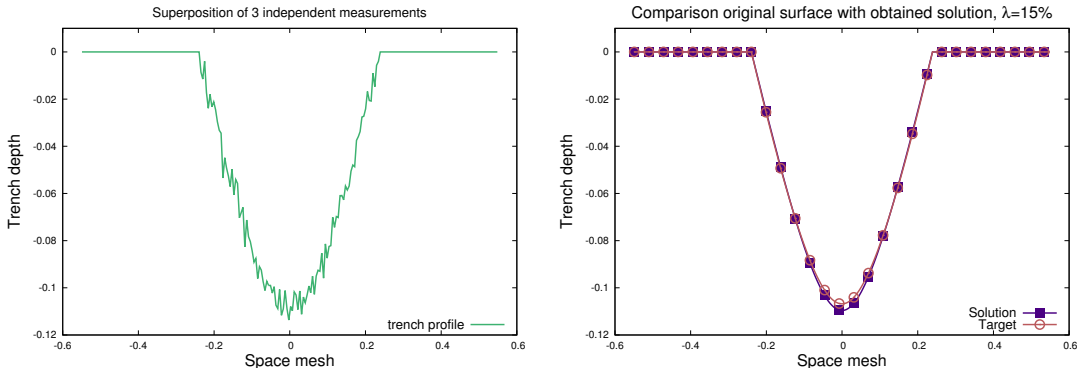

(c) Superposition of three trenches

Figure 5.8: Results of numerical experiments in the identification the Etching rate functions for AWJM model and reconstruction of the surface shapes based on different variants of cost functions in case the level of the measurement errors is 15%.

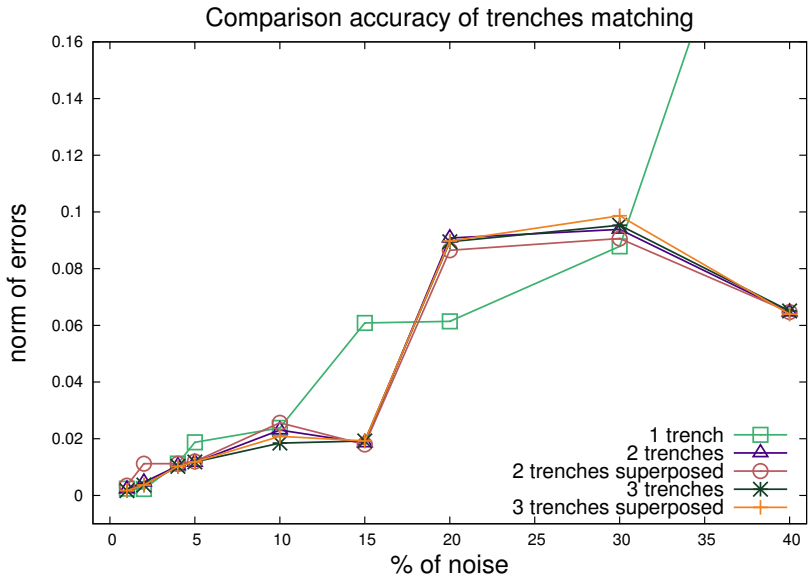

Figure 5.9: Accuracy of matching the obtained solutions to original profiles for different cost functions considering different levels of measurement errors.

The difference between using two and three measurements is not very impressive due to random nature of the noise applied to the input, and could be strongly increased by involving hundreds of experimental observations to reduce the influence of the errors. Such strategy will turn out the returning back to the completely smooth averaged input, which was used in section 4.3 of chapter 4.

But it is already possible to claim that use of three trench measurements instead of two (what is still reasonable unlike the hundreds of them) mostly gives more close and correct shape of the trench, and allows us to identify a more acceptable Etching rate function in the manufacturing.

Figure 5.9 gives an overview of the results of involvement the different cost function depending on the level of noise. It demonstrate the significant improvement in the several cases of identification achieved by introducing different approaches to define the cost function. Keeping the acceptable level of accuracy (less than 10%) in terms of (4.5) in matching between experimental measurement and obtained solution, introduction of more complex cost functions (5.1) and (5.3) gives us the opportunity

Trenches	1%	2%	5%	10%	15%	20%	30%	40%
Single	2.37×10^{-3}	2.24×10^{-3}	1.87×10^{-2}	2.38×10^{-2}	6.08×10^{-2}	6.14×10^{-2}	8.78×10^{-2}	0.272735
2 independent	2.23×10^{-3}	4.66×10^{-3}	1.15×10^{-2}	2.30×10^{-2}	1.84×10^{-2}	9.08×10^{-2}	9.38×10^{-2}	6.46×10^{-2}
2 superposed	3.43×10^{-3}	1.12×10^{-2}	1.19×10^{-2}	2.56×10^{-2}	1.79×10^{-2}	8.64×10^{-2}	9.06×10^{-2}	6.43×10^{-2}
3 independent	1.68×10^{-3}	3.66×10^{-3}	1.18×10^{-2}	1.84×10^{-2}	1.92×10^{-2}	8.94×10^{-2}	9.53×10^{-2}	6.50×10^{-2}
3 superposed	1.68×10^{-3}	3.65×10^{-3}	1.18×10^{-2}	2.08×10^{-2}	1.92×10^{-2}	8.97×10^{-2}	9.86×10^{-2}	6.39×10^{-2}

Table 5.2: Comparison of the accuracy in the prediction of the trench profile, corresponding to different cases of the cost functions and different levels of applied noise.

to identify more applicable and convenient AWJM model parameters. In general the more trenches measurements are available the higher accuracy in the surface prediction can be achieved due to elimination of the measurement errors by averaging the input data. But it goes beyond our interest to be able to identify model parameters from only one or couple of real measurements.

Cost functions (5.1) and (5.2) are not identical, but they theoretically have the same gradient. However numerical implementation gives different results and flexibility to find more suitable realization for each particular problem, what has to be taken into account. The same situation is for the pair of cost functions (5.3) and (5.4). More detailed results of comparison between all proposed approaches are presented in Table 5.2.

One could notice that in most of the results the use of several trenches instead of only one can improve the accuracy in the parameters identification, leading to reducing the errors in the prediction of the surface profile up to 20% in cases of low level of noise. In cases of very noisy input data (see columns related to noise higher than 20%) the use of several measurements plays strong role in decreasing the mismatch in reconstruction of the trenches. This effect could be explained by nature of the distribution of the applied noise. Certainly, it should be noted that sometimes only one measurement is available, and it might be enough to obtain the model parameters required to reconstruct the profile. Moreover, superposition of the trenches involved in the identification process which can be interpreted as an average of the input experiments usually also

leads to higher accuracy, but mostly on the "long distance" - the quantity of available measurements.

It reaffirms that the use of two or three measurements of the noisy profile can not ensure the strong improvement of the identification of unknowns due to the random behavior of the noise. But it demonstrates that when there are only couple of data measurements are available, the proposed approach is capable to identify acceptable for machining model parameters, the use of which will predict the surface formation very preciselly.

5.4 Noise as a model parameter

Identification of the AWJM model parameters in case of noisy input data is challenging and intractable problem due to the unclear form of the trench. As we demonstrated in previous sections, it always depends on the level and exact distribution of the noise, but in all the cases the accuracy of the surface prediction becomes lower with the increase of the noise. It is obvious that the most accurate results are given by the most clear and realistic measurements.

One of the possible solution to ameliorate the input for our task is to use the numerous measurements to obtain the average. We demonstrated this approach previously. Another proposition is to assume the noise as the independent unknown model parameter, which can be considered in the identification process, based on the following model:

$$\frac{\partial \boldsymbol{Z}}{\partial t} = -\frac{\boldsymbol{E}(x)\mathrm{e}^{a\boldsymbol{Z}}}{\left(1+\boldsymbol{Z}_x{}^2\right)^{k/2}} + \boldsymbol{\varepsilon}_{\exp} \ . \tag{5.5}$$

We propose to extend the number of unknown parameters $\boldsymbol{u} = \{\boldsymbol{E}, \boldsymbol{\varepsilon}_{\exp}\}$ which need to be found. In this way, our cost function changes to the following:

$$\boldsymbol{J}(\boldsymbol{u}) = \frac{1}{2}\int\limits_{\Omega} \|\boldsymbol{Z}(x,T) - \boldsymbol{Z}_{\exp}(x)\|^2 \mathrm{d}x + \frac{\alpha}{2}\|\nabla \boldsymbol{E}\|^2 + \frac{\beta}{2}\|\boldsymbol{\varepsilon}_{\exp}\|^2, \tag{5.6}$$

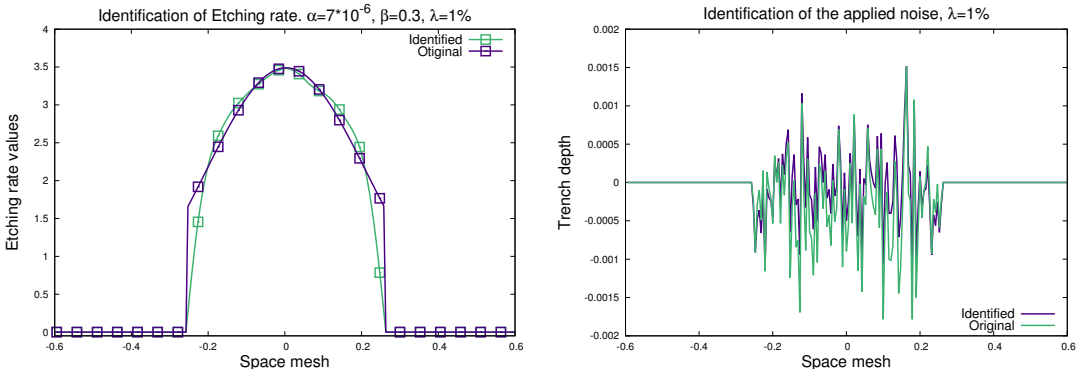

Figure 5.10: Coupled identification of the Etching rate function and applied noise with level equal to 1%.

where β is the Tikhonov regularization coefficient corresponding to the measurement errors.

The idea is to identify simultaneously the Etching rate function but apart from the noise in the input data. When the noise can be determined correctly, it will lead to the more precise identification of function $\boldsymbol{E}$, and of course to more proper surface forecast.

We generate again the artificial trench profiles for all the diapason 0 - 40% of noise, applied to the initial clear surface. This set of numerical experiments contain the identification based only on one available observation for each case. The regularization parameters α and β have to be re estimated numerically for each simulation to fit the values of the cost function.

Ivolvement of the measurement errors in the set of model parameters $\boldsymbol{u}$ increases the number of unknowns to be idetified and influences on the time and costs of the minimization process. The minimization takes from 49 to limit of 200 iterations depending on the each special case regardless the level of applied noise.

The numerical results of the joint identification of the Etching rate function and measurement errors are presented on Figures 5.10 - 5.17 respectively to the level of considered noise.

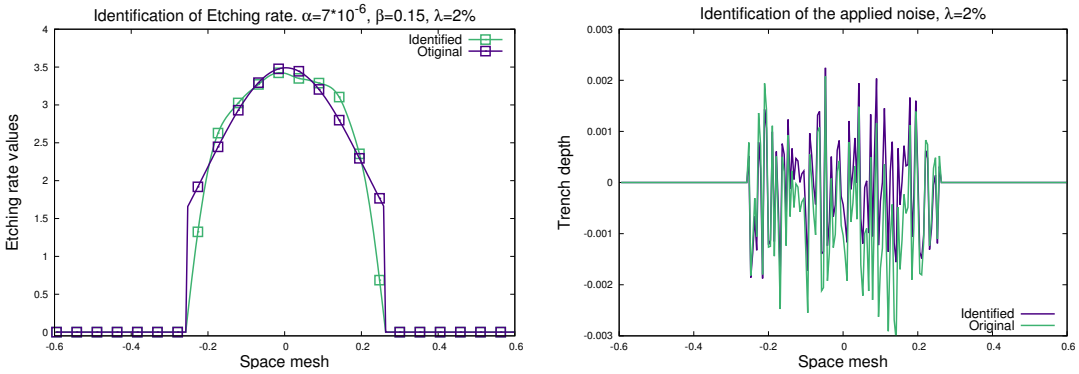

Figure 5.11: Coupled identification of the Etching rate function and applied noise with level equal to 2%.

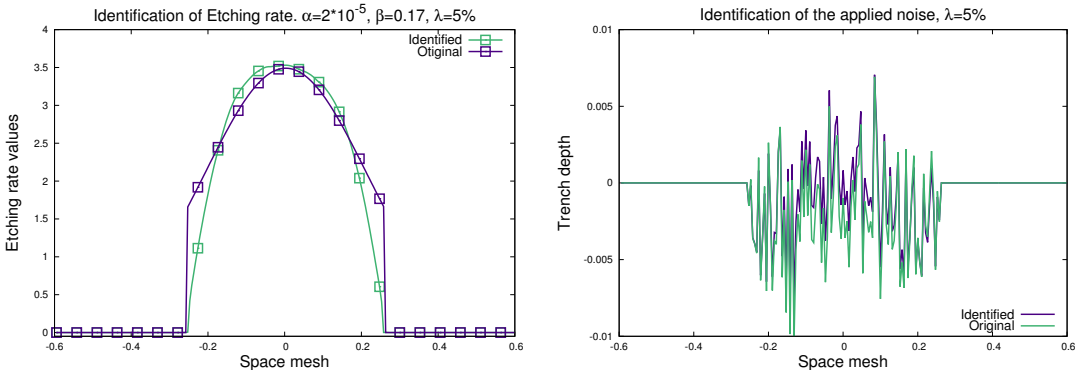

Figure 5.12: Coupled identification of the Etching rate function and applied noise with level equal to 5%.

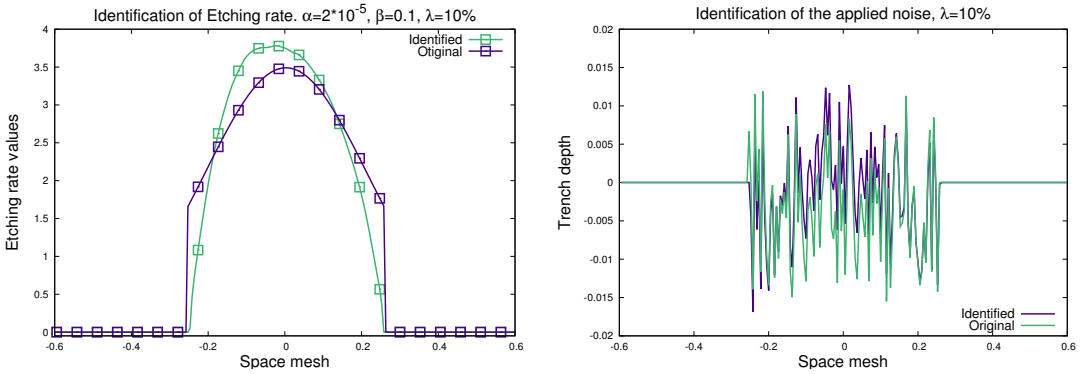

Figure 5.13: Coupled identification of the Etching rate function and applied noise with level equal to 10%.

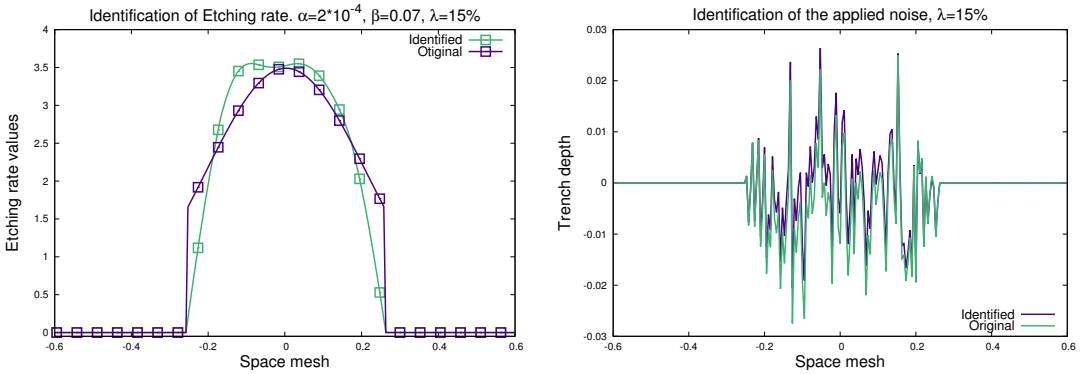

Figure 5.14: Coupled identification of the Etching rate function and applied noise with level equal to 15%.

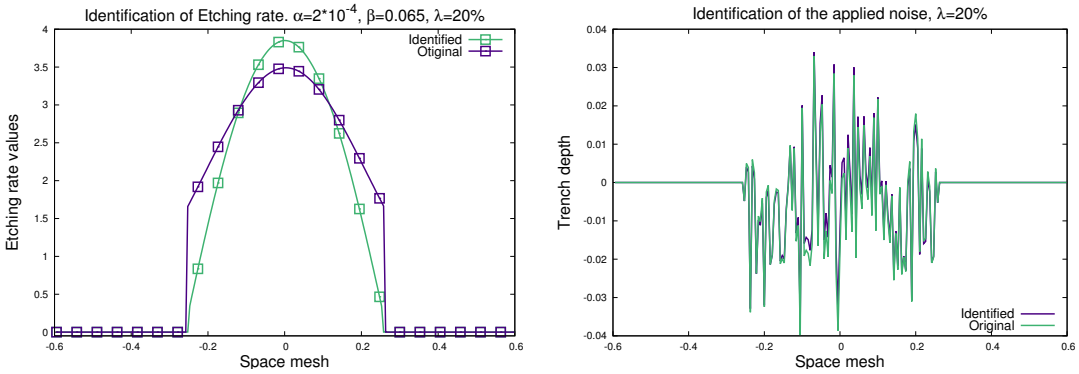

Figure 5.15: Coupled identification of the Etching rate function and applied noise with level equal to 20%.

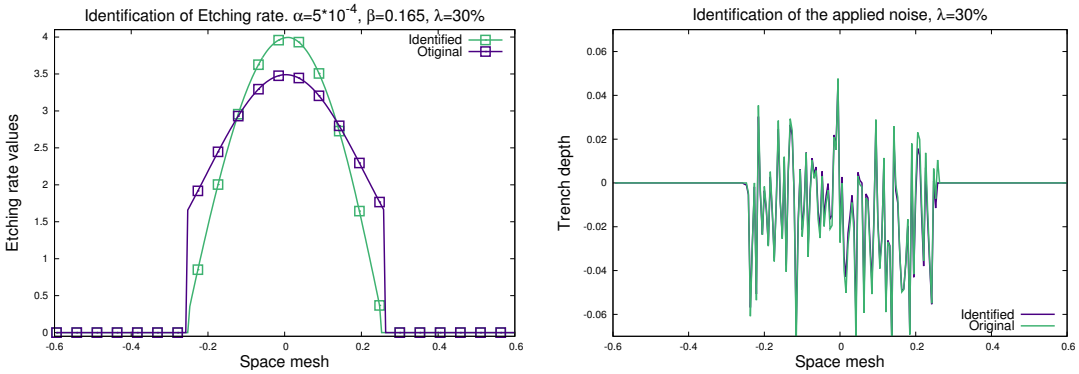

Figure 5.16: Coupled identification of the Etching rate function and applied noise with level equal to 30%.

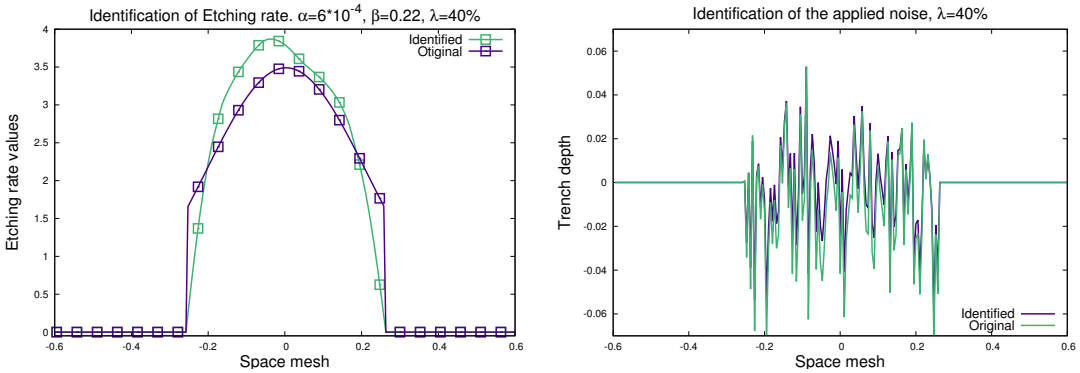

Figure 5.17: Coupled identification of the Etching rate function and applied noise with level equal to 40%.

When the surface profile is not very noisy (less than 5%), we can observe the small changes in compare with the initial approach. Moreover, depending on the exact distribution of the noise, the attempt to include the measurement errors in the set of model parameters can lead to decline of the accuracy in the surface prediction. It can be explained by very small rank of the noise values which were used. When the identification of the noise is not ideal, the wrong estimation of the values conversely increase the difference between experimental geometry of the shape and numerical solution, and moves us away from the target. But despite this, the form of the Etching rate function $\boldsymbol{E}$ in these cases becomes much closer to the original.

We can either notice the improvement of the identification of applied noise with the growth of its level, what in its turn improves the identification of the model parameter $\boldsymbol{E}$. Only one exception here is the case of 40% of the noise - either minimizer stucks in the local minimum with the particular distribution or the influence of the noise is too strong in general. Another reason can be the not optimal choice of the regularization parameters α and β. Furthermore, we can see how the wrong evaluation of the noise influences on the values of the Etching rate function, what entails not symmetry and some problems at the corresponding points during the identification.

Also, we observe much better identified form of the Etching rate function from the

Method	1%	2%	5%	10%	15%	20%	30%	40%
Standard	2.37×10^{-3}	2.24×10^{-3}	1.87×10^{-2}	2.38×10^{-2}	6.08×10^{-2}	6.14×10^{-2}	8.78×10^{-2}	0.272735
Noise - param	1.05×10^{-2}	1.11×10^{-2}	1.21×10^{-2}	3.34×10^{-2}	3.73×10^{-2}	2.23×10^{-2}	4.10×10^{-2}	7.82×10^{-2}

Table 5.3: Comparison of the accuracy in the prediction of the trench profile for standard approach and considering the measurement errors as model parameter.

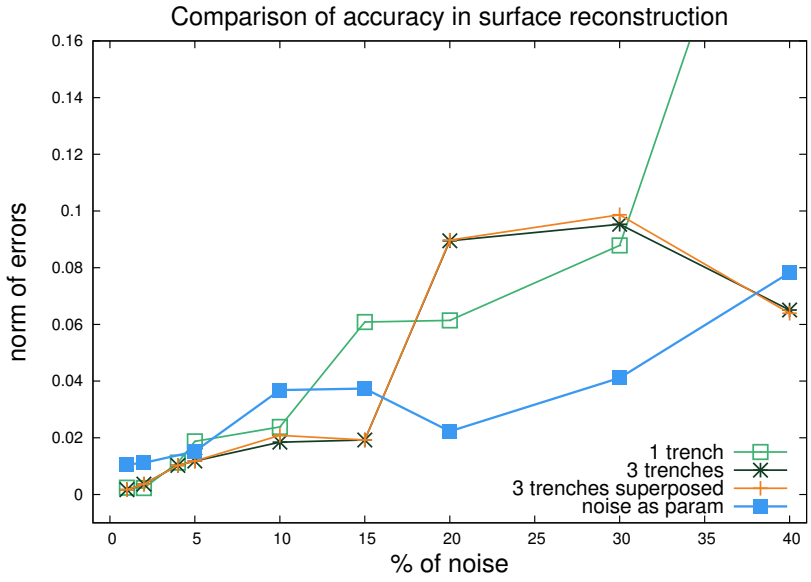

Figure 5.18: "Noise as model parameter" case in comparison with previous results of the surface prediction.

very noisy input data (30% and 40%) in compare with the results in the section 5.2. The function is not compressed at the bottom and the width is found correctly, what forms the remaining part more properly.

The results of the surface reconstruction and accuracy in its prediction are given in the Table 5.3. The row named "Noise-param" complies the current variant of the parameters identification, and the row "Standard" reminds the results obtained in the section 5.2 with only single available measurement for the input.

The corresponding comparison of the results obtained before with the consideration the measurement errors as model parameters is demonstrated on the Figure 5.18.

For the most important cases with the high level of noise, when we confront with the inaccuracy in the standard approach, we have very good improvement now. With the highly noisy experimental measurements (more than 15% of the measurement errors) the coupled identification of the noise and model parameter $\boldsymbol{E}$ gives the gain in the surface prediction approximately in two or three times. For the rest of the cases we still have very low level of the errors between the numerical solution and epxerimental geometry of the surface. The cases with the level of noise less than 5% are still very smooth and acceptable for the identification process with standard method. The possibility to identify the applied noise helps the minimizer to focus on the missed parameters - Etching rate function and strongly rises up the quality of the results.

5.5 Model errors caused by wrong initial estimation

The abrasive waterjet milling process can be done with different machining settings, some of which are directly linked with the parameters of proposed AWJM model (3.1). Thus, one of the parameters which has to be truly known before the identification and surface prediction, is the diameter of the nozzle which was used in experiments. In our model the scalar parameter a describes the radius of the AWJ nozzle.

When we base the parameters identification on the real experimental measurements, some information about the machining settings can be unreachable or even one can make a mistake with the provided information. We propose the case, when the wrong initial estimation of the parameter a is used for the numerical simulation. For this aspect of the model sensitivity study we suppose two variants - when the initial estimation of the nozzle radius is bigger the actual $a_1 > a_0$ and otherwise $a_1 < a_0$. This type of mistakes usually is called as model errors.

Numerically we examine both smooth and noisy input data. The initial surface was generated with the initial value $a_0 = 0.25$. First, we consider the case without any errors in the measurements. We perform the search of unknown Etching rate function and reconsstruction of the trench geometry for two wrong assumptions by choosing the

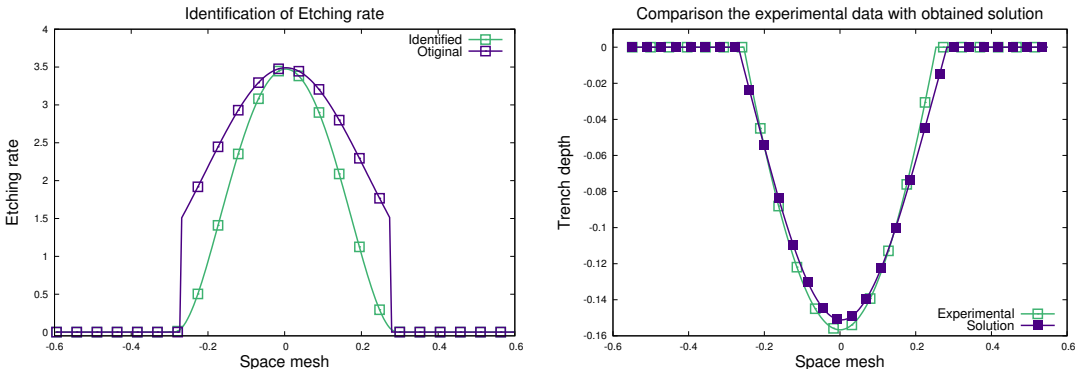

Figure 5.19: Identification of the Etching rate and surface prediction with wrong estimation $a_1 = 0.28$.

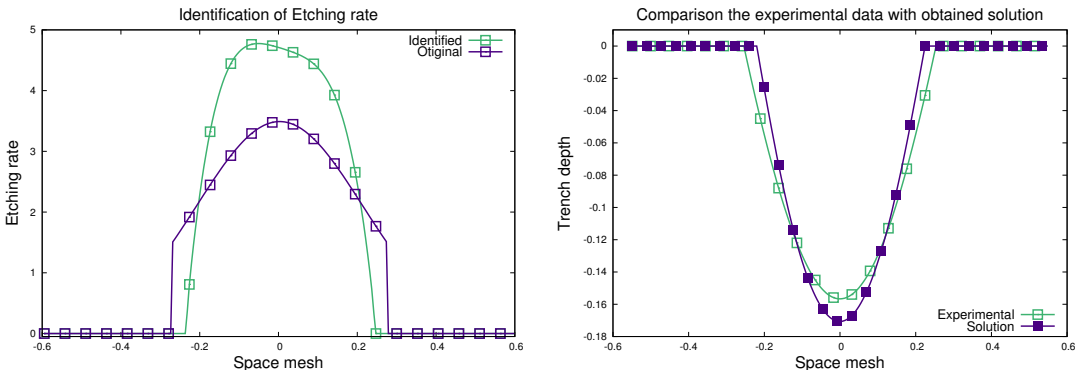

Figure 5.20: Identification of the Etching rate and surface prediction with wrong estimation $a_1 = 0.22$.

values $a_1 = 0.28$ and $a_1 = 0.22$. Numerical results are presented on Figures 5.19 and 5.20 respectively, where the initial surface is named "Experimental".

The second step is to perform the same simulations using the noisy profile as input, which was obtained by considering the noise of 10%. Appropriate results are given on Figures 5.21 and 5.22.

Wrong initial estimation of the parameter a related to the AWJ nozzle diameter leads to the essential mismatch in the trench profile forecast, even the mistake is quite small. We can see that if the chosen value a_1 is higher than original one, the identified

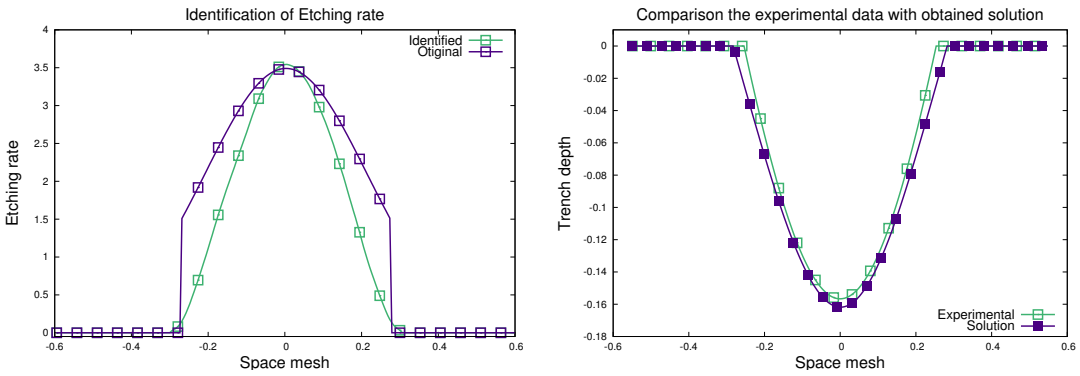

Figure 5.21: Identification of the Etching rate and surface prediction with wrong estimation $a_1 = 0.28$.

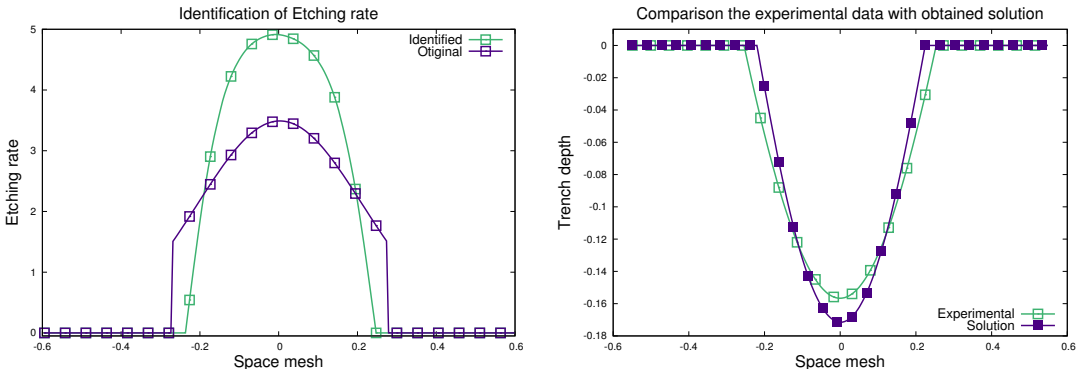

Figure 5.22: Identification of the Etching rate and surface prediction with wrong estimation $a_1 = 0.22$.

Etching rate function differs not so much from the original, and we can obtain smooth solution. The proposed method is able to partially addapt the sought unknown function to the input requirements. By the selecting the value a_1 smaller than initial, we cut the domain of the jets impact what gives completely wrong geometry of the surface.

As a temporary conclusion we can summarize that in lack of knowledge about the real size of the nozzle diameter, it is more rational to approximate it from the width of the measured trench with slightly bigger values to be able to identify the required unknowns more precisely.

Chapter 6

Identification of Etching rate function for moving waterjet

Contents

6.1 Introduction

In this chapter we want to present the concept of more challenging problem of the optimal parameters identification comprising the moving Abrasive Waterjet model. The considered movement of the waterjet is always straightforward among the workpiece (Figure 6.1). The feed speed can differ but be constant during the milling process and moreover it can vary within the changing the position of the jet. The cases of the linear acceleration and deceleration are studied in present work.

The identification of the model parameters in the 3D case comes from the similar principles and results obtained for linearized 2D case. There several different

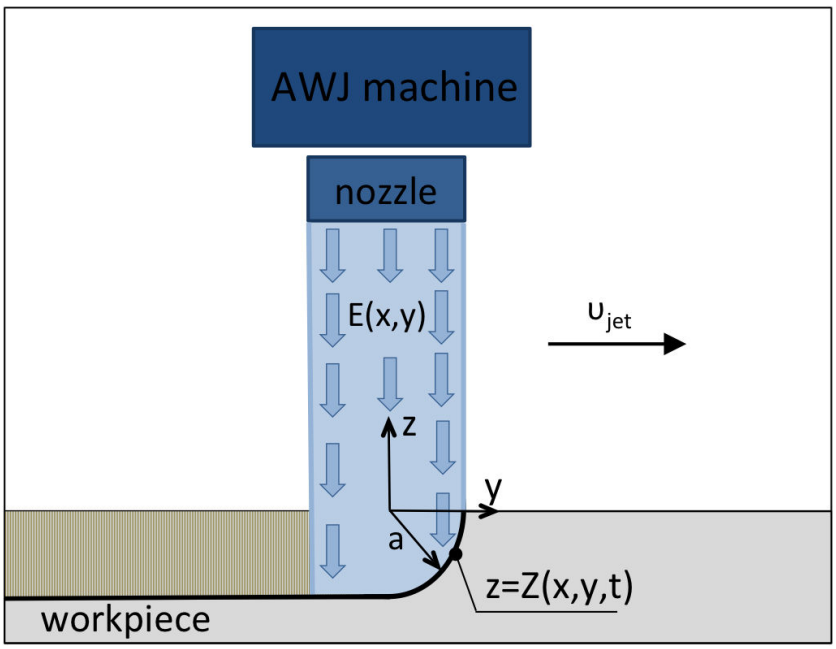

Figure 6.1: Schematic cross-view of the AWJM process and surface formation for moving waterjet.

approaches are demonstrated to form the cost function and proceed the optimization algorithm according to available input and their quantity.

As previously, the presented work of this chapter is possible to split into two parts: identification based on an self-generated input data, and involvement of the real experimental measurements. Although, we introduce the use not only of the average cross-sections (and surfaces obtained from it) but also the exact original measurements of the part of the trench. A part of this chapter has been accepted for publication in International Journal of Engineering Mathematics [5].

6.2 Evenly moving waterjet

6.2.1 Standing with self-generated data

Starting the work in the case of moving waterjet requires the conformation of the possibility to operate with such problem and amount of unknowns. When the waterjet

moves along a straight path regardless of the feed speed and its changes, the milled surface becomes the trench. On one hand it is possible to consider the similar formulation of the identification problem as in 2D case of stationary jet, but from the other - we are interested in the identification of the complete form of the Etching rate function, not only cross-section of it. It means that to identify the correct form of Etching rate function we have to study the milling process and pose the minimization problem not on the trench profile anymore. Instead of trench profile the part of the trench has to be assumed now as an input. We measure some interval of any given trench, where we pose our problem and perform the identification process.

Another aspect to change the type of the input is to consider the erosion effect produced by the jet through each point of the workpiece. In terms of the discretized formulation the spot of the beam impact is much bigger than the discretization step of the domain, what leads to the multiple hitting the each point of the surface.

In case of evenly moving abrasive waterjet we use the proposed AWJM model (3.1) which describes the evolution of the surface geometry by the impact of the waterjet beam in the ideal conditions when no measurement errors or model errors are considered:

$$\frac{\partial \boldsymbol{Z}}{\partial t} = -\frac{\boldsymbol{E}(x,y)\mathrm{e}^{a\boldsymbol{Z}}}{\left(1+\boldsymbol{Z}_x{}^2+\boldsymbol{Z}_y{}^2\right)^{k/2}}\,, \tag{6.1}$$

with initial and boundary conditions:

$$\begin{cases} \boldsymbol{Z}\,|_{t=0} = 0, \\ \boldsymbol{Z}\,|_{\partial\Omega_1} = 0. \end{cases}$$

Here $\boldsymbol{Z}_x$ and $\boldsymbol{Z}_y$ stand for the partial derivatives of $\boldsymbol{Z}$ with respect to x and y respectively.

In this subsection we study two different cases, when the input data are considered as self-generated surfaces and as averaged experimental observations. For the first one we generate the input surface with the fixed a priori known set of parameters $\boldsymbol{u}$, which we are going to identify later and see how is it possible. In the second case, we take

the averaged trench profile used for 2D case in previous chapter 4 and extend it in the y-direction among the movement of the jet.

There is no reason to start the identification for the real experimental measurements, when we have no information about the right type and form of the model parameters, which should be used in the direct simulations to reconstruct the surface geometry. In order to state that proposed method is correct we first have to proove it with the artificial input, and compare the obtained parameters with the initial.

For the numerical implementation we define a domain $\Omega_1 = \{(x, y) : x \in [-x_1; x_1], y \in [0; y_1]\}$, where x_1 always depends on the actual experimental parameters or measurements, due to the changes of the jets radius, and $y_1 = 10 \times x_1$. In fact, we restrain the minimization problem to a squared part in the middle of the trench $\Omega_2 = \{(x, y) : x \in [-x_1; x_1], y \in [\frac{y_1}{2} - x_1; \frac{y_1}{2} + x_1]\}$ which is presented on Figure 6.2(b). From the experiments done in collaboration with STEEP project partners, we set $x_1 = 0.5472$ mm. A regular grid of 228×1140 points with the steps $\Delta x = \Delta y = 0.048$ mm is chosen for discretizing Ω_1 accordingly to available data. For both cases the time interval is taken as unit $t \in [0, 1]$ with $\Delta t = \frac{\Delta x^2}{4}$. The general centered difference approximation for several variables in space and forward difference in time is used for the numerical implementation.

The "pseudo-experimental" surface was generated with arbitrary values of model parameters $a = 0.25$, $k = 0.1$ and Etching rate function $\boldsymbol{E}_0(x, y)$ defined on Ω_2 (Figure 6.2(a)).

In order to obtain a smooth solution ($E(x, y) \in \mathbb{H}^1(\Omega)$ instead of $\mathbb{L}^2(\Omega)$), we change the regularization term in the cost function to the one with the gradient of Etching rate function:

$$\boldsymbol{J}(\boldsymbol{E}) = \frac{1}{2} \int\limits_{\Omega_2} \|\boldsymbol{Z}(x, y, T) - \boldsymbol{Z}_{\exp}(x, y)\|^2 \mathrm{d}x\mathrm{d}y + \frac{\alpha}{2} \|\nabla \boldsymbol{E}\|^2. \tag{6.2}$$

The value of Tikhonov regularization multiplier $\alpha = 10^{-5}$ suitable for this concrete problem was obtained by L-curve method [33, 26].

To overcome the possible increase of the computing costs and instability in behavior

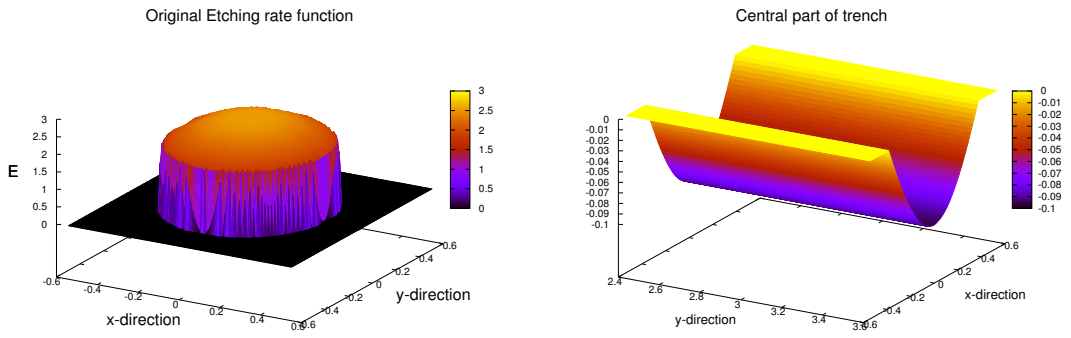

(a) Initial Etching rate function (b) Central part of the trench

Figure 6.2: Initial Etching rate function and corresponding surface.

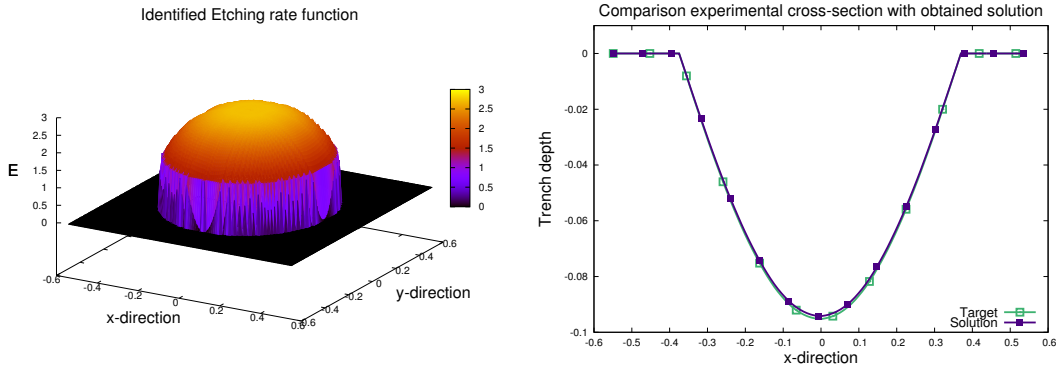

Figure 6.3: Identified Etching rate function and comparison of the cross-sections of obtained solution and input data (Target).

of the Etching rate function, we estimate it as the circularly symmetrical projection of the centred vector by the cubic spline interpolation [1].

Based on the demonstrated correctness of the identification process reported in the previously, the determined Etching rate function and comparison of the corresponding trench profile with the single cross-section of input data are presented on Figure 6.3. The minimization process is performed using N2QN1 minimizer from the "MODULOPT" library [22].

From the obtained results shown on Figure 6.3 we can notice that due to the ill-

posedness of the inverse problem the identified shape of the Etching rate function differs from the original but suitable for AWJM model and leads to very high accuracy in reconstruction the surface geometry in the ideal conditions under the consideration that no measurement or model errors are included. These results allow us to conclude that proposed approach is able to be used for the identification of unknown AWJM model parameters in 3D case.

6.2.2 Extension of the averaged trench profile

Further, we base the search of the AWJM model erosion rate $\boldsymbol{E}$ on the trench surface obtained from the real experimental measurements by extending the average cross-section in the direction of the jet movement (Figure 6.4). This input data has some peculiarity caused to some extent by specific of the milling process and corresponds to milling process with a jet feed speed of 2000 mm/min, and nozzle diameter of AWJ machine of 0.5 mm. This value was used as a background to estimate the model parameter a. All the numerical settings stay the same as in the previous experiment except the value of the Tikhonov regularization factor α, which has to be re-estimated.

The selection of the regularization multiplier is very thorough process and should be done very carefully for each particular problem. Even the small difference in the values of α can provoke serious deviations in the form of Etching rate function, despite the very high accuracy in the surface forecase. The comparison of identified functions $\boldsymbol{E}$ in case of various wrong and choosen as optimal regularization factors is demonstrated on Figures 6.5 - 6.9. It is possible to notice that almost all cases lead to accurate surface prediction, except the case of relatively large value $\alpha = 10^{-2}$, but the shapes of the Etching rate function can not be assumed as acceptable. Moreover, we want to mention that even very unsignificant difference in the regularization values lead to completely wrong results of the identified parameters. It may be explained by the too small or too high weight of the reguarization factor in compare to the values of the cost function and values of the Etching rate function. The chosen α also influences not only on the shape of the function $\boldsymbol{E}$ but on its scale as well. Due to the ill-posedness of

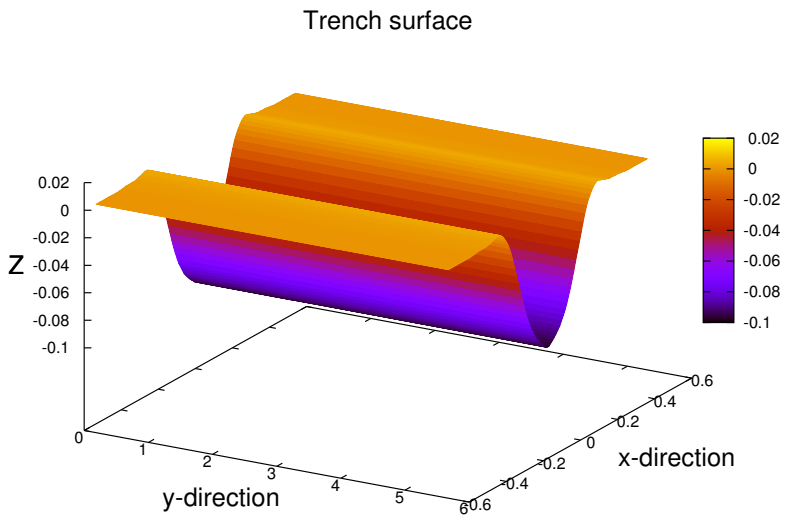

Figure 6.4: Extended average cross-section profile to the trench surface.

the inverse problem the picking of optimal conditions plays one of the important roles in obtaining the required results.

Unlike the previous occasion, we have no estimation of the Etching rate function that was used in the produced experiment, thus we start the determination from the zero assumption $\boldsymbol{E}_0 = \mathbf{0}$. Also in this situation we are not able to estimate the range of values of the Etching rate function to determine the diapason of possible regularization multipliers, thereby we have to study wide band of it and pick some close to the optimal. The precision of the optimal value could be higher what will increase the accuracy in surface prediction.

Here we provide the results of the identification of inaccessible from the experiments AWJM model parameters which should be used in the direct simulation to reproduce the required workpiece shape. The identified Etching rate function, which describes the formation of the waterjet energy beam, takes acceptable uniform shape, where the highest effect is focused in the centre of the beam. This type of the function $\boldsymbol{E}$ was obtained with the regularization term $\alpha = 10^{-6}$ which was chosen as nearest to the optimal. The use of these results in the direct simulation provides us reasonable

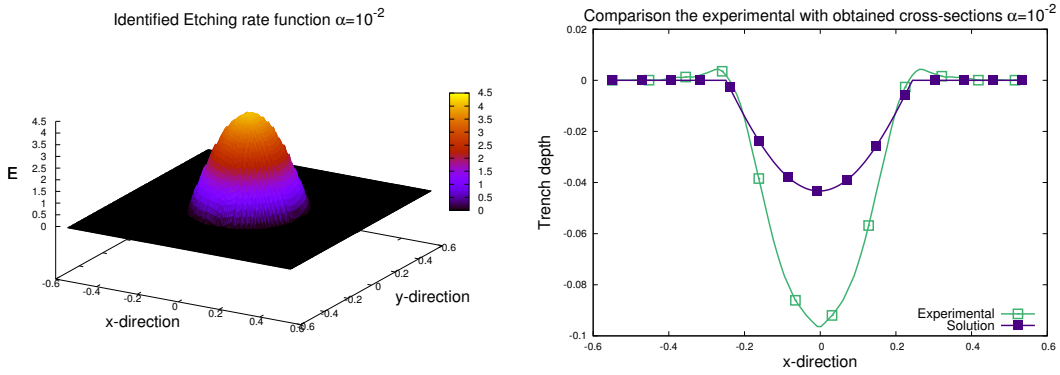

(a) Etching rate function (b) Cross-sections

Figure 6.5: Identified Etching rate function and surface prediction in case of not optimal selection of regularization factor $\alpha = 10^{-2}$.

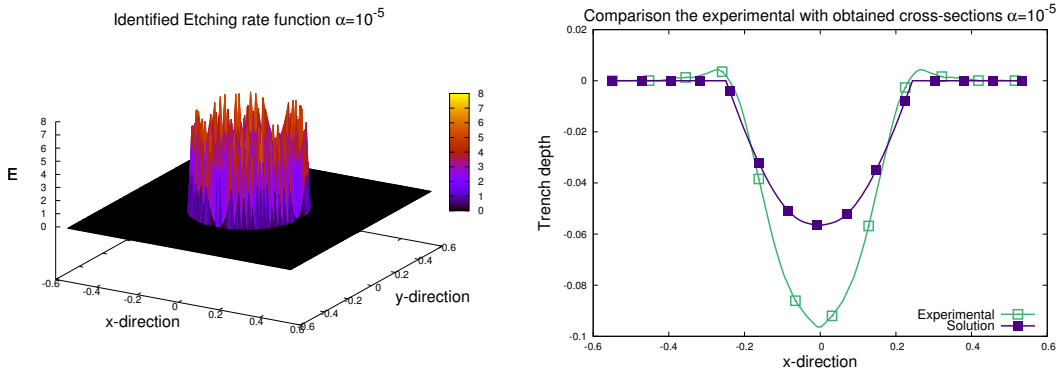

(a) Etching rate function (b) Cross-sections

Figure 6.6: Identified Etching rate function and surface prediction in case of not optimal selection of regularization factor $\alpha = 10^{-5}$.

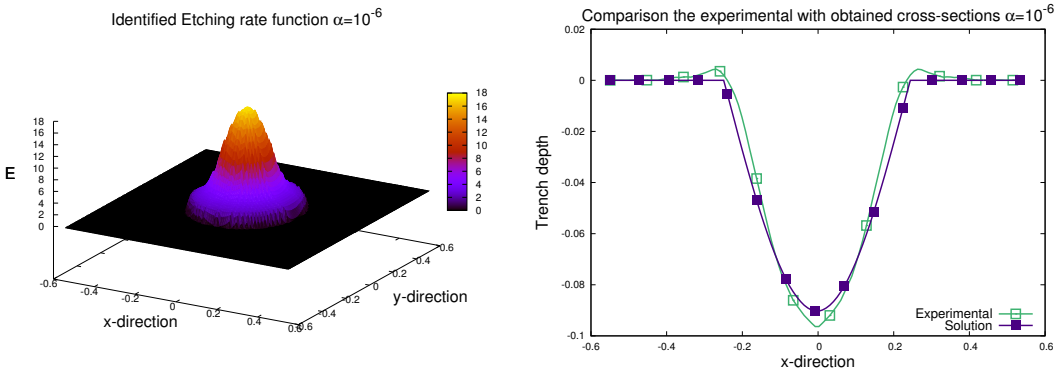

(a) Etching rate function (b) Cross-sections

Figure 6.7: Identified Etching rate function and surface prediction in case of good choice of regularization factor $\alpha = 10^{-6}$.

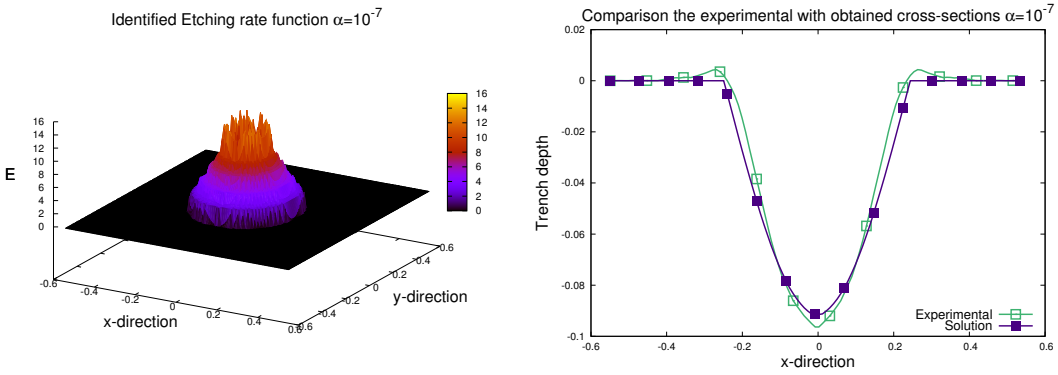

(a) Etching rate function (b) Cross-sections

Figure 6.8: Identified Etching rate function and surface prediction in case of not optimal selection of regularization factor $\alpha = 10^{-7}$.

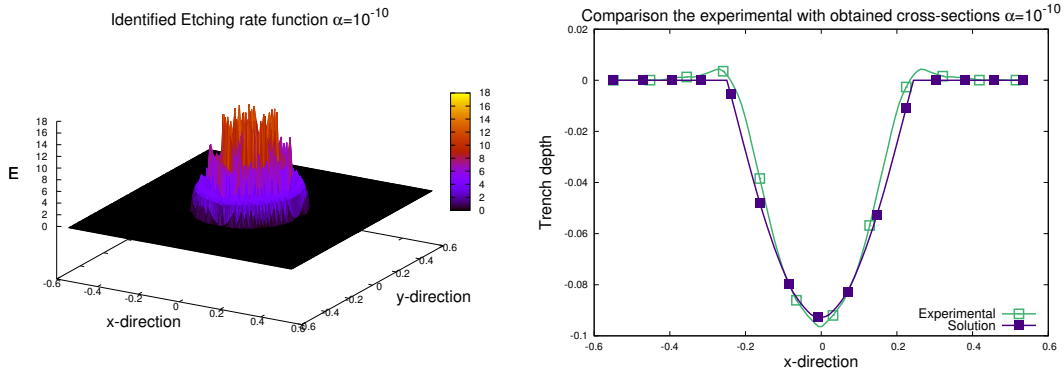

(a) Etching rate function (b) Cross-sections

Figure 6.9: Identified Etching rate function and surface prediction in case of not optimal selection of regularization factor $\alpha = 10^{-10}$.

match between cross-section of the numerical solution and experimental measurements (Figure 6.7). Thus, the required surface can be numerically predicted with an accuracy ε in terms of L^2 norm smaller than 6% by expression (6.3):

$$\varepsilon = \frac{\sqrt{\int_{\Omega_2} \left(\boldsymbol{Z}(x,y) - \boldsymbol{Z}_{exp}(x,y)\right)^2 \mathrm{d}x\mathrm{d}y}}{\sqrt{\int_{\Omega_2} \left(\boldsymbol{Z}_{exp}(x,y)\right)^2 \mathrm{d}x\mathrm{d}y}}. \tag{6.3}$$

One can observe the mismatch on the edges of the slopes of the trench, but this aspect was not considered and modeled in the used AWJM model (3.1). In practice these effects are explained by the redeposition of the target material and appear as the result of high power of the waterjet impact. Finally, this subsection demonstrates the ability to identify the unknown structure of the Etching rate function $\boldsymbol{E}$ which could be used to predict the evolution of the surface geometry for AWJM process.

6.2.3 Joint identification of all unknown parameters

In the very special subcase when there is completely no information about the model parameters, which was used in the experiments, it appears the necessity to identify all of them. Here we demonstrate the numerical results of the combined identification of set of unknown model parameters $\boldsymbol{u} = \{a, k, \boldsymbol{E}\}$ in one run. From the given input

data, we suppose only the background information for jets radius $a_b = 0.25$. We use the values $a_0 = 0.5$, $k_0 = 4$ and $\boldsymbol{E}(x, y) = \mathbf{0}$ as initial estimation for the identification process. According to available data we define the discretized squared domain Ω_2 by setting the $x_1 = 0.312$ mm with the steps $\Delta x = \Delta y = 0.024$ mm.

In this case we change the cost function $\boldsymbol{J}(\boldsymbol{u})$ to include the possible regularization terms.

$$\boldsymbol{J}(\boldsymbol{u}) = \frac{1}{2}\int\limits_{\Omega_2} \|\boldsymbol{Z}(x, y, T) - \boldsymbol{Z}_{\exp}(x, y)\|^2 \mathrm{d}x\mathrm{d}y + \\ + \frac{\alpha_1}{2}\|\nabla \boldsymbol{E}\|^2 + \frac{\alpha_2}{2}\|a - a_b\|^2. \tag{6.4}$$

Final identified Etching rate function $\boldsymbol{E}$ is presented on Figure 6.10(a) while the found scalar parameters are $a = 0.263$ and $k = 4.12 \times 10^{-5}$. Regularization multipliers $\alpha_1 = 10^{-10}$ and $\alpha_2 = 0.1$ were used. The use of all these values gives us very accurate surface recontruction, demonstrated on Figure 6.10(b), where the "Target" is the cross-section of input data and "Solution" is the cross-section of modelled trench. It is important to note that sought value of parameter a was found very pricesly, whereas the identified value of k is close to zero. This fact as well as the surface simulation with the use of this value demonstrates not high influence of it on evolution of the trench footprint. Moreover, wider freedom in adjustment of all model parameters leads to much better surface formation forecast. The required surface in this case can be numerically predicted with an approximate accuracy of 3% in terms of L^2 norm.

6.2.4 Experimental measurement based identification

Another side of our problem is the possibility to identify required model parameters not from the average surface geometry which is quite smooth and monotonous, but accepting the original measurements of the experimentaly produced trench. These measurements highly depend on settings and type of the instruments are used for. Being lucky we obtained not very roughly and noisy data, which we use as input for the inverse problem (Figure 6.11).

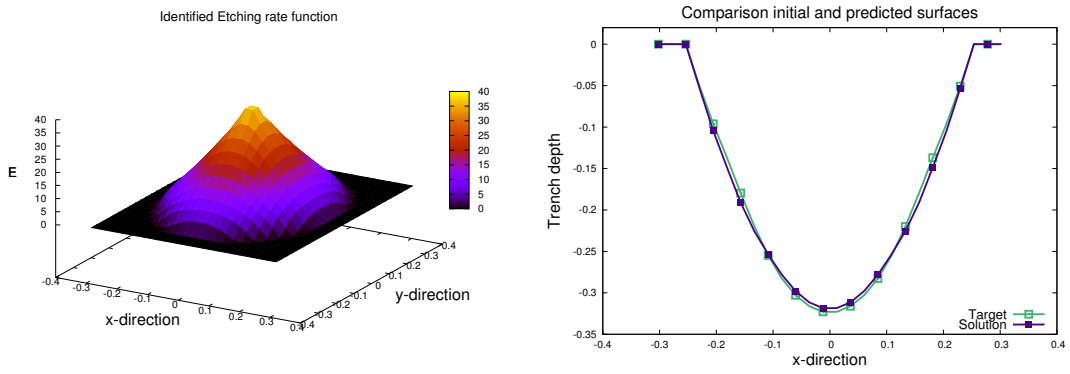

(a) Etching rate function

(b) Related cross-sections

Figure 6.10: Joint identification of the AWJM model parameters and comparison of the cross-sections of obtained solution and experimental measurements in case of evenly moving waterjet.

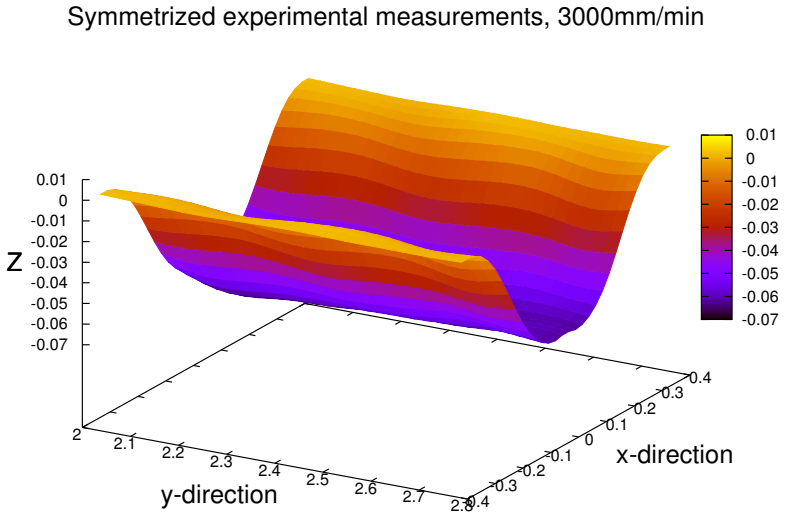

Figure 6.11: Original measurements of the part of the trench, milled by micro-waterjet machine.

Accordingly to the considered mathematical model we still assume the constant movement of the jet in straight direction with fixed physical parameters of the waterjet machining tool.

Usually parameter identification problems induce various difficulties caused by model errors and rather measurement ones. And working with the original observations of the experiments it is necessary to consider it. To be able to search unknowns from rough and noisy initial measurements we include in the AWJM model the error term $\boldsymbol{\varepsilon}_{\text{exp}}$, which represents the errors as random variables with a Gaussian probability density function and a zero mean, normalized in accordance with the maximum depth of the trench. This inclusion allows us to add the variation to the shape of the surface. In its turn it leads to higher flexibility of proposed approach to identify and adjust more correctly desired model parameters.

For the numerical simulations we use the following model:

$$\frac{\partial \boldsymbol{Z}}{\partial t} = -\frac{\boldsymbol{E}(x,y)\mathrm{e}^{a\boldsymbol{Z}}}{\left(1+\boldsymbol{Z}_x{}^2+\boldsymbol{Z}_y{}^2\right)^{k/2}} + \lambda\,\boldsymbol{\varepsilon}_{\text{exp}}\ , \tag{6.5}$$

where λ is the factor corresponding to the percentage of the errors also describes the presence of the measurement noise with the required level.

In this part of the work the available experimental measurements differ from the previous ones and correspond to waterjet milling process with the jet feed speed of 3000 mm/min. Due to provided data we define the discretized squared domain Ω_2 by setting the $x_1 = 0.384$ mm with the steps $\Delta x = \Delta y = 0.024$ mm related to the choosen part of the milled trench, where we minimize the cost function.

Results of the determination of the Etching rate function and comparison of the predicted surface ("Solution") with the original profile ("Target") are given on Figures 6.12(a) and 6.12(b) in case of jet feed speed equal to 3000 mm/min. We can notice that respectively to the decrease of the density in the input measurements we have the small lost in the smoothness of the final function shape what causes not significant lost in the surface restoring precision. Despite this we still have very high accuracy in the surface prediction using presented identification technique what is expressed as level of

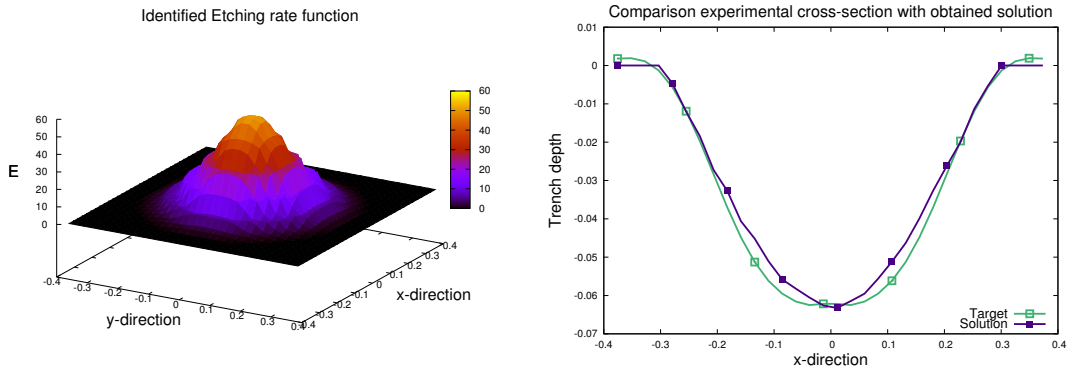

(a) Etching rate function

(b) Cross-sections

Figure 6.12: Identification of the Etching rate function and comparison of the cross-sections of obtained solution ("Solution") and experimental measurements ("Target") in case of evenly moving waterjet.

error (less than 5%) in terms of L^2 norm.

6.3 Waterjet feed speed variations

We propose another special case of the identification of Etching rate function for the moving waterjet with not constant feed speed. To extend the possibility of the application of demonstrated identification mechanism in the manufacturing, this particular problem belonging to the variations of the feed speed during the milling process was studied.

The idea is to meet the practical capabilities of waterjet machine, because of what we assume that it accelerates constantly during the movement from the initial position to final. The case of deceleration of the waterjet is considered as opposite problem and will not be studied separately. For the numerical implementation this problem is described as a change of the time spent by jet beam on the each position of the workpiece where we examine the problem. This assumption was done respectively to the technical properties of the AWJM machine and the experimental measurements provided by the partners of the project.

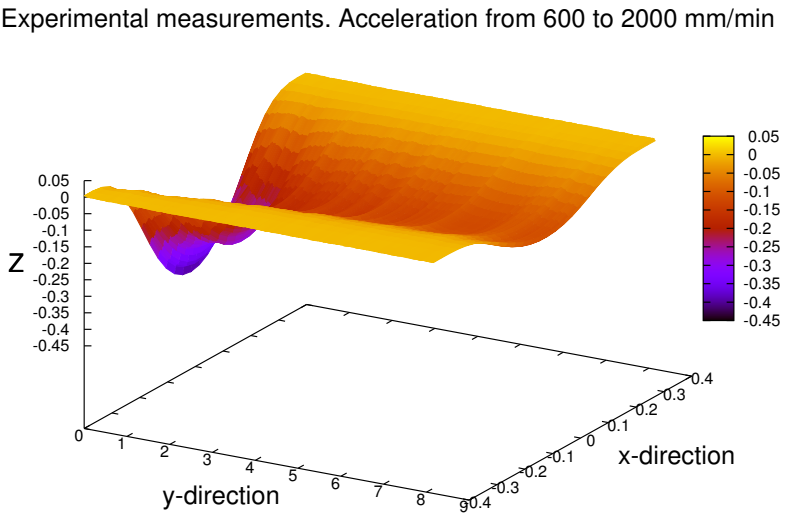

Figure 6.13: Averaged experimental measurements of the trench, milled by micro-waterjet machine with a feed speed change from 600 to 2000 mm/min.

The shape of the trench profile changes at each discretized point of observations during all the time of jets movement owing to the variations of the jet feed speed. It leads to the necessity of increasing the domain Ω to capture the most effective area.

We define the domain Ω_1 by choosing $x_1 = 0.396$ mm accordingly to available experimental measurements. As previously the regular grid with the steps $\Delta x = \Delta y = 0.033$ mm was used to discretize the domain Ω_1 to satisfy numerical simulations with the experimental measurements. The existing input data (Figure 6.13) correspond to the abrasive milling process done with AWJ machine with permanent acceleration from the feed speed of 600 mm/min to 2000 mm/min. In order to level and smooth the noisy input data a noise filter was applied basing on the averaging of measurements of the several trenches done with identical machining parameters. The real feed speed of the waterjet was recorder and correspondingly adjusted to the numerical simulations.

A Tikhonov regularization factor $\alpha = 10^{-11}$ was chosen with a L-curve method for this specific problem. The selection of the value α more predictable and suitable in case of evenly moving jet, because of the similar form of the trench on each cross-section.

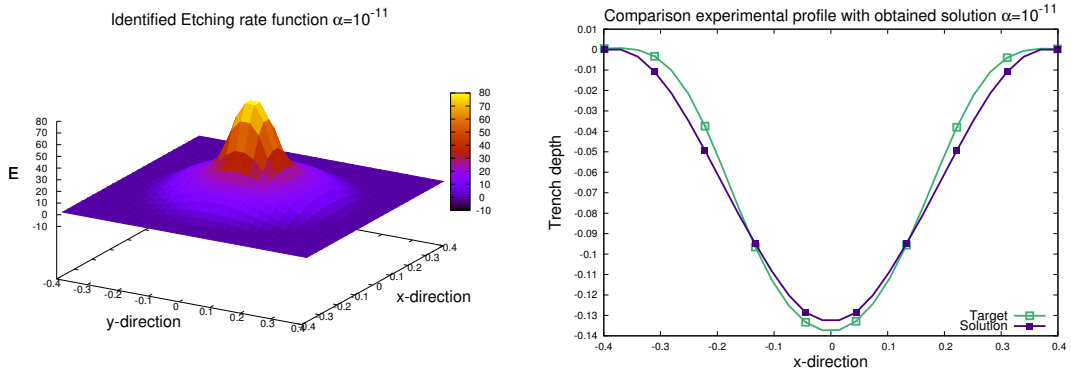

(a) Etching rate function

(b) Cross-sections

Figure 6.14: Numerical results of the identification of the Etching rate function and comparison of the cross-sections of obtained solution ("Solution") and experimental measurements ("Target") for the feed speed acceleration of the waterjet.

In case of jets feed speed variations the shape changes quickly, and the regularization term in the cost function can become not optimal, but anyway it allows us to regularize the solution in general and to accelerate the minimization process. With the use of regularization we can achieve our requirements of smoothness and stable behavior of the sought Etching rate function $\boldsymbol{E}$.

Results of the identification and comparisons of central profiles of the simulated trench with the experimnetal observations are shown on Figures 6.14(a) and 6.14(b) respectively. These results confirm the possibility to identify the unknown Etching rate function suitable for the AWJ machining and satisfying defined conditions. By the use of it we are able to predict the trench surface in case of varied waterjet feed speed. Due to the increase of complexity of the problem and changeability of the surface profile one can observe some decrease of the accuracy in the surface forecast in comparison with the results related to the evenly moving waterjet. Even so we still have the opportunity to predict the shape formation with acceptable level of error around 7% in terms of L^2 norm.

Chapter 7

Sensitivity study in case of uniform AWJ movement

Contents

7.1 Introduction

Sensitivity study in 3D case of constantly moving jet represents itself versatile problem due to the complexity of the model and random origin of the measurement errors. The process usually is very routine and meticulous because of the numerous of unknown parameters. The importance is contained in the influence of the data noise on the accuracy in the parameters detection, when on the other hand successful recognition of the noise in the input data helps to avoid mistakes in the trench surface anticipation. Moreover it allows to deeply understand the behavior of the model and improve the correctness of the identification process.

Because of the ill-posedness of the inverse problem we assume the variance-based method for the identification procedure. Valuable changes in the identification ap-

proach and in formulation of the minimization problem demonstrate the perspective and not obvious numerical results.

In this chapter we deliver the comparison of different methods to build the cost function to measure the difference between simulated trench and input noisy data, which affect to the precision in the surface reconstruction. We make an overview of the dependence between the noise level in the input data and the accuracy in surface prognosis in respect with chosen variants.

An interesting fact about the hidden model errors is discovered by the joint identification of the measurement errors and Etching rate function. The outlook of the obtained results demonstrates the imperfection of the proposed AWJM model and the ways of post-improving of the numerical results in order to predict the trench geometry formation more efficiently. The research and numerical results presented in this chapter have been accepted for publication in International Journal of Engineering Mathematics [5].

7.2 Variety of input measurements

In this section we demonstrate and compare the numerical results of the proposed approach to identify the Etching rate function $\boldsymbol{E}$ under different levels of measurement errors in the simulated data. The appearance of the noise is almost impossible to avoid in real observations. This part of the study explains and demonstrates the capability of the proposed approach to cope with wide range of the problem regardless on the quality of the provided experimental information. Hence, the identification process bases on the self-generated data obtained manually, which represents wide spectrum of possible real situations. Using the given 3D AWJM model (6.5) we generated various trench surfaces with predetermined parameters $\boldsymbol{E} = \boldsymbol{E}_0, a = a_0, k = k_0$. Respectively to chosen numerical tests, we add random uncorrelated noise with different levels (from 1% to 40%) to obtain the set of input data for various cases of identification process.

Further these noisy trenches are used separately or in superposition as the only

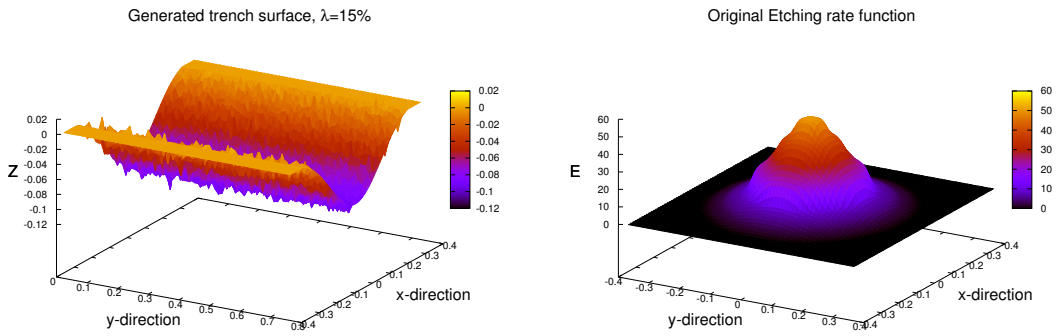

(a) Generated input data

(b) Initial Etching rate function

Figure 7.1: Self-generated surface measurements with 15% of applied noise and form of the initial Etching rate function.

input of the suggested identification method to find out the unknown AWJM model parameters suitable for the surface prediction requirements and machining process. For the numerical implementation the same as in section 6.2.4 of chapter 6 initial assumptions and parameters of the discretization are used except $\Delta x = \Delta y = 0.012$ mm which are used in order to increase the density of the grid and improve the accuracy. We also assume that initial Etching rate function $\boldsymbol{E}_0$ (Figure 7.1(b)) is circularly symmetric and obtained by the cubic interpolation from the centred vector.

In this case our inverse problem is ill-posed again with the big number of unknowns to be identified. The used Tikhonov regularization term plays strong improvement role with proper choice of the values of factor α. In compare with the identification from the smooth self-generated data or averaged one, we now include a lot of instability in the input data and for each separate situation it is necessary to fit the regularization terms.

As explained above, the simulated input data is obtained by adding a Gaussian white noise of various levels of intensity to the initial trench surface (e.g. Figure 7.1(a) demonstrates the case of 15% noise), generated by use of the Etching rate function $\boldsymbol{E}_0$ (Figure 7.1(b)).

The general purpose is to identify the unknown parameter $\boldsymbol{E}$. The use of this values

in the direct simulation with AWJM model (6.1) will produce the trench, which idealy has to be the closest to the initial one. The middle cross-sections of the experimental trenches are named "Target" on the figures in this chapter.

In order to find acceptable for production and smooth solutions, first we base the minimization process on the cost function (6.2). The only one trench measurement was used as input for each particular case according to the level of applied noise. The use of Tikhonov regularization term on the gradient could bring the essential absence of high oscillations in the identification output. Regularization coefficient has to be re-estimated through a L-curve method because of the modification of the grid size.

Detailed results of the identification of the Etching rate function $\boldsymbol{E}$ based on a single trench measurement for all the cases of applied noise with levels in range of 1 - 40%, and comparison of the middle cross-sections of noisy ("Input"), original ("Target") and predicted ("Solution") trenches are given on Figures 7.2(a) - 7.4(b).

It is possible to see the monotone modifications of the results with increase of the noise level, applied to the initial data. The accuracy in the surface prediction gradually declines, but the geometry of the simulated trench keeps similar form. In case of 20% and more of considered measurement errors, the solution becomes significantly deeper and wider. Such behavior is caused foremost by the identified Etching rate function $\boldsymbol{E}$. The evolution of the identified erosion rate from case to case shows that the influence of the noise and its particular peaks grows and makes more difficult to fit the input requirements. From the other side, the range of the Etching rate values stays the same.

The stability of these results indicates that it is still possible to find the unknown AWJM model parameter $\boldsymbol{E}$ even from the measurements with very high level of the noise. Also, it demonstrates that the nature of the noise is irrelevant for the identification mechanism.

The use of these obtained values leads to high enough accuracy in the direct modelling and prediction of the trench surface despite the not ideal matching of the identified function $\boldsymbol{E}$ to the initial one.

Further we assume that there are several different available experimental measure-

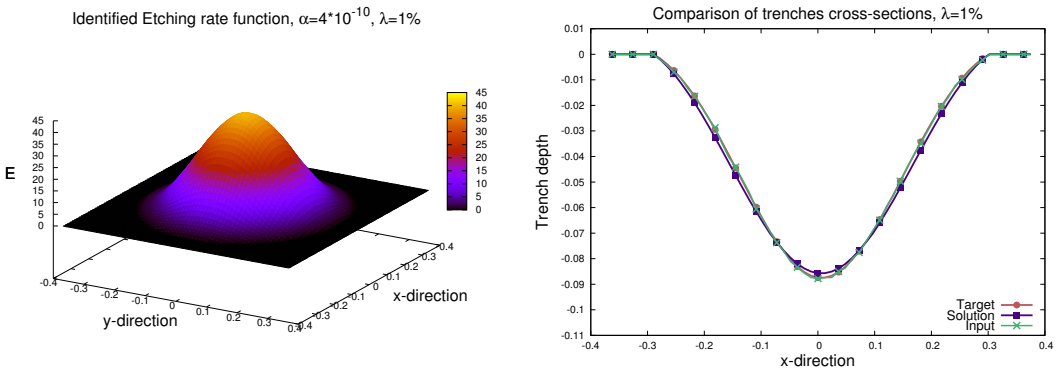

(a) Single trench, 1% of noise

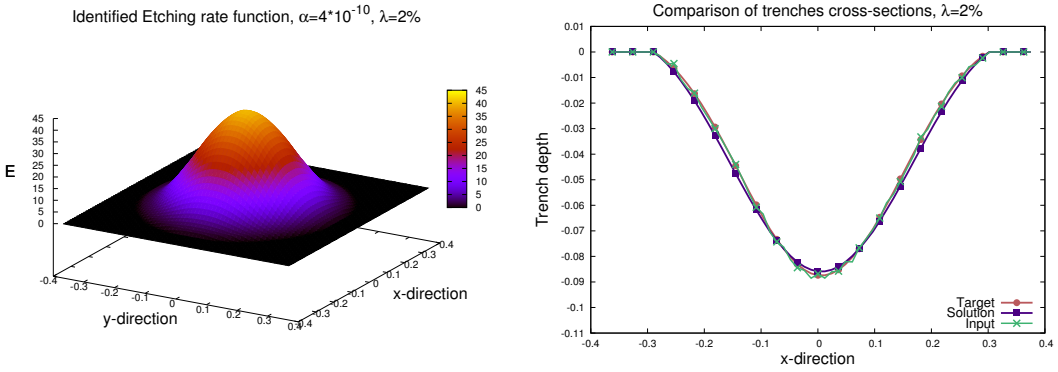

(b) Single trench, 2% of noise

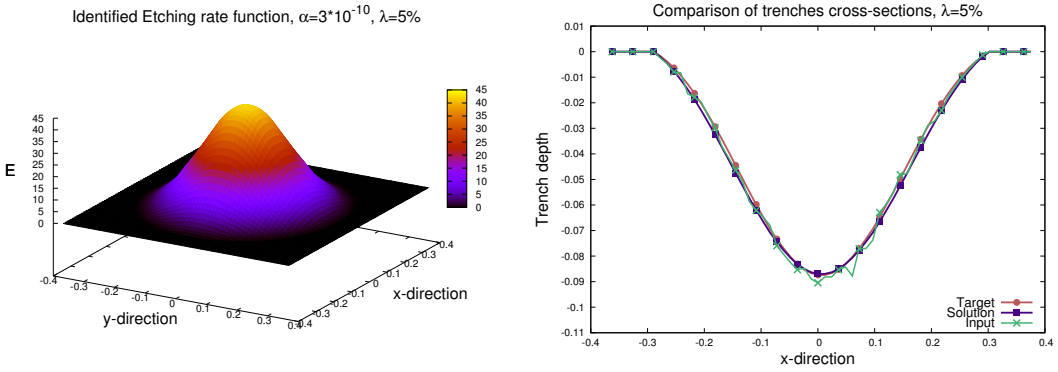

(c) Single trench, 5% of noise

Figure 7.2: Results of numerical identification of the Etching rate functions for 3D AWJM model and prediction of the surface shapes ("Solution") based on single trench measurement with applied noises of 1%, 2% and 5% respectively, compared with original trench profile ("Target") and noisy input ("Input").

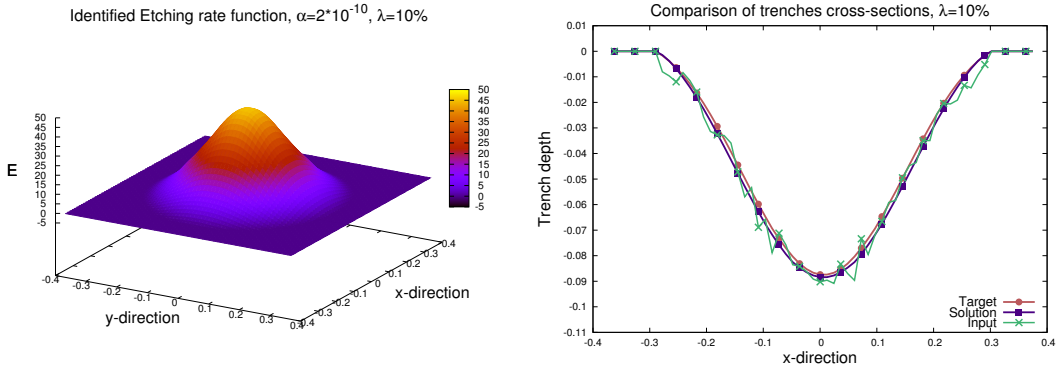

(a) Single trench, 10% of noise

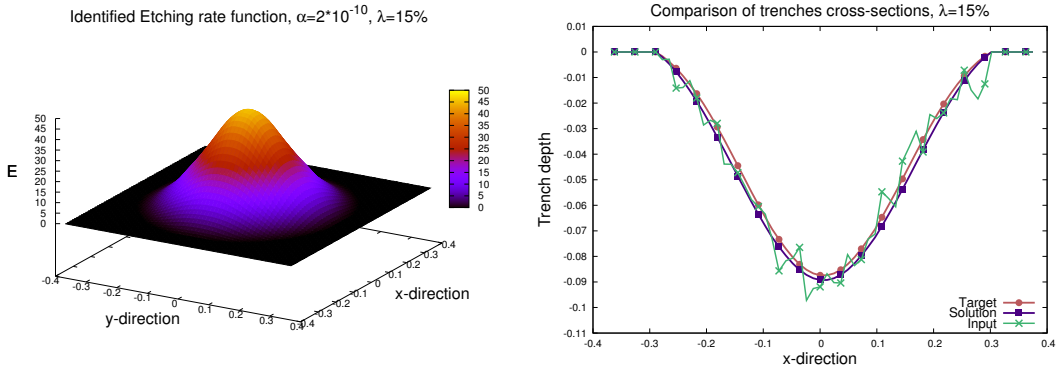

(b) Single trench, 15% of noise

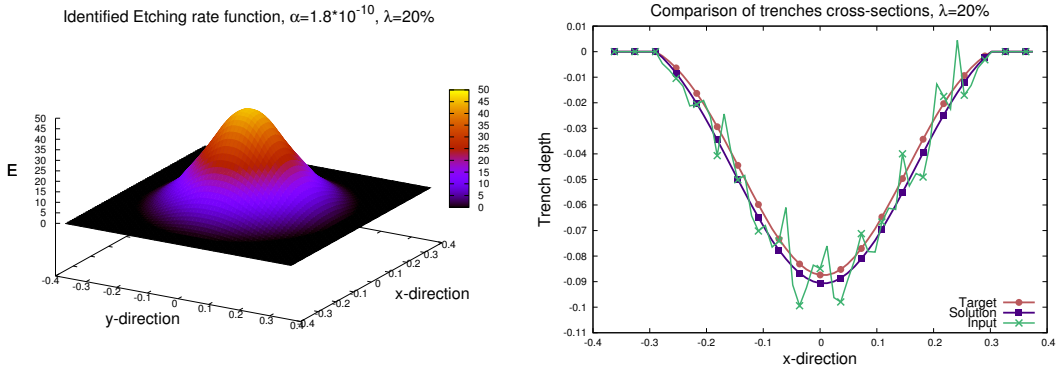

(c) Single trench, 20% of noise

Figure 7.3: Results of numerical identification of the Etching rate functions for 3D AWJM model and prediction of the surface shapes ("Solution") based on single trench measurement with applied noises of 10%, 15% and 20% respectively, compared with original trench profile ("Target") and noisy input ("Input").

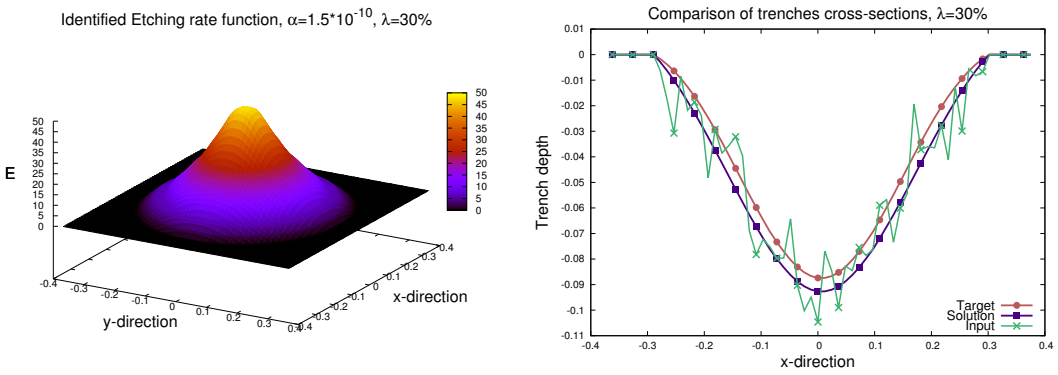

(a) Single trench, 30% of noise

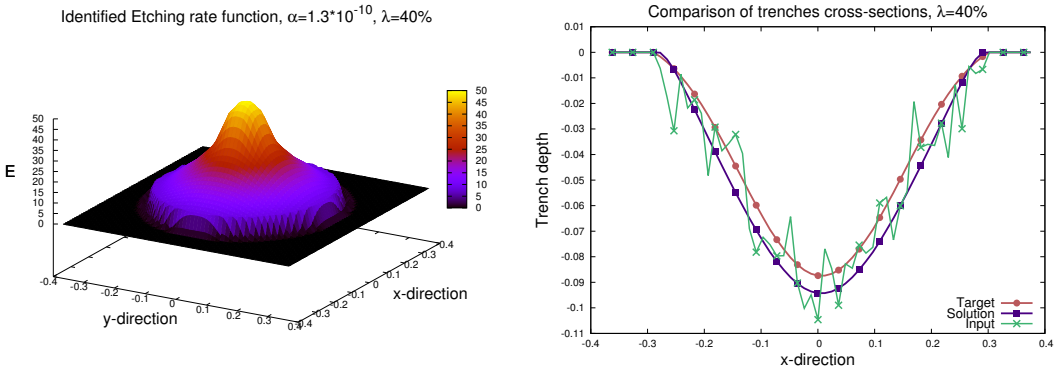

(b) Single trench, 40% of noise

Figure 7.4: Results of numerical identification of the Etching rate functions for 3D AWJM model and prediction of the surface shapes ("Solution") based on single trench measurement with applied noises of 30% and 40% respectively, compared with original trench profile ("Target") and noisy input ("Input").

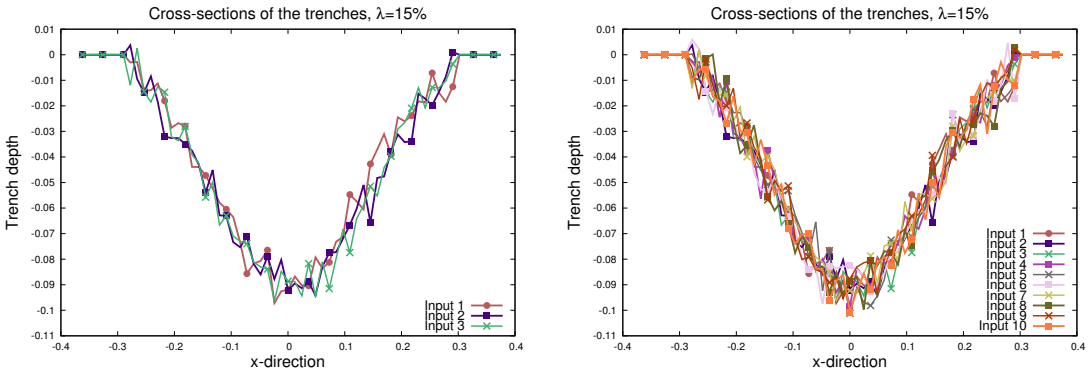

(a) 3 input measurements (b) 10 input measurements

Figure 7.5: Diversity of the available input measurements for different cost functions in case of 15% applied noise.

ments of exactly the same trench that can be used to identify the unknown AWJM model parameters and to model the required surface. In lack of real experimental measurement, to implement this situation we have to generate required amount of surfaces with the same parameters.

The distribution of the noise is always random, so the difference between them is only the random noise applied to the initial surface. In this way we simulate the case of duplicating measurements of the milled trench. To diversify the study we assume two different cases when there three or ten measurement input are available, which are shown on Figures 7.5(a) and 7.5(b).

The cost function involved in the identification process has to be modified in accordance with each considered case. When the identification bases on the minimization of the distance between numerical solution and each of the experimental observation separately, our cost function transforms to

$$\boldsymbol{J}(\boldsymbol{E}) = \sum_{i=1}^{n} \frac{1}{2n} \int_{\Omega_2} \left\| \boldsymbol{Z}(x,y,T) - \boldsymbol{Z}_{\exp_i}(x,y) \right\|^2 \mathrm{d}x\mathrm{d}y + \frac{\alpha}{2} \|\nabla \boldsymbol{E}\|^2, \tag{7.1}$$

where $n = 3$ either $n = 10$ depending on number of available inputs which are taken into account.

The use of several independent trench measurements leads to very similar numerical results in the identification of the unknown function $\boldsymbol{E}$ and prediction the required trench surface. The most significant improvement which brings to the better surface reconstruction can be observed with high level of noise more than 30%.

On Figures 7.6(a) - 7.6(c) and 7.7(a) - 7.7(c) the appropriate results are shown. Released results relate to the identification of Etching rate function in case of the use of three and ten detached measurement input with noise levels of 5%, 15% and 40% respectively. It is possible to sight that results are very close visually, but actually small improvement exists and precision results are listed in the Table 7.1.

Given numerical results of the surface prediction demonstrate very similar accuracy of matching the modeled surface to the original trench regardless of the use more inputs. It is necessary to notice that this approach does not bring very high change in the surface reconstruction precision. From the other side it means that our identification approach allows to determine the AWJM model unknowns fairly truly even with only one available input, despite the high oscillations in the data caused by the measurement errors.

But looking more attentively on the identified Etching rate function $\boldsymbol{E}$, smoothness of the solution has been increased. This effect may be essential in the further realization of the micro-waterjet milling process in the real manufacturing, where the form and behavior of the beam energy parameters need to be strictly determined and suitable for machine parameters.

Considering several independent trench measurements as input for the identification process can be interpreted as the averaging of the surfaces in some sense. To clarify this aspect we demonstrate the numerical results belonging to the another situation when several trench measurements are superposed and used as only input.

Analytically, the gradients of the cost function with respect to the unknown model parameter $\boldsymbol{E}$ have to be the same in both cases, but results in numerical implementations can differ. The point that discrete adjoint state is obtained from the discrete direct formulation but not from the continious, and it leads to the discrepancy be-

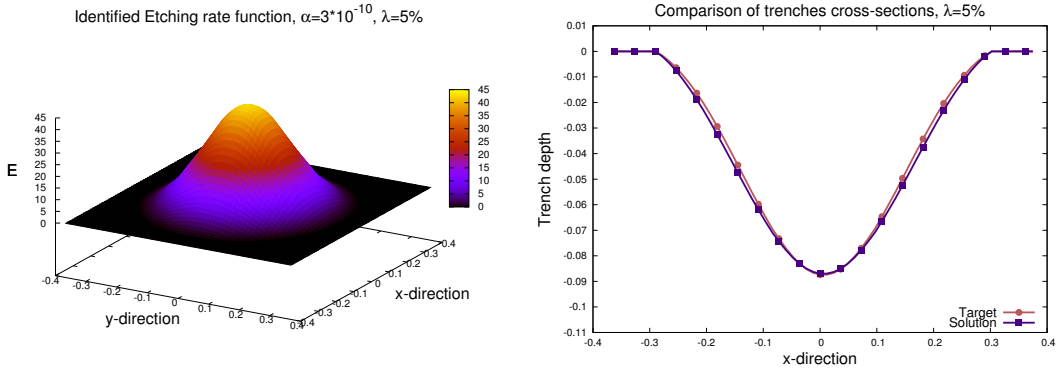

(a) 3 independent trenches, 5% of noise

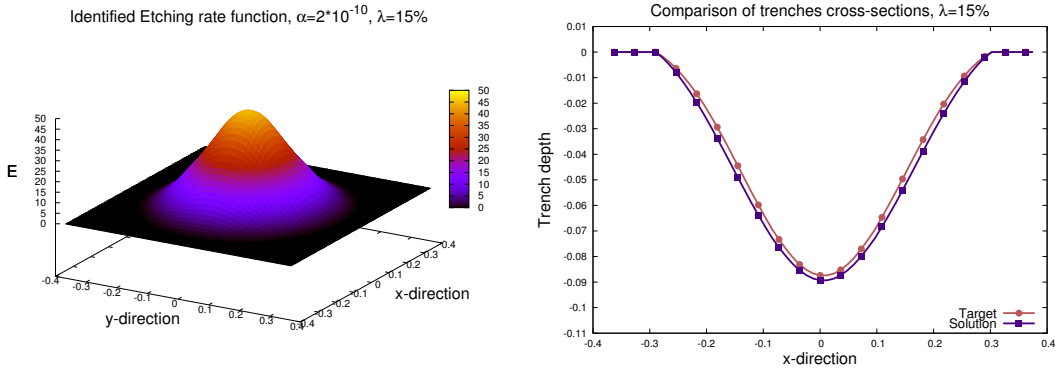

(b) 3 independent trenches, 15% of noise

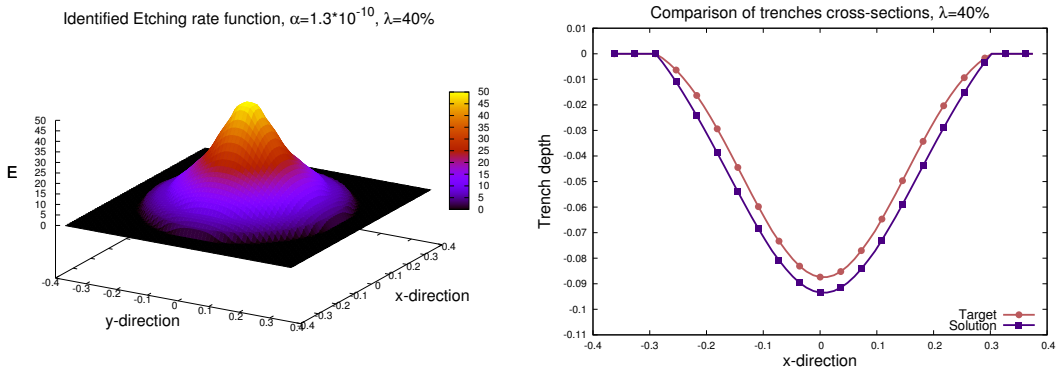

(c) 3 independent trenches, 40% of noise

Figure 7.6: Results of identification of the Etching rate functions and reconstruction of the surface shapes ("Solution") based on 3 independent trench measurements with 5%, 15% and 40% level of the measurement errors, compared with original trench profile ("Target").

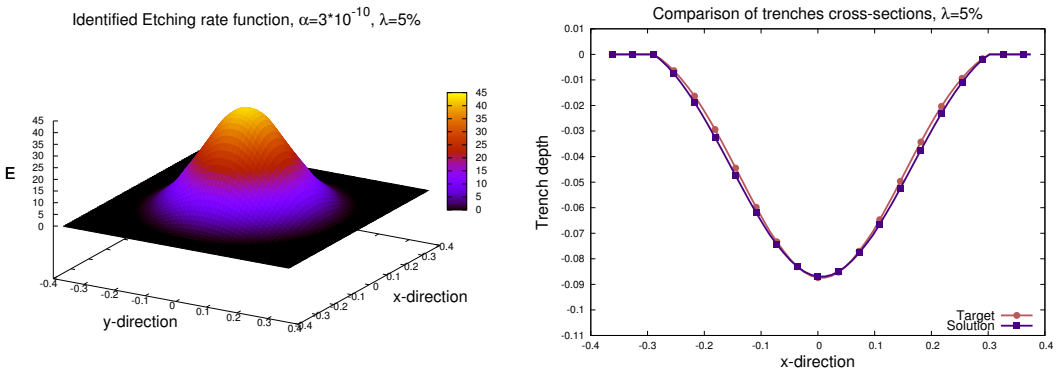

(a) 10 independent trenches, 5% of noise

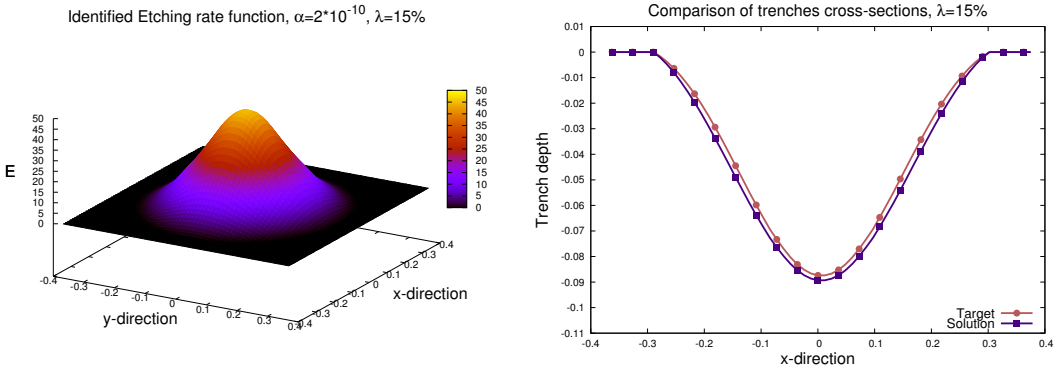

(b) 10 independent trenches, 15% of noise

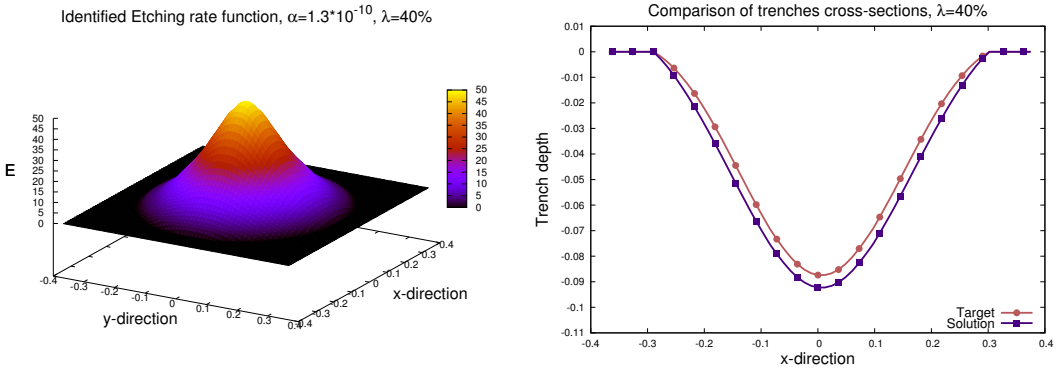

(c) 10 independent trenches, 40% of noise

Figure 7.7: Results of identification of the Etching rate functions and reconstruction of the surface shapes ("Solution") based on 10 independent trench measurements with 5%, 15% and 40% level of the measurement errors, compared with original trench profile ("Target").

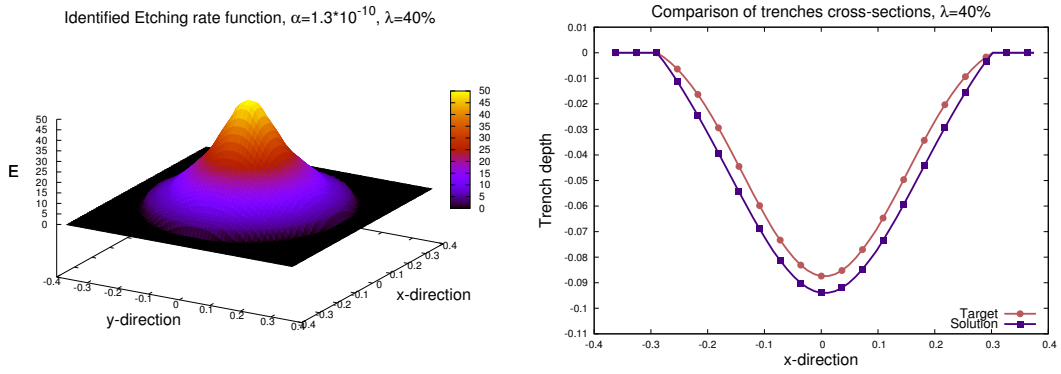

Figure 7.8: Results of identification of the Etching rate functions and surface prediction based on superposition of 10 trench measurements with 40% level of the measurement errors.

tween numerical results in paramter identification. In theory the use of the average of the noisy trenches will provide less rough and noisy input data and will lead to the identification of model parameters more precisely, what in its turn implies the better prediction of the required surface.

Based on that proposition we introduce the superposition of the ten experimental observation, which are taken from the previous test and introduced in the cost function as follows:

$$\boldsymbol{J}(\boldsymbol{E}) = \frac{1}{2}\int\limits_{\Omega_2} \left\| \boldsymbol{Z}(x,y,T) - \left(\frac{\sum_{i=1}^{n} \boldsymbol{Z}_{\exp_i}(x,y)}{n} \right) \right\|^2 \mathrm{d}x\mathrm{d}y + \frac{\alpha}{2}\|\nabla \boldsymbol{E}\|^2, \tag{7.2}$$

where $n = 10$ in accordance with the chosen case.

The results of the identification of Etching rate function and accuracy in trench formation prediction are almost the same as in case of independent measurements except the case of 40% of the noise (Figure 7.8). Suddenly, the surface geometry forecast is less precise in this situation than previously, but still better than in case of the use of one or three trenches as input.

A comparison of the accuracy in surface geometry prediction for various configurations of the cost function is represented on Figure 7.9.

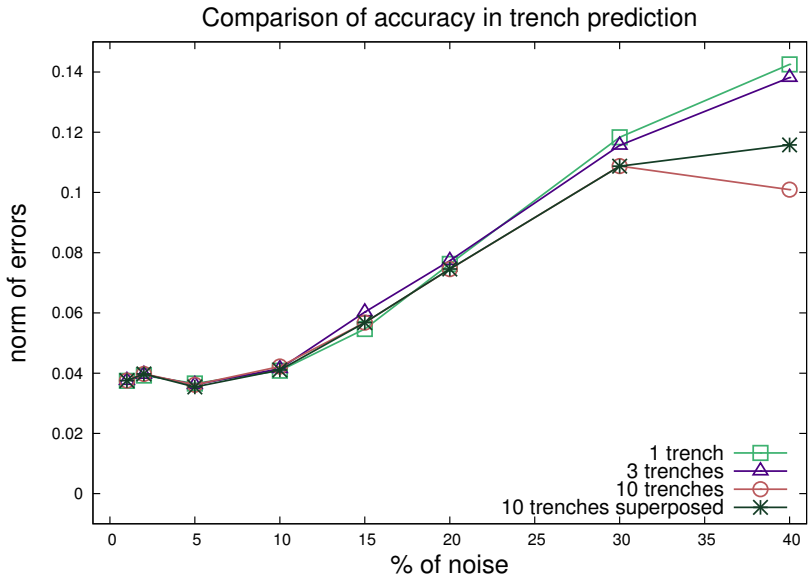

Figure 7.9: Comparison of the proposed constructions of the cost function, based on different amount of the available experimental observations.

Holding the acceptable level of accuracy (less than 10%) in the surface reconstruction in comparison with the experimental measurements, using several input or either of their average (7.1) and (7.2) provides better opportunity to match the required trench profile. The use of the average of the input measurements demand in its turn to adapt the regularization coefficient due to the change of the behavior of the input.

The difference between using one and several measurements is not very impressive due to random nature of the noise applied to the input, and could be strongly increased by involving hundreds of experimental observations to reduce the influence of the errors and by adjusting the regularization coefficient according to the averaging of the input. Given overview of the identification based on 1, 3 or 10 trenches shows us that from the other side, we can identify unknowns with reasonable accuracy even with only one trench measurement.

Cost functions (7.2) and (7.1) for $n = 10$ are not identical, but theoretically they have the same gradient. Nevertheless numerical implementation of these two cases shows the difference in obtained results and gives the flexibility to find more suitable

Trenches	1%	2%	5%	10%	15%	20%	30%	40%
1 trench	3.74×10^{-2}	3.92×10^{-2}	3.65×10^{-2}	4.08×10^{-2}	5.46×10^{-2}	7.62×10^{-2}	0.118329	0.142537
3 trenches	3.75×10^{-2}	3.95×10^{-2}	3.61×10^{-2}	4.14×10^{-2}	6.02×10^{-2}	7.73×10^{-2}	0.115635	0.138153
10 trenches	3.75×10^{-2}	3.97×10^{-2}	3.61×10^{-2}	4.22×10^{-2}	5.67×10^{-2}	7.45×10^{-2}	0.108759	0.100952
superposition of 10	3.75×10^{-2}	3.97×10^{-2}	3.54×10^{-2}	4.10×10^{-2}	5.67×10^{-2}	7.45×10^{-2}	0.108724	0.115774

Table 7.1: Comparison of the accuracy in the ternch surface prediction, corresponding to different cases of the cost functions and different levels of applied noise.

way for each particular problem. More detailed and precise results of the surface prediction are given in Table 7.1.

The analysis of the obtained results induces to think about the particular random distribution of the noise, applied with high level to the original input, which has very high influence on the identification process. The trench surface simulated with the use of the identified Etching rate function is quite close to the input (noisy or average of several trenches) in all the cases, which were not alligned and fitted to the original surface due to the fairly random distribution of the noise. It engenders the conclusion that the use of much larger number of measurement can negotiate the noises or make them more uniform, calibrate and fit by this the inputs to the original data and improve the accuracy of the surface prediction.

Mostly the use of several trenches (and their average) instead of only one can essentially improve the accuracy in the parameters identification, conducting to reduction of the errors in the surface prediction up to 20% in cases of adverse available inputs. Particularly, in case of high level of the applied noise (40%), the use of 10 separate measurement allows to improve the surface prediction accuracy by 30%. Certainly, it should be noted that sometimes only one measurement is available, and it might be enough to obtain the model parameters required to reconstruct the profile.

7.3 Noise as model parameter

7.3.1 Identification of the measurement noise

The identification of the unknown AWJM model parameter Etching rate function $\boldsymbol{E}$ in the previous section demonstrates a high straight dependency of the accuracy on the level of the noise. The accuracy of the surface prediction always decreases with the increase of the noise level reagardless of the proposed approach to construct the cost funciton.

One of the possibilities to improve the quality in surface prediction and accuracy of the identification process is to take into account and identify the measurement errors by considering them as unknown model parameters in the AWJM model:

$$\frac{\partial \boldsymbol{Z}}{\partial t} = -\frac{\boldsymbol{E}(x,y)\mathrm{e}^{a\boldsymbol{Z}}}{\left(1+\boldsymbol{Z}_x{}^2+\boldsymbol{Z}_y{}^2\right)^{k/2}} + \boldsymbol{\varepsilon}_{\exp}\ . \tag{7.3}$$

We now assume that $\boldsymbol{u} = \{\boldsymbol{E}, \boldsymbol{\varepsilon}_{\exp}\}$ and we consider new following cost function:

$$\boldsymbol{J}(\boldsymbol{u}) = \frac{1}{2}\int\limits_{\Omega_2} \|\boldsymbol{Z}(x,y,T) - \boldsymbol{Z}_{\exp}(x,y)\|^2 \mathrm{d}x\mathrm{d}y + \frac{\alpha}{2}\|\nabla \boldsymbol{E}\|^2 + \frac{\beta}{2}\|\boldsymbol{\varepsilon}_{\exp}\|^2, \tag{7.4}$$

where α stays the regularization multiplier for Etching rate function and β is the Tikhonov regularization coefficient corresponding to the measurement errors.

To ensure first the correctness of this idea and possibility to identify the existing noise in the input data, we firstly use the "true" values of $\boldsymbol{E}_0$ as the initial estimation of the Etching rate function and focus on the identification of measurement errors, which is represented as normaly distributed random values among all the working domain Ω_2. Numerically it leads to the sufficient growth of the amount of unknowns and slows down the minimization process. Here and in all the next numerical tests in this section we use the same parameters and assumptions as in section 7.2.

Firstly, it is necessary to check if the minimizer is able to faithfully determine the randomly distributed values of the model parameter. The initial noise applied to the

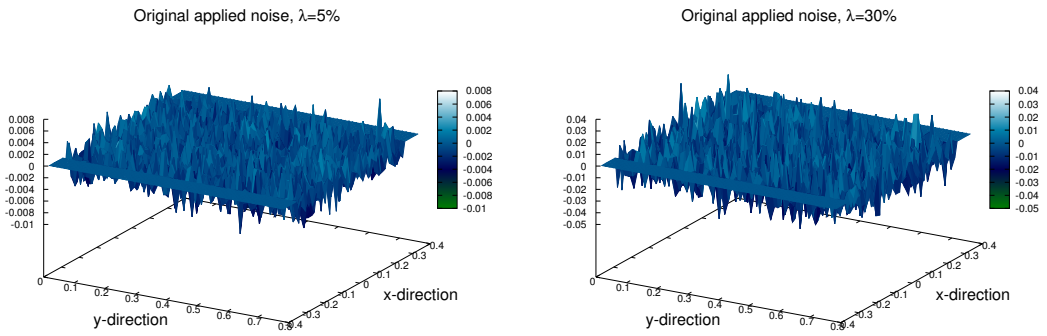

(a) Initial generated noise of 5% (b) Initial generated noise of 30%

Figure 7.10: Original generated noise of 5% and 30% level respectively.

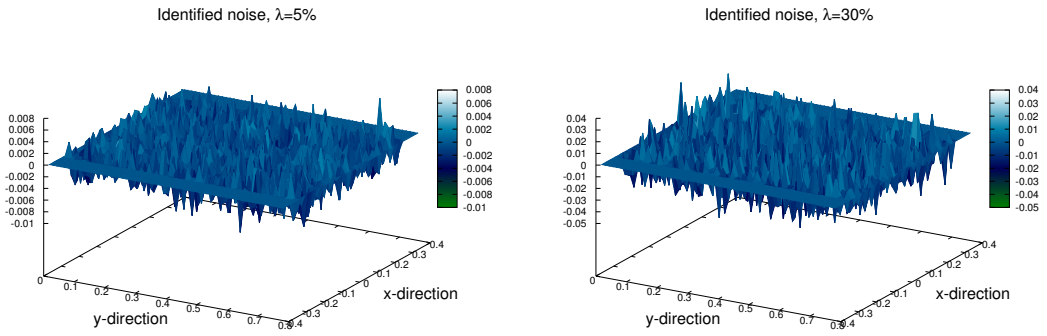

(a) Identified noise in case of 5% (b) Identified noise in case of 30%

Figure 7.11: Identifiied noise related to the cases of 5% and 30% level respectively.

trench with the levels of 5% and 30% is shown on Figure 7.10. The numerical results of the identification of the noise for both cases are given on Figure 7.11.

The main goal of these experiments is to show the availability of the announced method to reliably identify acceptable values of the simulated measurement errors regardless of error intensity.

The above illustrations clarify very strong capability to determine the measurement errors from the unclear input data having correct information about all other AWJM model parameters in advance. In compare with the original distribution of the noise the mismatch is very negligible despite its behavior.

Usually there is no information about the behavior and type of the Etching rate function $\boldsymbol{E}$ that should be used to predict the right form of the surface. Moreover, most of the available measurements are noisy and unclear. So we now face with the problem when it is necessary to identify the unknown model parameter $\boldsymbol{E}$ and measurement errors $\boldsymbol{\varepsilon}_{\text{exp}}$ at the same time, in order to improve the quality of the surface reconstruction.

Considering that we continue the identification process in the similar conditions and with the same configuration as previously, we can use some assumptions about the form of the Etching rate function $\boldsymbol{E}$, which we have already obtained in section 7.2, to simplify the continuation of identification process. The original clear surface of the trench was generated with the same model parameters, and the only difference is the random generation of the noise imposed on it.

Selected results of the combined identification of the Etching rate function and measurment errors for the cases of 5% and 30% levels are presented on Figures 7.12 and 7.13. The forms of the found Etching rate function $\boldsymbol{E}$ are almost identical in both demonstrated cases, and evenmore it keeps the same for all the range of studied noises. It proves the correctness in the joint parameters identification.

In compare with the simple identification of the noise, the shapes of the noise in these cases are not so perfect and demonstrate the dependence on other model unknowns. The disparity of the results is more distinct with smaller values of the measurement errors while in case of 30% the behavior of the identified noise is very simillar to previous case.

The comparison of the central cross-sections of initial ("Target") and identified ("Solution") Etching rate functions and related trench prediction results for the 5% noise case are given on Figure 7.14.

Considering the identification result for all the range of noise levels, we can note that with the decrease of the measurement errors, their influence on the surface formation decrease as well and become less significant. It leads to the modification of the form of identified noise, what can be distinctly seen on Figure 7.12(a), where the noise takes in

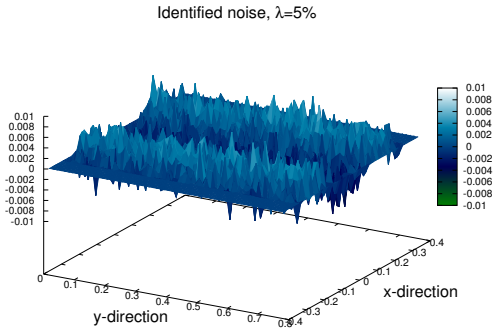

(a) Identified measurement errors 5%

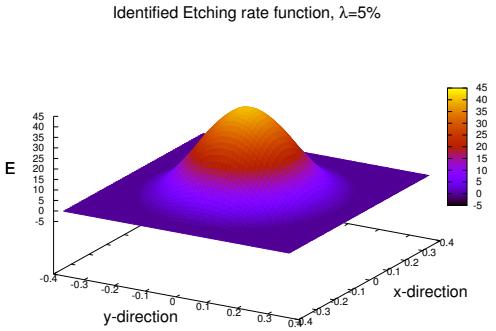

(b) Identified Etching rate function in case of 5% of noise

Figure 7.12: Jointly identified noise form and Etching rate function in case of 5% of applied noise.

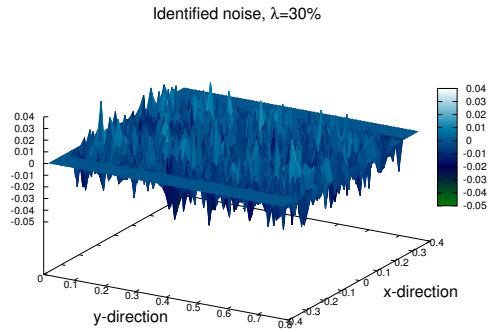

(a) Identified measurement errors 30%

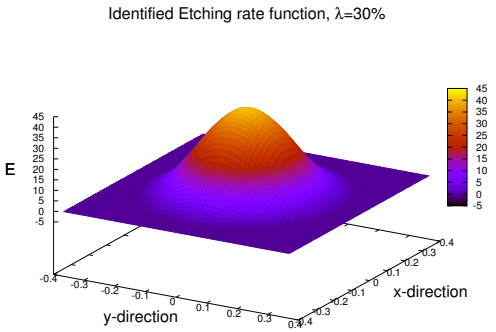

(b) Identified Etching rate function in case of 30% of noise

Figure 7.13: Jointly identified noise form and Etching rate function in case of 30% of applied noise.

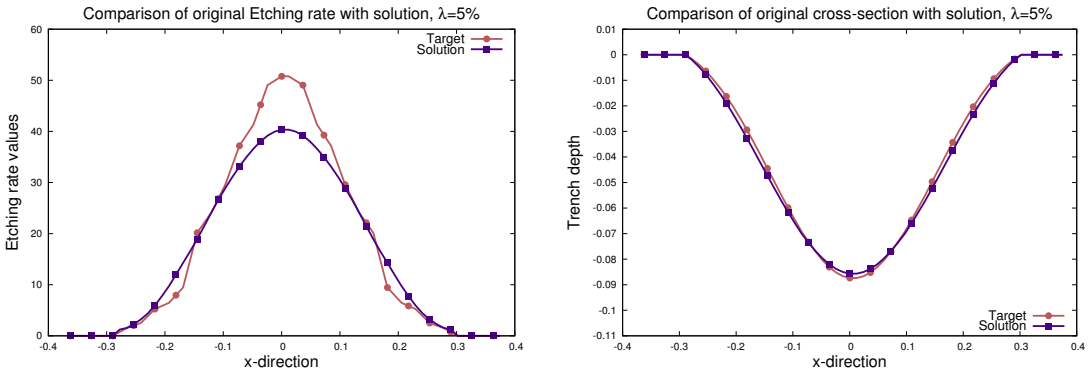

(a) Identified Etching rate function

(b) Surface reconstruction

Figure 7.14: Numerical results of the Etching rate identification (identified is called "Solution" and initial - "Target") and trench surface reconstruction with identified measurement noise of 5%.

some sense the shape of the trench surface. It is possible to conclude, that during the identification, the method tried to adjust the unknown model parameters to better fit the given input and changed the form of more flexible one - noise.

This kind of results can be very useful to understand how the final identified form of $\boldsymbol{E}$ (Figure 7.14(a)) should be actualized to reconcile the form of the noise and to improve the accuracy in the surface prediction via direct simulation with the use of optimal AWJM model parameters.

From the other side, when the measurement errors are much higher (e.g. 30% on the Figure 7.13(a)) the values and influence of it greatly rise up in comparison with Etching rate function $\boldsymbol{E}$, and it turns into several problems for the minimizer to correct the exact unknowns in the right ways and inability to adjust model parameters more precisely. But even with actual results the level of errors in the surface prediction is less than 4% in terms of L^2 norm.

7.3.2 Removing the measurement noise

One more interesting aspect of this work is the ability to improve the surface reconstruction by the improvement of the input data.

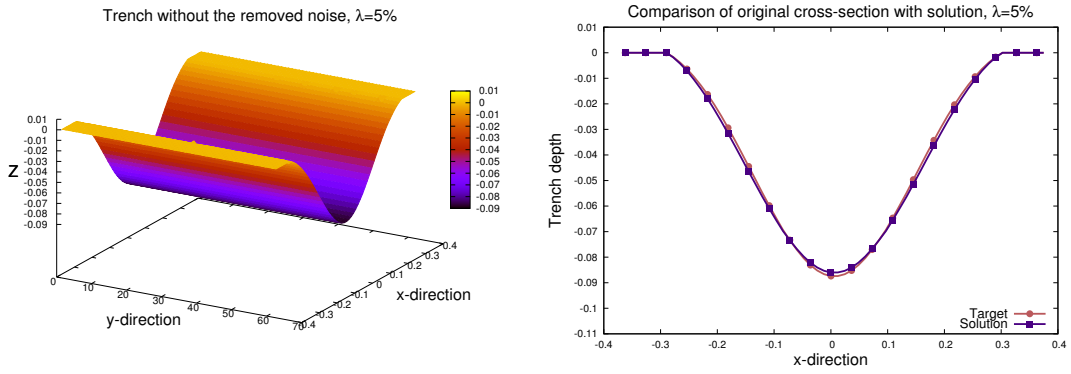

(a) Trench without the removed 5% noise

(b) Comparison of central cross-sections

Figure 7.15: Numerical results corresponding to the removed noise of 5% from the initial measurements, and prediction ("Solution") of the milled trench.

The general idea is to find the possibility to use the identified noise in order to improve the accuracy in surface prediction. As we demonstrated previously, proposed identification of the model parameters is able to properly determine the measurement noise from the input data. These obtained results can be used to improve the shape of the input data by removing the supposed noise from it.

Assume now that we identified quite acceptable and useful values of the measurement erros (e.g. Figure 7.11), which affect most strongly the identification of the AWJM model parameter $\boldsymbol{E}$ and the accuracy of surface prediction. We can further use this information to reduce the measurement errors, even if it is not ideally determined, from the initial input and obtain much smooth and clear trench.

The set of numerical implementations of this approach is presented on Figures 7.15(a) - 7.18(a). To demonstrate the applications diversity of this approach in practice the results are given for problems of 5%, 15%, 30% and 40% of the measurement noise. For each of the cases the trench surface with removed noise is illustrated as well as the comparison of the central cross-sections of the predicted ("Solution") and original ("Target") trenches.

By removing the noise from the input data we are able to obtain much better shape of the trench for each case of the noise level. Moreover, by studying the improved

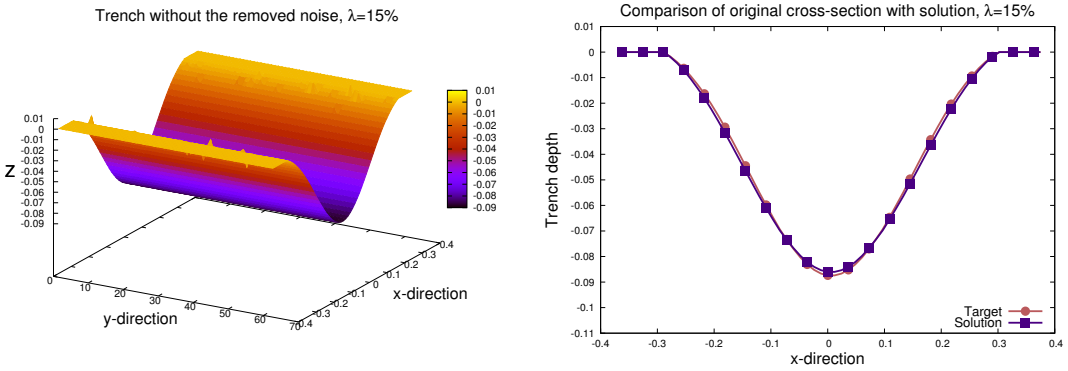

(a) Trench without the removed 15% noise (b) Comparison of central cross-sections

Figure 7.16: Numerical results corresponding to the removed noise of 15% from the initial measurements, and prediction ("Solution") of the milled trench.

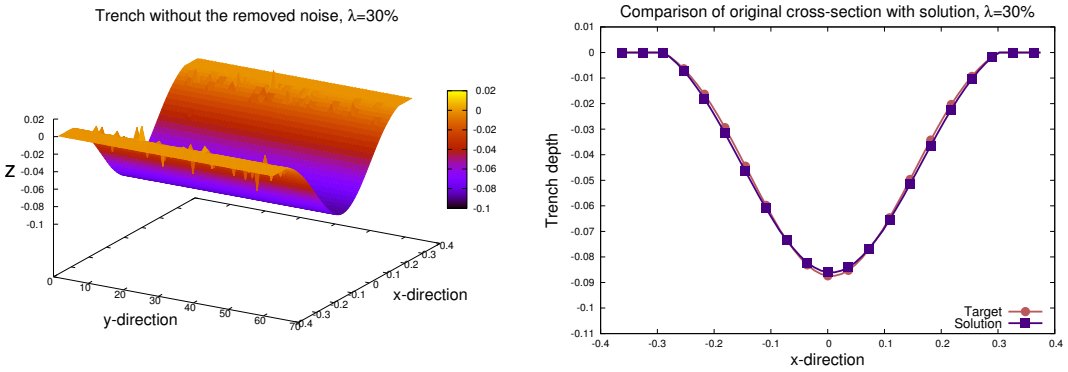

(a) Trench without the removed 30% noise (b) Comparison of central cross-sections

Figure 7.17: Numerical results corresponding to the removed noise of 30% from the initial measurements, and prediction ("Solution") of the milled trench.

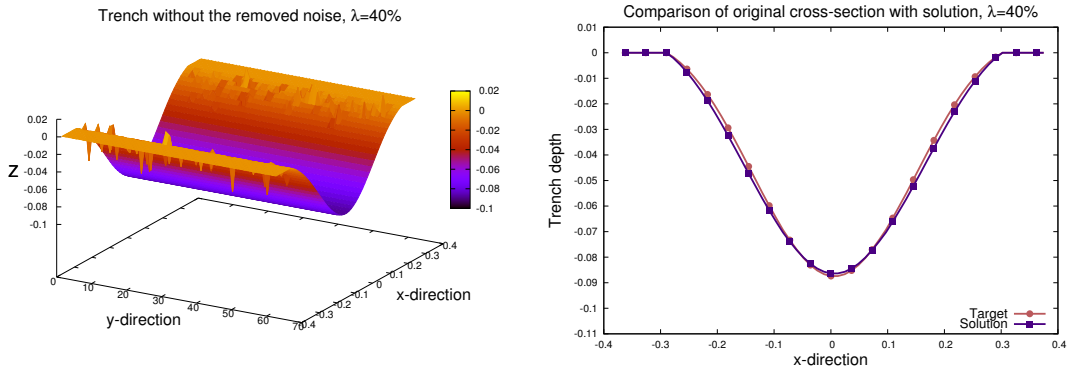

(a) Trench without the removed 40% noise

(b) Comparison of central cross-sections

Figure 7.18: Numerical results corresponding to the removed noise of 40% from the initial measurements, and prediction ("Solution") of the milled trench.

surfaces we can notice that the identified noise is very close to the applied one, and as smaller noise was in the measurements as more correct its determination.

After the use of such manipulation we can perform again the identification of the unknown AWJM model parameter $\boldsymbol{E}$ as it was demonstrated in section 7.2. By such decision we are able to reduce the influence of the measurement and model errors and really enhance the accuracy of the surface prediction 7.15(b) - 7.18(b).

The complete description of the identification results for all the span of the error levels is given in the Table 7.2. One could see that almost for all the cases our identification approach gives the very high accuracy in the surface prediction regardless of the type of input record and let us to predict the surface in direct simulation with level of error less than 3%. In cases of 15% and 20% of noise we have the increase of the precision in more than two times, while for 30% and 40% of noise we improve the accuracy of the surface prediction in more than four times.

Measurement errors	1%	2%	5%	10%	15%	20%	30%	40%
Removed noise	2.87×10^{-2}	2.94×10^{-2}	2.54×10^{-2}	2.98×10^{-2}	2.57×10^{-2}	3.27×10^{-2}	2.66×10^{-2}	3.50×10^{-2}
Noisy input	3.74×10^{-2}	3.92×10^{-2}	3.65×10^{-2}	4.08×10^{-2}	5.46×10^{-2}	7.62×10^{-2}	0.118329	0.142537

Table 7.2: Accuracy in the trench surface prediction, corresponding to different levels of applied noise. 1 measurement as input.

Chapter 8

Conclusions et perspectives (français)

Conclusions

Le principal objectif de ce travail était d'étudier le comportement du modèle d'usinage par jet d'eau abrasif en fonction des différents paramètres et de développer une méthode permettant de prédire l'évolution de la surface usinée par jet d'eau abrasif, malgré la relative qualité des données expérimentales et le manque d'information sur les paramètres d'usine des machines.

Nous avons étudié différents aspects de l'identification de paramètres pour le modèle d'usinage par jet d'eau abrasif, et les possibilités correspondantes de prédire la forme des tranches usinées avec l'aide de ces paramètres. L'identification des paramètres de ce modèle non-linéaire est particulièrement délicate lorsque les données sont bruitées, rendant le problème mal posé.

Dans ce travail, nous avons appliqué la théorie des problèmes inverses, avec une approche variationnelle, à ce problème concret et industriel. L'utilisation de la méthode de l'adjoint et d'algorithmes de minimisation efficaces nous a permis d'identifier rapidement et précisément les valeurs inconnues des paramètres du modèle. L'identification de ces paramètres permet alors de modéliser et prédire le profil des tranches usinées par jet d'eau abrasif. L'utilisation de l'approche proposée a permis d'obtenir des prévisions très précises de la formation de la surface.

Les différentes idées pour identifier les paramètres ont d'abord été introduites dans le cas de données générées par le modèle, pour un jet d'eau stationnaire. Puis nous avons procédé à l'identification de paramètres à partir de données expérimentales réelles, permettant de relier notre approche à une application industrielle. Nous avons montré

qu'un niveau même très faible de bruit ou d'erreurs de mesure peut grandement influencer l'identification et conduire à des erreurs considérables sur l'identification de la surface prédite. L'utilisation de mauvaises valeurs d'ébauche pour les autres paramètres du modèle conduit également à une moins bonne identification. L'utilisation de méthodes efficaces comme l'algorithme L-BFGS pour la minimisation, et le logiciel TAPENADE pour la différentiation automatique, a permis d'aborder ce type de problème.

L'identification généralement très précise des paramètres du modèle nous donne une bonne opportunité de prédire et simuler la formation des tranches usinées, relativement indépendamment de la qualité et densité des données expérimentales.

Dans le cas d'un déplacement uniforme ou non du jet d'eau, avec différentes vitesses, l'identification devient un problème nettement plus compliqué, en raison de l'augmentation sensible du nombre d'inconnues, et encore de l'instabilité par rapport aux données. Nous avons montré que l'approche proposée pouvait également résoudre ce problème, et ce, indépendamment du type et de la taille des données, de la profondeur de la tranche usinée, de la vitesse d'alimentation du jet d'eau, du type de déplacement du jet, et du niveau de bruit sur les données. De plus, l'identification simultanée de tous les paramètres recherchés en une seule opération montre que le modèle est réaliste, et qu'il possible de prédire avec une grande précision la surface en se focalisant sur les paramètres les plus influents.

Nous avons également étudié l'identification dans le cas d'absence de connaissances a priori sur les paramètres du modèle. En identifiant le bruit comme un paramètre supplémentaire, l'identification des autres paramètres du modèle est alors toujours possible avec une grande précision, même lorsque les données expérimentales sont peu nombreuses et imprécises.

Nous avons également comparé différentes reformulations de la fonction coût pour tenir compte de la disponibilité de plusieurs jeux de données, permettant d'aboutir à des améliorations notables de l'identification lorsque le bruit est très élevé. Nous avons considéré que le bruit faisait partie du modèle, et nous avons introduit des termes de régularisation de Tikhonov pour compenser sa présence. Nous avons montré qu'un

niveau de bruit très élevé pouvait complètement changer l'identification, et qu'il était nécessaire d'ajuster les termes de régularisation en fonction de la structure et forme des tranches usinées.

Afin de pouvoir prévoir la surface usinée dans des conditions bruitées, nous avons aussi mis en œuvre une méthode d'identification dans laquelle le bruit est identifié seul, indépendamment des autres paramètres du modèle. L'idée consiste alors à utiliser le bruit identifié pour le retirer des données, puis à identifier les autres paramètres du modèle avec ces nouvelles données. Cela augmente la qualité de l'identification des paramètres. Et les résultats numériques correspondants pour la surface usinée confirment l'intérêt de cette approche. Nous avons enfin présenté une approche d'identification globale de tous les paramètres simultanément, afin de montrer l'étendue des capacités de la méthode proposée.

Perspectives

Cette étude a principalement porté sur l'identification de paramètres pour le modèle d'usinage par jet d'eau abrasif, dans le cas de mouvements assez simples du jet, impactant une surface initialement plane. Il y a donc plusieurs perspectives naturelles d'extension de ces travaux:

Extension à des surfaces initiales non planes. Ce problème peut être abordé en considérant un problème de chevauchement ou recouvrement dans le processus d'usinage, en séparant les cas transverse et longitudinal. Dans le cas de surfaces initialement non planes, le modèle doit être recalibré pour tenir compte des variations de la distance entre la pièce et l'orifice du jet, l'augmentation du diamètre du panache et de la surface d'impact du jet, les modifications dans les forces mécaniques, ..., en fonction des variations géométriques de la surface.

Déplacement non linéaire du jet. Dans le cas d'un jet qui ne se déplace pas en ligne droite, il faut modifier le modèle numérique pour tenir compte des changements de propriétés de l'impact du jet sur la surface. Cette perspective est sans doute cruciale

d'un point de vue applicatif, afin de permettre la prévision de formes libres dans le processus de fabrication industrielle.

Étude de différents types de bruits. Nous n'avons étudié ici que le bruit blanc Gaussien additif. Mais il serait nécessaire d'étudier d'autres types de bruits, afin de pouvoir traiter certaines données expérimentales plus réalistes.

Étude de sensibilité par rapport au bruit sur des données expérimentales réelles. Nous n'avons pu étudier la sensibilité au bruit que dans le cas de données synthétiques. En effet, les données expérimentales sont très coûteuses à obtenir. En plus de l'intérêt évident de cette étude, cela permettrait de considérer le cas de bruits dont le niveau varie, impactant sérieusement le processus d'identification et de prévision de formation de la surface usinée.

Chapter 9

Conclusions and perspectives (english)

Conclusions

The main objective of this work was to study the behavior of the Abrasive Waterjet Milling model according to the physical machining system and to develop the method allowing to predict the evolution of the surface geometry for the abrasive waterjet milling process despite the quality of experimental observations and background information about machine settings.

We studied different aspects of the optimal parameters identification for AWJM model and possibilities to predict the shape of the milled trenches with the use of these parameters. The identification of Abrasive Waterjet Milling model parameters especially from the noisy data is a challenging problem because of its ill-posedness and nonlinearity of the proposed direct model.

In this work we presented the application of inverse problems theory, based on variational approach, in the real production. The use of adjoint technique and minimization methods allows to quickly and efficiently find unknown values of the required model parameters with high accuracy. The identification of optimal model parameters indeed gives a chance to model and predict the trench profile for AWJ machining. The use of demonstrated techniques leads to very precise prediction of the surface formation.

The general ideas and methods which might be used in order to identify different parameters of AWJM model were firstly demonstrated in case of self-generated input data for stationary waterjet model. Further, the averaged experimental observations were involved in the identification process in order to link this approach with real manufacturing problems. We illustrated how an even small level of measurement errors

or noise can influence on the identification results and occasionally leads to considerable errors in surface forecast. Wrong background estimation of the initial values of model parameters also decreases the accuracy of the numerical results and has to be carefully verified in advance. The involvement of efficient approaches and techniques as L-BFGS minimization method and automatic differentiation software TAPENADE shows their capacity to be used for this type of a problem.

The general high precision of the AWJM model parameters identification provides good opportunity to predict and simulate the milled trench surfaces regardless of the quality and density of available experimental observations.

In case of uniform or uneven movement of the waterjet with varied feed speed, the parameters identification problem turns out to be a more tough question due to increase of the number of unknowns and instability of the input measurements. We showed the capability of the proposed method to cope with different cases independently of type and size of the input data, depth of the milled trench, micro-waterjet feed speed, kind of the jet movement and level of the measurement noise. Furthermore, joint identification of all sought model parameters in one run reveals the nonideality of the proposed AWJM model, and gives the chance to highly improve the accuracy in the surface prediction by focusing on the most active and possible neglecting of less important parameters in surface formation.

We also presented a way to estimate the required surface profile in the lack of knowledge of exact AWJM model parameters. Proposed model coupled with measurement errors which were taken into account can precisely model the surface shape by identifying optimal values of the model parameters even with very poor and inaccurate experimental observations.

The comparison of different approaches of the cost function formulation in accordance with various number of available data indicates several particular improvements in cases of high level of measurement noise. We considered measurement errors that were included in the mathematical model, which we tried to compensate by adding Tikhonov regularization terms. Moreover, we explained how the high level of noise

could completely change the identification process and why it is necessary to keep the regularization terms adjusted for each particular problem to get a more precise structure and shape of the reconstructed trench.

In order to control the surface prediction under the noisy conditions, we implemented the technique to identify the measurement noise independently from the other model parameters. The global idea is to use the found values to be removed from the input data for the minimization problem, thereby to increase the quality of the optimal parameters identification. Obtained numerical results confirm the necessity of these manipulations by refining the quality of surface shape prediction. Also, the combined identification of all the possible and not fixed model parameters was presented in this work, to explain how widely this approach can be used regardless of available input data.

Perspectives

This study is mainly focused on the identification of the AWJM model parameters in the case of a straightforward movement of the waterjet impacting on initially plain surface. Thus, several following possibilities to extend the research are proposed:

Extension to non planar initial surfaces. Thus, it generally might be formulated as an overlapping problem for the waterjet milling process and can be splitted to transversal and longitudinal cases. Involvement of the non flat initial surface of the workpiece requires some calibrations in the proposed AWJM model due to the growth of the stand-off distance of the jet, widening of the impact spot and changes of the jet plume forces according to the variations of the surface geometry.

Non straightforward jet milling path. Consideration of this modification in the waterjet milling process requires to calibrate again the AWJM model due to the changes of the impact properties and surface geometry caused by the jets displacement. This perspective of the work can highly increase the application of the proposed method in the manufacturing in order to control the freeform milling process.

Consideration of the different types of noise. In this work we only introduced the measurement noise assumed as additive white Gaussian noise, but nonetheless other types of the stochastic processes can be considered in the AWJM model in order to operate with more realistic experimental data.

Sensitivity analysis based on the real experimental noisy data. This extension of the work can be very useful and important but remains very expensive due to the experiment costs. Moreover, the level on the noise in the experimental input data may vary and be not only of the fixed range, which in turn may affect the accuracy of the surface geometry prediction.

Bibliography

[1] J. H. Ahlberg, E. N. Nilson, and J. L. Walsh. *The Theory of Splines and Their Applications*. Academic Press, New York/London, 1967.

[2] L. Armijo. Minimization of functions having Lipschitz continuous first partial derivatives. *Pacific J. Math.*, 16(1):1–3, 1966.

[3] R. C. Aster, B. Borchers, and C. H. Thurber. *Parameter Estimation and Inverse Problems (Second Edition)*. Elsevier, 2013.

[4] D. Auroux and V. Groza. Optimal parameters identification and sensitivity study for Abrasive Waterjet Milling model. 2016. Sumbitted.

[5] D. Auroux and V. Groza. Sensitivity studies and parameters identification for noisy 3D moving AWJM model. *International Journal of Engineering Mathematics*, 2016. Article ID 9608584, 15 pages, doi:10.1155/2016/9608584.

[6] D. A. Axinte, D. S. Srinivasu, J. Billingham, and M. Cooper. Geometrical modelling of abrasive waterjet footprints: A study for 90° jet impact angle. *CIRP Annals - Manufacturing Technology*, 59:341–346, 2010.

[7] D. A. Axinte, D. S. Srinivasu, M. C. Kong, and P. W. Butler-Smith. Abrasive waterjet cutting of polycrystalline diamond: a preliminary investigation. *Int. J. Mach. Tool Manuf.*, 49:797–803, 2009.

[8] H. Banks and K. Kunisch. *Parameter Estimation Techniques for Distributed Systems*. Birkhäuser, Boston, 1989.

[9] H. T. Banks. *Control and Estimation in Distributed Parameter Systems*. SIAM, Philadelphia, 1992.

[10] H. Barrett. Image reconstruction and the solution of inverse problems in medical imaging. *Medical Images: Formation, Handling and Evaluation*, 98:3–42, 1992.

[11] J. Beck, B. Blackwell, and C. S. Clair. *Inverse Heat Conduction: Ill–Posed Problems*. Wiley, New York, 1985.

[12] M. Bertero and P. Boccacci. *Introduction to Inverse Problems in Imaging*. Inst. of Physics Publ., Bristol, 1998.

[13] A. Bilbao Guillerna, D. A. Axinte, and J. Billingham. The linear inverse problem in energy beam processing with an application to abrasive waterjet machining. *International Journal of Machine Tools & Manufacture*, 99:34–42, 2015.

[14] J. Billingham, C. B. Miron, D. A. Axinte, and M. C. Kong. Mathematical modelling of abrasive waterjet footprints for arbitrarily moving jets: PartII - Overlapped single and multiple straight paths. *International Journal of Machine Tools & Manufacture*, 68:30–39, 2013.

[15] D. Colton, H. Engl, A. K. Louis, J. McLaughlin, and W. Rundell. *Surveys on Solution Methods for Inverse Problems*. Springer-Verlag Wien, 2000.

[16] D. Colton and R. Kress. *Inverse Acoustic and Electromagnetic Scattering Theory*. Springer, Berlin, 1992.

[17] A. M. Denisov, E. V. Zaharov, A. V. Kalinin, and V. V. Kalinin. Application of Tikhonov regularization method for numerical solution of inverse problem of electrocardiography. *MSU Vestnik*, 15, 2008.

[18] H. W. Engl. Regularization methods for the stable solution of inverse problems. *Surveys on Mathematics for Industry*, 3:71–143, 1993.

[19] H. W. Engl, M. Hanke, and A. Neubauer. *Regularization of inverse problems*, volume 375 of *Mathematics and its Applications*. Kluwer Academic Publishers Group, Dordrecht, 1996.

[20] H. W. Engl and W. Rundell. *Inverse Problems in Diffusion Processes*. SIAM, Philadelphia, 1995.

[21] J.-C. Gilbert and C. Lemaréchal. Some numerical experiments with variable storage quasi-Newton algorithms. *Math. Prog.*, 45:407–435, 1989.

[22] J.-C. Gilbert and C. Lemaréchal, 2013.

[23] C. W. Groetsch. *Inverse Problems in the Mathematical Sciences*. Vieweg, Braunschweig, 1993.

[24] J. Hadamard. *Lectures on Cauchy's Problem in Linear Partial Differential Equations*. New Haven Yale University Press, 1923.

[25] J. Hadamard. *Quelques cas d'impossibilité du problème de Cauchy*. In mem. Lobatchewsky. Kazan, 1927.

[26] P. C. Hansen and D. P. O'Leary. The use of the L-curve in the regularization of discrete ill-posed problems. *SIAM J. Sci. Comput.*, 14:1487–1503, 1993.

[27] L. Hascoët and V. Pascual. The Tapenade Automatic Differentiation tool: Principles, Model, and Specification. *ACM Transactions On Mathematical Software*, 39(3), 2013.

[28] V. Isakov. *Inverse Problems in Partial Differential Equations*. Springer, Berlin, New York, 1998.

[29] B. Kaltenbacher, A. Neubauer, and O. Scherzer. *Iterative Regularization Methods for Nonlinear Ill-Posed Problems*, volume 6 of *Radon Series on Computational and Applied Mathematics*. Walter de Gruyter GmbH & Co, Berlin, 2008.

[30] A. Kirsch. *An Introduction to the Mathematical Theory of Inverse Problems*. Springer, New York, 1996.

[31] M. C. Kong, S. Anwar, J. Billingham, and D. A. Axinte. Mathematical modelling of abrasive waterjet footprints for arbitrarily moving jets: PartI - single straight paths. *International Journal of Machine Tools & Manufacture*, 53:58–68, 2012.

[32] M. M. Lavrentiev, V. G. Romanov, and S. P. Shishatskii. *Ill-Posed Problems of Mathematical Problems*, volume 64. AMS, Providence, 1986.

[33] C. L. Lawson and R. J. Hanson. *Solving Least Squares Problems*. SIAM, Philadelphia (PA), 1995.

[34] J.-L. Lions. *Optimal Control of Systems Governed by Partial Differential Equations*. Springer-Verlag, 1971.

[35] D. C. Liu and J. Nocedal. On the limited memory BFGS method for large scale optimization. *Math. Prog.*, 45:503–528, 1989.

[36] P. Lozano Torrubia, J. Billingham, and D. A. Axinte. Stochastic simplified modelling of abrasive waterjet footprints. *Proc. R. Soc. A*, page 2016 472 20150836, 2016.

[37] F. Natterer. *The Mathematics of Computerized Tomography*. Teubner, Stuttgart, 1986.

[38] A. Quarteroni. *Numerical Models for Differential Problems*. Springer-Verlag, 2009.

[39] A. G. Ramm. *Scattering by Obstacles*. Reidel, Dordrecht, 1986.

[40] A. Saltelli, M. Ratto, T. Andres, F. Campolongo, J. Cariboni, D. Gatelli, M. Saisana, and S. Tarantola. *Global Sensitivity Analysis: The Primer*. John Wiley & Sons, 2008.

[41] D. K. Shanmugam, J. Wang, and H. Liu. Minimisation of kerf tapers in abrasive waterjet machining of alumina ceramics using a compensation technique. *Int. J. Mach. Tool Manuf.*, 48:1527–1534, 2008.

[42] P. Slikkerveer and F. In't Veld. Model for patterned erosion. *Wear*, 233:377–386, 1999.

[43] A. Tarantola. *Inverse Problem Theory and Methods for Model Parameter Estimation*. SIAM, Philadelphia, 2005.

[44] U. Tautenhahn. Lavrentiev regularization of nonlinear ill-posed problems. *Vietnam Journal of Mathematics*, 32:29–41, 2004.

[45] A. N. Tikhonov and V. Y. Arsenin. *Solutions of ill-posed problems*. John Wiley & Sons, New York, 1977.

[46] A. N. Tikhonov and V. B. Glasko. Use of the regularization method in non-linear problems. *Zh. Vychisl. Mat. Mat. Fiz.*, 5(3):463–473, 1965.

[47] H. K. Tönshoff, F. Kross, and C. Marzenell. High pressure water peening—a new mechanical surface strengthening process. *Ann. CIRP*, 46:113–116, 1996.

[48] F. Veersé and D. Auroux. Some numerical experiments on scaling and updating L-BFGS dianogal preconditioners. Research Report 3858, INRIA, 2000.

[49] C. Vogel. *Computational Methods for Inverse Problems*. SIAM, Philadelphia, 2002.

[50] P. Wolfe. Convergence conditions for ascent methods. *SIAM Rev.*, 11(2):226–235, 1969.

[51] M. Zuhair Nashed and O. Scherzer. *Inverse Problems, Image Analysis, and Medical Imaging: AMS Special Session on Interaction of Inverse Problems and Image Analysis*. American Mathematical Soc., New Orleans, Louisiana, 2002.